RAMAN SPECTROSCOPY OF THE INTERFERON-INDUCED 2', 5'-OLIGOADENYLATES

1987

WHITE

Report Documentation Page

Form Approved
OMB No. 0704-0188

Public reporting burden for the collection of information is estimated to average 1 hour per response, including the time for reviewing instructions, searching existing data sources, gathering and maintaining the data needed, and completing and reviewing the collection of information. Send comments regarding this burden estimate or any other aspect of this collection of information, including suggestions for reducing this burden, to Washington Headquarters Services, Directorate for Information Operations and Reports, 1215 Jefferson Davis Highway, Suite 1204, Arlington VA 22202-4302. Respondents should be aware that notwithstanding any other provision of law, no person shall be subject to a penalty for failing to comply with a collection of information if it does not display a currently valid OMB control number.

1. REPORT DATE **JUN 1987**	2. REPORT TYPE **N/A**	3. DATES COVERED **-**

4. TITLE AND SUBTITLE **Raman Spectroscopy of the Interferon-Induced 2',5'-Oligoadenylates**	5a. CONTRACT NUMBER
	5b. GRANT NUMBER
	5c. PROGRAM ELEMENT NUMBER
6. AUTHOR(S)	5d. PROJECT NUMBER
	5e. TASK NUMBER
	5f. WORK UNIT NUMBER
7. PERFORMING ORGANIZATION NAME(S) AND ADDRESS(ES) **Uniformed Services University Of The Health Sciences Bethesda, MD 20814**	8. PERFORMING ORGANIZATION REPORT NUMBER
9. SPONSORING/MONITORING AGENCY NAME(S) AND ADDRESS(ES)	10. SPONSOR/MONITOR'S ACRONYM(S)
	11. SPONSOR/MONITOR'S REPORT NUMBER(S)

12. DISTRIBUTION/AVAILABILITY STATEMENT
Approved for public release, distribution unlimited

13. SUPPLEMENTARY NOTES

14. ABSTRACT

15. SUBJECT TERMS

16. SECURITY CLASSIFICATION OF:			17. LIMITATION OF ABSTRACT **SAR**	18. NUMBER OF PAGES **184**	19a. NAME OF RESPONSIBLE PERSON
a. REPORT **unclassified**	b. ABSTRACT **unclassified**	c. THIS PAGE **unclassified**			

Standard Form 298 (Rev. 8-98)
Prescribed by ANSI Std Z39-18

UNIFORMED SERVICES UNIVERSITY OF THE HEALTH SCIENCES
F. EDWARD HÉBERT SCHOOL OF MEDICINE
4301 JONES BRIDGE ROAD
BETHESDA, MARYLAND 20814-4799

APPROVAL SHEET

Title of Thesis: Raman Spectroscopy of the Interferon-Induced
                  2',5'-Oligoadenylates

Name of Candidate: Major Joseph C. White, MS, USA
                    Doctor of Philosophy Degree
                    June 25, 1987

Thesis and Abstract Approved:

_____   _____
Committee Chairperson   Date
                                        7/20/87

_____   _____
Committee Member   Date
                                        7/17/87

_____   _____
Committee Member   Date
                                        7-17-87

_____   _____
Committee Member   Date
                                        7-17-87

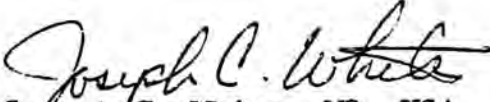_____   _____
Committee Member   Date
                                        7-17-87

i

The author hereby certifies that the use of any copyrighted
material in the dissertation manuscript entitled:

"Raman Spectroscopy of the Interferon-Induced

2',5'-Oligoadenylates

beyond brief excerpts is with the permission of the copyright
owner, and will save and hold harmless the Uniformed Services
University of the Health Sciences from any damage which may arise
from such copyright violations.

MAJ Joseph C. White, MS, USA
Department of Biochemistry
Uniformed Services University
   of the Health Sciences

ii

ABSTRACT

Title of Thesis: Raman Spectroscopy of Interferon Induced

2',5'-Oligoadenylates

Joseph C. White, Doctor of Philosophy, 1987

Thesis directed by: M. I. Johnston, Ph.D., Biochemistry Department

Raman spectra of model compounds and of 2',5'-
oligoadenylates in D_2O were utilized to assign the Raman vibrational
bands of 2',5'-oligoadenylates. pH titration experiments revealed
that the 5'-terminal phosphate group has a pKa of about 6.1 and
probably does not interact with other portions of the molecule.
Band assignments for the C_6-NH_2 groups of pA2'pA2'pA were verified
by the position of the band assigned to these groups in the Raman
spectra of pA2'pA2'pA in H_2O and D_2O. The Raman spectrum of
pA2'pA2'pA was altered slightly by elevations in temperature, but
not in a manner supporting the postulate that 2',5'-oligoadenylates
possess intermolecular base stacking. Major differences in the
Raman spectrum of 2',5'- and 3',5'-oligoadenylates were observed in
the 600-1200 cm^{-1} portion of the spectrum that arises predominately
from ribose and phosphate vibrational modes. Phosphodiester
backbone modes in A3'pA3'pA and pA3'pA3'pA produced a broad band at
802 cm^{-1} with a shoulder at 820 cm^{-1}, whereas all 2',5'-
oligoadenylates contained a major phosphodiester band at 823 cm^{-1}
with a shoulder at 802 cm^{-1}. The backbone mode of pppA2'pA2'pA
contained the sharpest band at 823 cm^{-1}, suggesting that the
phosphodiester backbone may be more restrained in the biologically
active, 5'-triphosphorylated molecule. This is the first evidence
that relates biological activity to a physicochemical property of

2-5A. Modified forms of 2',5'-oligoadenylates were examined, including the biologically active pA2'(8BrA)2'p(8BrA) which had bands in the 1200-1300 cm^{-1} portion of the spectrum that were different compared to the inactive brominated analogues, p(8BrA)2'pA2'pA and pA2'p(8BrA)2'pA. Preliminary studies on the binding interaction of 2',5'-oligoadenylates with a monoclonal antibody specific for pA2'pA2'pA were initiated. Such studies, utilizing a specific and available antibody, would serve as the basis for the future analysis of the binding of pppA2'pA2'pA to the naturally-occurring 2',5'-oligoadenylate-dependent ribonuclease. Significant progress was made and the next logical step of using resonance Raman spectroscopy rather than conventional argon laser Raman spectroscopy was clearly defined. Such research will be valuable to those who design modified 2',5'-oligoadenylates as potential therapeutic drugs.

RAMAN SPECTROSCOPY OF THE INTERFERON

INDUCED 2',5'-OLIGOADENYLATES

by

Joseph C. White

Thesis submitted to the Faculty of the Department
of Biochemistry Graduate Program of the Uniformed
Services University of the Health Sciences in partial
Fulfillment of the requirements for the degree of Doctor of
Philosophy, 1987

DEDICATION

To Susan, Bryan, and Julie

ACKNOWLEDGEMENTS

I would like to sincerely thank my advisor Dr. M. I. Johnston for her invaluable assistance in completing this research. Her systematic approach to science and her demand for excellence not only improved the quality of this research, but also set a standard which I will attempt to emulate throughout my scientific career.

I would also like to thank Dr. Robert W. Williams for many hours of instruction on the Raman instrument. Thanks to his expertise with complex electronics and instrumentation, the Raman instrument was always operational and reliable.

I would like to thank the members of my dissertation committee for their encouragement and for many helpful discussions. I wish to particularly acknowledge Dr. Fred Bollum and Dr. Bill Ruyechan for their assistance and advice.

The constructive criticism and useful suggestions I received from Postdoctoral Fellows Dr. William G. Hearl and Dr. Deborah Hurt improved the quality of this work and was greatly appreciated. Also, I would especially like to thank Mary O'Connor, Karen Winestock, Sheila Loughran, and Ruth Starman for their assistance with technical problems and their never ending humor and good spirit.

I am grateful to my parents, Ena and Joseph White and to my parents-in-law Mary Ellen and Sam Thompson for their continuing support. Above all, I am very grateful for the love and support I received from my wife, Susan. Without her constant encouragement, this thesis would not have been possible.

Table of Contents

LIST OF FIGURES

LIST OF TABLES

.

.

[1] Abbreviations: BSA, bovine serum albumin; OA, ovalbumin; ELISA, enzyme linked immunosorbent assay; Ficoll-pA$_3$, pA$_3$ conjugated through 5'-phosphate to AECM-Ficoll; AECM-Ficoll, [N-(2-aminoethyl)carbamoyl]methylated Ficoll; PBS, 0.01 M sodium Phosphate, pH 7.4 and 0.15 M NaCl; Tween 20, poly(oxyethylene)sorbitan monolaurate; PBS + Tween, PBS with 0.05% Tween20; ABTS, 2,2'-azinobis(3ethylbenzothiazolone-6-sulfonic acid); IFN, interferon; dsRNA, double stranded RNA; mRNA, messenger RNA; t-RNA, transfer RNA; DNA, deoxyribonucleic acid; NK cells, natural killer cells; PC, phosphocellulose; DEAE, diethyl amino ethyl; eIF-2, eukaryotic initiation factor 2; LADH, liver alcohol dehydrogenase; NADH, nicotinamide adenine dinucleotide; TEAB, triethyl ammonium bicarbonate; TEA, triethyl ammonium ion; CD circular dichroism; NMR, nuclear magnetic resonance; 2-5A or pppA$_3$, trimer triphosphate, 5'-O-triphosphoryladenyl-(2',5')adenylyl(2',5') adenosine, pppA2'p(A2'p)nA, where n is usually 1-3; trimer monophosphate, pA2'pA2'pA or pA$_3$, 5'-O-monophosphoryladenylyl-(2',5')adenylyl(2',5') adenosine; pA2'pA3'pA, 5'-O-monophosphoryl-adenylyl(2',5')adenylyl(3',5') adenosine; pA3'pA2'pA, 5'-O-mono-phosphoryladenylyl(3',5')adenylyl(2',5') adenosine; trimer core, A2'pA2'pA, adenylyl(2',5')adenylyl(2',5') adenosine; A3'pA3'pA, adenylyl(3',5')adenylyl(3',5') adenosine; pA2'pA8Br2'pA8Br, 5'-O-monophosphoryladenylyl(2',5')8-bromoadenylyl 8-bromoadenosine; RNase L, 2-5A dependent endoribonuclease; HEPES,4-(2hydroxyethyl)-1-piperazineethanesulfonic acid.

I. Introduction

Development of cell-free protein synthesis systems in the early 1970's have made possible the elucidation of many complex biochemical processes at the molecular level. Use of these systems has been largely responsible for the insight gained about the mechanism of interferon (IFN)[1] action.

Interferons are a family of proteins, many of which share some sequence homology (Lengyel, 1982 and references therein). They occur in a wide variety of vertebrates from fish to man and are important modulators of cell function. Unless they are induced, their concentration is below the level of detection in most organs and cell culture systems.

Human interferons are historically classed into three antigenically distinct types, alpha, beta, and gamma. Alpha interferons are produced mainly by myeloid cells, beta interferons are produced mainly by solid tissue types such as fibroblasts, and gamma interferons are produced by T-lymphocytes. Alpha and beta interferons can be induced by a variety of agents including certain viruses, certain bacteria and protozoa, and natural or synthetic double stranded RNA (dsRNA) such as poly(I)·poly(C) (Lengyel 1982). Certain tumor derived or virus transformed cells are also reported to induce α-interferons in antigen, mitogen, or lectin stimulated T lymphocytes and in NK cells.

IFNs that are secreted by producing cells bind to surface receptors of responsive cells and induce numerous and diverse biological effects. Human IFN-α and β (type I) bind to the same high affinity (10^{-10} M) species specific receptors (Aguet &

Mogensen, 1983). These type I receptors are coded by a gene on chromosome 21 and number about 2,500/cell. The receptor may also interact with other proteins and gangliosides (Aguet & Mogensen, 1983). IFN- γ acts through type II IFN receptors which are not encoded by chromosome 21. These receptors are more abundant than type I receptors and number 25-50,000 per cell. The two types of IFN receptors appear to be independent because type I IFN's do not compete with the binding of IFN- γ to cells (Baglioni et al., 1983; Aguet et al., 1983; Raziuddin et al., 1984). IFN's bind rapidly to their receptors which are then internalized.(Aguet et al., 1983). IFN- β may bind to nuclear membranes as shown by the work of Kushnaryov et al (1985).

Binding of IFN to the cell membrane is an obligatory first step to induce the interferon effect. However, binding alone does not necessarily result in the activation of interferon's biological functions. An example of binding with no activation was shown by Revel & Chebath (1986). Their experiments show that there is no gene activation after binding of IFN at 4° C or when IFN- α or γ fragments that retain receptor binding activity are used. Other workers have shown that binding of IFN alone is sufficient to elicit a transmembrane signal. This was shown in experiments with insoluble IFN which was obtained by binding IFN to a large ligand incapable of penetrating the cell membrane (Ankel et al.,1973; Chany et al.,1974). Aguet (1980) and Aguet & Blanchard (1981) have shown that ^{125}I mouse IFN was not degraded after binding to the receptor and most was recovered as it was released from the cell. No internalized IFN was detected in these experiments. Other workers

have shown some internalization of IFN, but this may have resulted
from endocytic degradation of the receptor (Chany, 1984).

In light of the above discussion, the mechanism by which
IFN activates genes is not clearly understood but it probably
involves some function of receptor occupancy. However, in some
cases interferon resistant cells do not bind IFN (Gresser et al.,
1974) in other cases, no difference can be found between IFN binding
to sensitive and resistant cells. For example, a mouse embryo cell
line that had become resistant to IFN was found to bind mouse IFN to
the same extent as normal mouse L cells (Stewart, 1979).

Interferons are recognized as important biological mediators
that have numerous effects on the immune system, including
inhibition of viral replication (Stewart, 1979). Cell surface MHC
class I antigens are induced by all interferons, but IFN-γ
increases expression of MHC antigens at concentrations lower than
required to inhibit viral replication (Revel et al., 1984; Wallach
et al., 1982). The IFN-induced expression of MHC antigens would
enhance the killing of virus-infected cells by cytotoxic lymphocytes
that recognize viral antigens complexed with MHC-I antigens (Revel
et al., 1985; De Maeyer-Guinard & De Maeyer E., 1985). Tumor cells
may escape this killing by expressing few MHC-I antigens.
Interferon α and γ can restore class I HLA expression in tumor cells
and may account for IFN's antitumor effect. Cells expressing the
HLA-DR antigens are also involved in presentation of antigen to
helper T-cells involved in the production of antibody (Rosa &
Fellous, 1984; Collins et al.,1984). In addition, IFN appears to be
important in switching on the expression of MHC-I antigens during

differentiation (Yarden et al., 1984). IFN-γ activates natural killer cells (NK) cells while protecting responsive cells against NK killing. This NK-mediated cell killing may be another major immunoregulatory function of IFN-γ (Revel et al., 1985; DeMaeyer-Guignard & De Maeyer, 1985).

Interferons induce increased synthesis of certain sets of cell receptor proteins including Fc receptors, an unidentified 16 kd protein in T and B cells, and an unidentified 20 kd protein in Daudi cells (Revel M., 1984; Knight et al., 1985; De Maeyer-Guignard & De Maeyer, 1985). The synthesis of certain excreted proteins also increases (Revel & Chebath, 1986 and references therein). Secretion of lymphotoxin and tumor necrosis factor is increased by IFNs-α and γ (Revel et al.,1985).

The mode of action of an interferon may depend upon the type of cell, the type of interferon, and the agent that interferon is acting against i.e. virus, tumor, or parasite (Stewart, 1979, 1981). Interferon treatment leads to inhibition of translation of a wide variety of viral mRNA's (reviewed by Johnston & Torrence, 1984). However, some viruses, may have another site of interferon action as discussed below.

Interferons induce at least two double-stranded RNA-dependent proteins, 2',5'-oligoadenylate synthetase and protein P1 kinase, both of which are probably involved in the IFN-mediated inhibition of viral mRNA translation and have been implicated in other IFN-mediated activities as well (reviewed by Johnston & Torrence, 1984). 2',5'-Oligoadenylate synthetase polymerizes ATP into pppA(2'pA)n where n>2 (2-5A). 2-5A, in turn, activates a

latent cellular endoribonuclease, RNase L, that degrades RNA. In
the paragraphs that follow, the interferon response that results in
binding and activation of RNase L by 2-5A, will be reviewed.

**II.A.1. Mechanism of interferon action: The 2-5A system,
experiments in cell-free extracts.**

Treating cells with interferon evokes numerous biological
effects including growth inhibition and the arrest of virus
replication (Taylor-Papadimitriou, 1980).   Early studies on the
mechanism of IFN action focused on interferon's antiviral effects
(Stewart, 1979, 1981). Various studies have implicated interferon's
interference with almost every stage of virus replication.
Inhibition of transcription is proposed to be the primary mechanism
of IFN action against vesicular stomatitus virus (VSV) and SV40
(Johnston & Torrence, 1984 and references therein).
Pretreatment of mouse L cells with IFN inhibits the penetration of
VSV without affecting virus adsorption (Whitaker-Dowling et al.,
1983). IFN blocks the budding stage of replication of certain RNA
viruses (Bugany et al., 1983). Substantial evidence supports the
view that interferon blocks virus reproduction at the level of
translation in many cases (reviewed by Sonnabend & Freidman, 1973;
Metz, 1975; Freidman 1977). For example, Ball and White (1978) used
a coupled transcription-translation to study the effects of IFN
treatment in cell-free extracts of primary chick embryo cells. No
effect on transcription was observed, but translation of various
mRNA's was inhibited up to 70%.

The series of experiments that began to uncover the
molecular basis for this inhibition of translation were conducted in

cell-free extracts of mouse L cells (Friedman et al., 1972a,b). These extracts were subjected to various treatments and then the ability of the extract to carry out protein synthesis in response to exogenous mRNA was monitored. When mouse L cells were pretreated with interferon alone, no effect on protein synthesis was observed. When mouse L cells were first treated with interferon and then infected with vaccinia virus, extracts from these cells developed a dramatic decrease in their ability to translate EMC virus RNA or globin mRNA. These experiments suggested that interferon treatment produced a latent antiviral state in the cell. The mechanism of this antiviral state was further elucidated by the finding that double-stranded RNA such as Penicillium chrysogenum dsRNA could replace the requirement for the virus infection (Kerr et al., 1977). That is, the addition of dsRNA to extracts of interferon-treated mouse L cells resulted in a blockage of protein synthesis, but the addition of dsRNA had no effect on translation in extracts of untreated L cells.

II.A.2. The messenger: dsRNA

dsRNA acts to inhibit protein synthesis through production of a heat stable low molecular weight inhibitor of protein synthesis generated when extracts of interferon-treated mouse L cells are incubated in the presence of dsRNA and ATP (Roberts et al., 1976). Inhibition of translation was also shown in intact mouse L cells treated with IFN and dsRNA (Williams et al., 1978). The enzymatic activity responsible for synthesis of the inhibitor, now known to be 2-5A synthetase, could be adsorbed to a column of poly(I)·poly(C)-

Sepharose (Hovansessian et al., 1977), washed, and incubated with ATP to generate high concentrations of the inhibitor. The inhibitor was ionic in nature and consisted of several components that could be separated on an DEAE ion exchange column. The chemical structure of the inhibitor was deduced from a series of chemical and enzymatic degradations and found to be 5'-O-triphosphoryladenylyl-(2',5')adenylyl(2',5') adenosine, or 2-5A (Kerr & Brown, 1978). The inhibitor has the chemical structure depicted in Figure 1. This structure represented the first demonstration of the natural occurrence of a 2',5'-oligonucleotide.

Subsequently, other 2',5'-linked nucleic acids have been found. Geer et al. (1983) reported a ligase activity in E. coli extracts that joins tRNA halves to form a 2',5'-phosphodiester bond at the ligation juncture. Wallace and Edmonds (1982) described a "highly charged ionic component" from a total RNase T2 digest of nuclear polyadenylated mRNA that proved to be the trinucleotide splicing branch point in the mRNA splicing reaction. Subsequently, Padgett et al. (1984) and Ruskin et al. (1984) described a forked mRNA splicing intermediate containing both 2',5'-and 3',5'-phosphodiester bonds.

II.A.3. Targets of ds RNA: 2-5A Synthetase and Protein P_1 Kinase

2-5A synthetase has been found in cells of a wide variety of animals. Reptiles, mice, rabbits, dogs, chickens, guinea pigs, monkeys, and humans, but not yeast, amphibians or Drosophila have been reported to contain detectable levels of the synthetase (reviewed by Johnston & Torrence 1984).
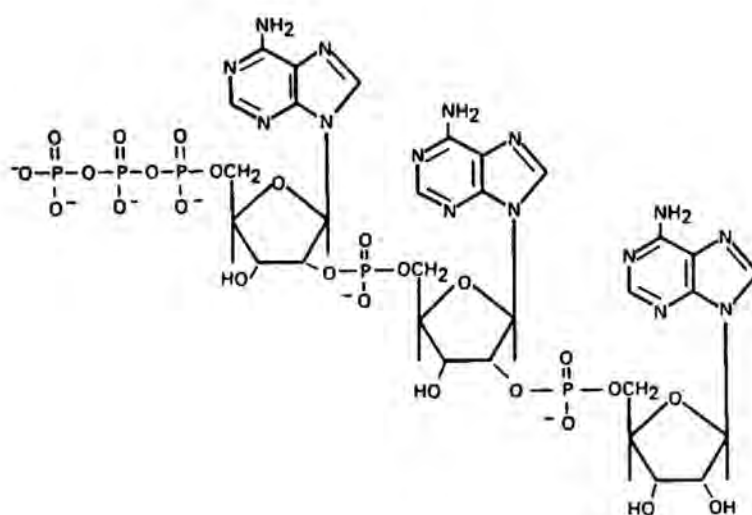
Figure 1. Structure of 2-5A [5'-O-triphosphoryladenylyl(2',5')-adenylyl(2',5') adenosine.

Evidence for at least three 2-5A synthetases exist: 1. An 85-120 kda form found predominately in the cytoplasm, 2. A 20-30 kda form found in the nucleus, and 3. An intermediate size (67 kda) associated with microsomes (Yang et al.,1981; Revel et al.,1982; St. Laurent et al., 1983; Revel et al., 1987). The different forms of 2-5A synthetase have different activation requirements. For example, the small enzyme was optimally activated when dsRNA was added in 100- to 1000-fold excess of the concentration activating the large 85-120 kda enzyme (Ilson et al., 1986). Ilson's work was repeated with identical results (Chebath et al.,1987) but the dsRNA activation requirement for the 67 kda form of the synthetase was not reported in this later study. The markedly different activation requirements of the three different synthetase enzymes, together with their different cellular locations, supports the concept of a complex enzymatic system that may be capable of localized responses to dsRNA. To date, two general synthetase mRNA message classes, 1.5 and 3.8 kb, have been isolated and translated in Xenopus oocytes to yield functional 2-5A synthetase (Revel et al., 1982). The 1.5 kb synthetase gene has since been cloned into E. coli (Merlin et al., 1983).

There is a second, independent mechanism of interferon action that is dsRNA-dependent and separate from the 2-5A system (reviewed by Johnston & Torrence, 1984). The main feature of this system is an interferon-induced protein kinase. This protein kinase was identified recently as protein P_1 kinase purified from mouse L_{929} cells (Berry et al.,1985). Four lines of evidence supported the conclusion that IFN treatment induces the synthesis of P_1 which

itself possess the dsRNA-dependent protein kinase activity. First, it was not possible to separate P_1 kinase activity from the dsRNA-dependent protein kinase using DEAE, PC and hexylamine agarose chromatography. Second, the molecular weight observed for the dsRNA-dependent protein kinase, 67 kda, is identical to the molecular weight observed for phosphorylated P_1. Third, P_1 contains a nucleotide binding site that has been photoaffinity labeled with ATP (Bischoff & Samuel, 1985). Fourth, the phosphorylation of P_1 was independent of reaction volume which suggests that this phosphorylation may be an intramolecular autophosphorylation (Berry et al., 1985).

IFN treatment of many types of cells induces P_1 kinase which then phosphorylates the α subunit of eIF-2. Phosphorylation of eIF-2 increases its affinity for eIF-2B, effectively sequestering the relatively smaller pool of eIF-2B since the pool of eIF-2B is only 10-20% of that of eIF-2. This, in turn, interferes with normal recycling of eIF-2 during protein synthesis initiation. Following binding of the ternary complex to the initiating $43S_N$ ribosomal subunit, eIF-2 is released as an inactive eIF-2·GDP complex. Normally, eIF-2·GDP is exchanged with eIF-2·GTP bound in an eIF-2B·eIF2·GTP complex (reviewed by Safer, 1983). Binding of Met-tRNA to eIF-2·GTP forms the ternary complex required for initiation. However, when eIF-2α is phosphorylated the resulting eIF2(αP)·GDP becomes sequestered into an inactive eIF-2B·eIF-2(αP)·GDP complex. After the remaining active pool of eIF-2 is utilized, translational inhibition occurs.

The protein P1 kinase/eIF-2 pathway as it relates to

interferon treatment of cells has been reviewed elsewhere (Johnston & Torrence, 1984; Torrence, 1985 and references therein) and will not be discussed further here.

II.A.4. The second messenger: 2-5A and its activation of RNase L

As mentioned above, treatment of cells with IFN results in the synthesis of two new dsRNA dependent proteins, P_1 and 2',5'-oligoadenylate synthetase. 2-5A synthetase then produces 2-5A from the cell's pool of ATP. 2',5'-Oligoadenylates activate a latent endoribonuclease (RNase L) that degrades RNA and contributes to the translational inhibition caused by double-stranded RNA (Kerr & Brown, 1978; Kerr et al., 1974; Lebleu et al., 1976; Sen et al.,1976). This 2-5A mediated degradation of RNA can be seen most dramatically in the 2-5A-dependent degradation of ribosomal RNA (Wreschner et al., 1981a). Studies on the sequence specificity of RNase L (Floyd-Smith et al.,1981; Wreschner et al., 1981b) demonstrated that, regardless of the RNA substrate, specific cleavage occurs at UpN sequences giving rise to oligomers terminating in UpNp.

RNase L has been partially purified from mouse L cells (Schmidt et al., 1978), mouse EAT cells (Slattery et al., 1979; Floyd-Smith et al., 1982) and rabbit reticulocyte lysates (Wreschner et al., 1982; reviewed by Johnston & Torrence, 1984). Floyd-Smith & Lengyel (1986) report a 4,750 fold purification of RNAse L from mouse EAT cells using DEAE cellulose, phosphocellulose, and poly(A)-agarose. Covalent cross-linking of RNase L and pppA2'A2'pA2'pA[^{32}P]pCp has been used to identify 2-5A binding

proteins and to estimate their molecular weight (Wreschner et al., 1982). RNase L purified from mouse EAT cells (Floyd-Smith & Lengyel, 1986) has a molecular weight of 77 kda as estimated by cross-linking techniques (St. Laurent et al., 1983). In crude extracts of several cell types, only one predominant protein of 70-90 kda molecular weight was labeled in cross linking studies. This indicates that RNase L is the only major 2-5A binding protein in the cell.

Regulation of RNase L levels has been reported to vary with IFN treatment, growth rate, and cell differentiation (Jacobsen, et al., 1983a,b). The treatment of JLS-V9R cells with IFN led to a 10-to 20-fold increase in RNase L levels. The extent of RNase L induction in JLS-V9R cells is several times that reported for murine L cells (Cayley et al., 1982), human Daudi (Silverman et al., 1982b) or HeLa cells (Silverman et al., 1982a) and may be the result of very low levels of RNase L in these cells before IFN treatment. Silverman et al. (1983) also reported that RNase L levels changed with the stage of growth of the JLS-V9R cells. Expression of active RNase L was also shown to be greatly enhanced during cell differentiation in F9, PYS and PSA 5E cells by analysis of the extent of rRNA breakdown that followed the introduction of $ppp(A2'p)_nA$ into the intact cells (Krause et al., 1985).

II.A.5. Degradation of 2-5A

The 2-5A cycle is completed by its degradation. Two pathways for 2-5A degradation can be perceived. One involves a phosphodiesterase that degrades 2-5A into pppA2'pA or nucleotides,

and the other involves a phosphatase activity that degrades 2-5A to pA2'pA2'pA, a molecule that can not activate RNase L. Phospho-diesterase activity that cleaves 2-5A to 5'-AMP and 5'-ATP has also been reported to occur in a variety of cultured cells (Williams et al., 1978; Schmidt et al., 1978). Evidence for the phosphatase pathway was revealed in studies by Hearl and Johnston (1984, 1987) who demonstrated the major species of 2-5A recovered from the tissues of mice injected with saline, poly(I)·poly(C), or EMC virus was A2'pA2'(pA)$_n$. The half life of 2-5A in the cell is relatively short and is on the order of 15-30 min (reviewed Johnston & Torrence, 1984). There is some evidence that the phosphodiesterase is slightly induced upon interferon treatment of mouse L cells (Kimchi et al., 1979; Schmidt et al., 1979) and human fibroblasts (Krishnan & Baglioni, 1981), but other researchers have not detected any interferon-mediated change in PDi activity in chick embryo cells (Ball, 1980), mouse L cells (Williams et al., 1978), HeLa cells (Minks et al., 1979; Verhaegen-Lewalle & Content, 1982), human RSa, IF, HEC-1, and WGA cells (Verhaegen-Lewalle & Content, 1982) and Daudi cells (Silverman, et al., 1982).

II.A.6. Summary

The preceding discussion on the mechanism of interferon's antiviral action is summarized in Figure 2. Interferon treatment leads to the production of at least two new proteins, 2-5A synthetase and protein P1 kinase. dsRNA present in the cell as a product of viral replication specifically activates the enzyme. The 2-5A molecule (pppA2'pA2'pA or ppA2'pA2'pA) activates a latent
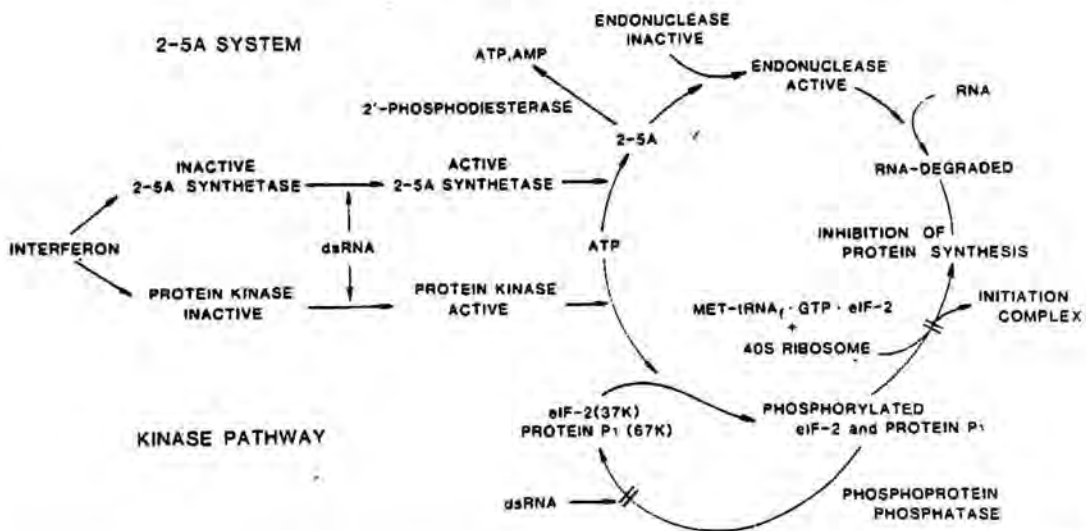
Figure 2. A schematic representation of the key components and actions of the 2-5A system.

endoribonuclease (RNase L) present in most cells regardless of interferon treatment. The activated RNase L then degrades RNA in the cell, including mRNA, leading to an inhibition of protein synthesis. The degradation of reovirus RNA in extracts of IFN-pretreated EAT cells was first demonstrated by Lengyel's group (Brown et al.,1976). The cycle is completed by degradation of the biologically active form of 2-5A to an inactive form by the action of a phosphatase or a phosphodiesterase or both.

II.B.1. The 2-5A molecule: Studies of the 2-5A-RNase L interaction

The unique nature of 2',5'-oligoadenyates stimulated investigation into the structural requirements for its binding to and activation of RNase L. Chemical modification of 2-5A has provided information about the parts of the molecule that are critical for binding or activation of RNase L. Interaction of analogues of 2-5A with RNase L has been followed using three different assay methods (reviewed by Torrence, 1983). The first assay is based on the mouse L cell cell-free protein synthesis system activated with EMC virus RNA (Torrence et al., 1981) and measures the analogue's ability to antagonize or prevent the translation or inhibitory effects of pppA2'pA2'pA. This antagonism results from competition of the modified oligonucleotide with 2-5A for the RNase L binding site and provides a measure of RNase L binding (Knight et al.,1980). In this system, the 2-5A concentration is held constant (at 20 nM) while increasing quantities of the oligomer are added until the inhibition caused by 2-5A is reduced by 50%. The second assay measures activation of the endonuclease

using the same system as above but without the addition of 2-5A. This approach measures the concentration of the analogue needed to effect 50% inhibition of protein synthesis and provides a measure of endonuclease activation. The third approach used to study the binding of analogues to RNase L uses pppA2'pA2'pA2'pA2'pA3'[^{32}P]pC3p as a radiolabeled probe that can be displaced by oligonucleotides that compete for the RNase L binding site (Knight et al.,1980). The concentration of the oligomer needed to prevent 50% of the radioactive probe from binding to RNase L is used to assess its binding to RNase L. New analogues of 2-5A are tested for binding and or activation by one of the above methods.

Recently, a specific and sensitive functional assay for 2-5A has been developed (Silverman, 1985). This assay employed 2-5A core-cellulose to which RNase L was added and mixed on ice to generate a 2-5A core-cellulose-RNase L complex. The cellulose was washed and suspended in an assay mix containing poly(U)-[3'-^{32}P]Cp. Addition of increasing concentrations of trimer and tetramer 2-5A resulted in the activation of RNase L which then degraded the labeled poly(U) to acid soluble fragments. The acid precipitable radioactivity captured on the glass-fiber filters was determined by scintillation counting. The advantage of this assay is that it is a functional assay specific for 2-5A.

II.B.2. Identification of the portions of the 2-5A molecule important in the binding and activation of RNase L.

Inspection of the structure of 2-5A in Figure 1 reveals a molecule that can be chemically modified in a number of positions. Indeed, analogues of 2-5A have been made by modifying the number of

5'-phosphate groups, the heterocyclic bases, phosphodiester linkages, or the ribose 2'- and 3'-hydroxyls. The effect of chain length has also been investigated. Assaying these analogues for binding or activation of RNase L provides a great deal of information about the parts of 2-5A important for this interaction. The results of these studies are summarized below.

II.B.2.a. 5'-Terminal Phosphate Isomers

The number of 5'-phosphates was shown to be important in determining the biological activity of 2-5A. Trimer 5'-triphosphate, pppA2'pA2'pA, and trimer 5'-diphosphate, ppA2'pA2'pA, bind and activate RNase L. Trimer 5'-monophosphate, pA2'pA2'pA, binds the endonuclease without activating the enzyme, but is capable of antagonizing the inhibition of protein synthesis by pppA2'pA2'pA. Trimer core, A2'pA2'pA, neither binds nor activates RNase L efficiently (Kerr & Brown, 1978; Torrence et al., 1981). However, trimer core at high concentrations has been implicated in the inhibition of DNA and RNA synthesis (Kimchi et al., 1981a,b). The mechanism of core action remains unknown.

II.B.2.b. Chain length isomers

As discussed above, no unphosphorylated oligomer is as active as the corresponding 5'-monophosphate in its ability to antagonize the binding of pppA2'pA2'pA to RNase L. For example, trimer core, A2'pA2'pA, is 100-fold less active than pA2'pA2'pA but tetramer and pentamer cores, A2'pA2'pA2'pA2' and A2'pA2'pA2'pA2'pA, are only 10-fold less active than their respective 5'-monophosphates

(Torrence, et al.,1982). The increase in antagonism of the tetramer and pentamer cores may be due to longer chain length. The longer cores contain the minimum structure ...pA2'pA2'pA and may be able to slip into the nuclease binding site. The same study shows that addition of adenosine nucleotides to pA2'pA2'pA to give pA2'pA2'pA2'pA and pA2'pA2'pA2'pA2'pA does not change activity indicating that chain length does not effect activity of 5'-monophosphorylated 2-5A's. Finally, at least three adenosine nucleotides are required for maximal activity. Dimer monophosphate, pA2'pA, is 100-times less active that pA2'pA2'pA (Torrence et al.,1983). However, removal of adenosine from the 2'-terminus of pA2'pA2'pA to give pA2'pA2'p results in a compound 5-fold less antagonistic than pA2'pA2'pA. This result may be due to increased resistance of pA2'pA2'p to degradation, or it may reflect the fact that the 2'-terminal nucleoside of pA2'pA2'pA is not required for binding RNase L.

II.B.2.c.. Phosphodiester Linkage Isomers

The importance of the 2',5'-phosphodiester backbone of 2-5A is demonstrated by analysis of the linkage isomers pA2'pA3'pA and pA3'pA2'pA. Replacing a single 2',5'-linkage with a 3',5'-linkage produces a 20- to 50-fold decrease in activity (Lesiak et al., 1983). If both 2',5' bonds are replaced with 3',5' bonds (i.e. 3-5A), activity decreases by a factor of 10^5.

Chemical synthesis of a 2',5'-phosphorothioate trimer and tetramer produced analogue structures that inhibit protein synthesis better and are more stable in cell-free extracts than authentic

pppA2'pA2'pA (Lee & Suhadolnik, 1985). In the assay for biological activity, seventy percent displacement of the radiolabeled probe, pppA2'pA2'pA2'A[^{32}P]pCp, is achieved with 2 nM tetramer phosphoro-thioate analogue or with to 10 nM authentic pppA2'pA2'pA2'pA. These analogues are more stable in cell free extracts than authentic 2-5A's presumably due to their increased resistance to PDi. After 60 minutes in an interferon-treated HeLa cell extract, 45% of the phosphorothioate analogues remain while only 5% of authentic 2-5A's are recovered.

2-5A's unique phosphodiester backbone is essential to provide the correct stereochemical fit of 2-5A and RNase L. Substitution of the diester oxygens for sulphur increases activity probably due to increased stability to phosphodiesterase.

II.B.2.d. Modifications of the ribose moiety of 2-5A

Replacement of all three 3'-hydroxyls of pA2'pA2'pA with hydrogens gives a cordycepin analogue of 2-5A that is much less active as a protein synthesis inhibitor than 2-5A itself (Sawai et al., 1983; Haugh et al.,1983). This analogue has low binding affinity for RNase L and does not activate it efficiently.

Modification of the 2'-ribose of 2-5A by periodate oxidation opens the 2'-terminal cis-diol to a dialdehyde that can be reacted with n-hexylamine and reduced with sodium cyanoborohydride to form a n-hexylmorpholine derivative (Imai et al., 1982). This analogue is ten times more active than 2-5A in a cell-free translation system due to its increased resistance to degradation. Also, when injected into HeLa cells infected with Mengo virus, this "tailed" compound is

at least ten fold more active than authentic 2-5A (DeFilippi et al., 1985).

II.B.2.e. Modifications to the heterocyclic bases of 2-5A.

Modification of the base moieties of 2-5A includes replacement or modification of the adenine rings. The bases of 2-5A have been modified in a systematic manner to identify the positions of the base critical for binding or activation of RNase L. When the adenine rings of 2-5A are replaced by pyrimidine rings (Sawai et al.,1981) or hypoxanthine (Sawai et al.,1981) or have a third ring added (etheno analogues) between the N1 and amino nitrogens of adenine (Lesiak et al.,1983), a dramatic loss of biological activity occurs.

Further insight into the requirement for biological activity is demonstrated by the synthesis of analogues where one adenosine is replaced by inosine to give pppI2'pA2'pA, pppA2'Ip2'pA, and pppA2'pA2'pI (Imai & Torrence 1985; Torrence et al.,1984). Replacement of the first base with inosine results in an analogue which is 200 times less active than 2-5A in its ability to bind RNase L. Replacement of the middle base with inosine results in a 2 to 3-fold decrease in binding and a 20-fold decrease in activation of RNase L. When the third base of 2-5A is replaced with inosine, a 1000-fold decrease in RNase L activation but virtually no decrease in binding RNase L is observed. These studies demonstrate the following: 1. The 5'-terminal N6 amino group of adenosine interacts with RNase L and is required for optimal binding. 2. The 3'-terminal amino group of adenosine interacts with RNase L and is

critical for activation. 3. The middle N6 amino group of adenosine in 2-5A does not appear to be critical to binding or activation of RNase L (Imai et al., 1985). A similar study was conducted on the 7-deazaadenosine (tubercidin) analogue of 2-5A (Jamoule et al., 1984). The only analogue that retained the ability to activate RNase L was the one in which the middle base was substituted to give $pppA2'p(c^7A)2'pA$. This study confirms the critical nature of the first and third base residues (in 2-5A) for binding and activation of RNase L. The middle nucleotide residue seems to play only a minor role in this process.

Perhaps the most interesting of all the base analogues are the 8-Br substituted 2-5A's. An analogue brominated at the C8 position of adenine, $pA2'pA^{8Br}2'pA^{8Br}$, displayed unexpected biological activity. This 5'-monophosphate shows 8% of the inhibitory activity of 2-5A itself or about 13% of the activity of its parent compound, $pppA2'pA^{8Br}2'pA^{8Br}$ (Torrence et al., 1985; Torrence & Lesiak, 1986; Torrence et al.,1987). This unexpected result demonstrates that biological activity does not always require a 5'-terminal di- or triphosphate and implies that the biological activity of different 2',5'-oligoadenylates may be dictated by a structural feature other than the number of 5'-terminal phosphates.

In summary, efficient binding to RNase L requires the N6 amino group of the 5'-terminal adenine (Torrence et al., 1984; Imai & Torrence, 1985; Imai et al., 1985), and two 2',5'-phosphodiester bonds (Lesiak et al., 1983). Activation of RNase L requires the N6 amino group of the 2'-terminal adenine (Torrence et al., 1984; Imai & Torrence, 1985; Imai et al., 1985) and the 3'-OH of the ribose

ring (Sawai et al., 1983; Haugh et al., 1983).

II.C.1. Raman Spectroscopy, Historical Perspectives

While investigating the scattering of light in liquids, C. V. Raman made a discovery that has proved to be of great importance for the investigation of molecular structure (Raman & Krishman, 1928). Raman noted that when a substance is irradiated with light of a certain frequency, the scattered beam contains not only light of the same frequency, Rayleigh scattering, but also lines with slightly lower frequencies, Stokes lines, and slightly higher frequencies, anti-Stokes lines. Raman made a through study of these shifted spectral lines with sunlight focused through several lenses to generate an intense beam of light. He was awarded the Nobel prize in 1930 as a result of his efforts.

Raman spectroscopy is frequently referred to as Raman scattering because it is a light scattering phenomenon. Scattered light can be broken down into an elastic component (Rayleigh scattering) and an inelastic component. Raman scattering results from the inelastic collision of an incident photon with a molecule which is either in its ground or excited energy state. In contrast to phosphorescence or fluorescence, the Raman effect does not require the incident light to be coincident with an absorption band because the photon is never entirely absorbed. Instead, the molecule is perturbed into a "virtual" state that induces a vibrational translation. Thus, any wavelength of light may be used to study the Raman effect.

Raman scattering is affected by the polarizability of the

molecule and the dipole moment induced or distorted by the electric field of the incident radiation (Wilson et al., 1980). The selection rules for a vibrational Raman spectrum depend on whether the polarizability changes when the molecule vibrates. If it does, then the vibration is Raman active. For example, suppose that a molecule is irradiated with light of frequency v. The polarizability, α, depends upon one of the normal-mode displacements Q_i with frequency v_i then

$$\mu = \alpha\xi$$

Substituting

$$\alpha = \alpha_0 + \alpha_i Q_i$$

$$Q_i = Q_{io} \cos(2\pi v_i t)$$

$$\xi = \xi_0 \cos(2\pi v t)$$

where $\alpha_i' = (d\alpha/dQ_i)_{Qi=0}$. The induced dipole moment is now given by

$$\mu = (\alpha + \alpha_i Q_i)\xi$$

Substituting for Q_i and E

$$\mu = \alpha_0 + \alpha_i [Q_{io} \cos(2\pi v_i t)]\xi_0 \cos(2\pi v t)$$

and multiplying

$$\mu = \alpha_0 \xi_0 \cos(2\pi v t) + \alpha_i Q_{io}\xi_0 \cos(2\pi v t) \cos(2\pi v_i t)$$

Applying the trigonometric identity

$$\cos(\alpha + \beta) = \cos\alpha \cos\beta + \sin\alpha \sin\beta$$

one obtains

$$\mu = \alpha_0 \xi_0 \cos(2\pi v t) + 1/2 \ \alpha_i Q_{io}\xi_0 \cos[2\pi(v-v_i)t]$$
$$+ 1/2\alpha_i \ Q_{io}\xi_0 \cos[2\pi(v+v_i)t]$$

From the equation above, the scattered light has three frequencies at which the induced dipole moment oscillates, v, $v - v_i$, and $v + v_i$

(Figure 3). These are the Rayleigh, Stokes, and anti-Stokes lines, respectively. Raman scattering is observed with frequency shifts corresponding to the frequencies of each normal mode Q_i for which α_i is not zero. These normal modes are said to be Raman active.

The vibrational selection rules of the Raman effect are based upon symmetry considerations. That is, if the structure of the molecule were known, a thorough application of normal mode vibrational analysis could be used to determine the number of fundamental vibrational frequencies as well as the entire Raman spectrum (Cotton, 1971). The vibrations of common groups of atoms or functional groups are relatively independent of the rest of the molecule and vibrate within a specific range of frequencies. This group frequency approach is often used to fingerprint experimental spectra against compounds of known structure. If two separate structures are proposed for an unknown compound then one could calculate a different Raman spectrum for each structure. A comparison of the calculated Raman spectra with the experimental Raman spectrum would then tend to support one proposed structure over the other.

II.C.2. Raman Spectroscopy of Nucleic Acids

Classical Raman spectroscopy has numerous advantages when compared to other techniques. Raman spectroscopy results in minimal or no damage to the sample. Relatively little interference from water bands is observed in the Raman spectrum. Sample volumes as low as 1-5 uL can be scanned. The vibrational information obtained is representative of specific conformations. Raman spectra of the

$$\begin{array}{ccc} | & | & | \\ \nu - \nu_i & \nu & \nu + \nu_i \\ \text{Stokes} & \text{Rayleigh} & \text{anti-Stokes} \end{array}$$
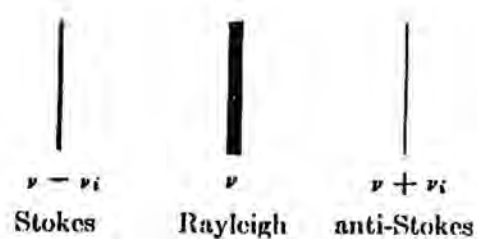
Figure 3. The Rayleigh and Raman lines in the radiation scattered from a substance with a single Raman-active vibration of frequency ν_i.

same sample in different forms, i.e. crystal, fiber, or solution, can be compared. Thus, the conformation in solution can be compared with the crystal structure obtained from x-ray diffraction studies. Disadvantages of visible, non-resonance Raman method are: the potential to destroy sample in the laser beam if high power or high energy light is being used, the need for relatively concentrated samples of 10-100 mg/mL, and fluorescense from impurities. Some samples require 3-4 hours in the light path before fluorescence decreases to a level where high quality Raman spectra can be obtained.

The Raman spectra of nucleic acids arise from vibrations of two parts of the of the molecule between which there is little vibrational coupling. Figure 4 shows the primary backbone and base structure of RNA. One set of vibrations originates from the symmetric vibrations of the ribonucleic acid bases and from the furanose-phosphate backbone. Many of the base bands are Raman active and produce strong bands that provide valuable information concerning base stacking interactions and interbase hydrogen bonding (reviewed by Peticolas et al, 1987).

Conformation-dependent alterations in the base bands in the Raman spectrum are of two general types: 1. an increase or decrease in the band intensity without a change in frequency (Tomlinson & Peticolas, 1970; Peticolas, 1970; Small & Peticolas, 1971a; Small & Peticolas, 1971b), and 2. an increase or decrease in band intensity accompanied by a shift in frequency. Type 1 changes are observed in helical nucleic acids and result in a decrease in band intensity upon helix formation. This effect is termed Raman hypochromism and
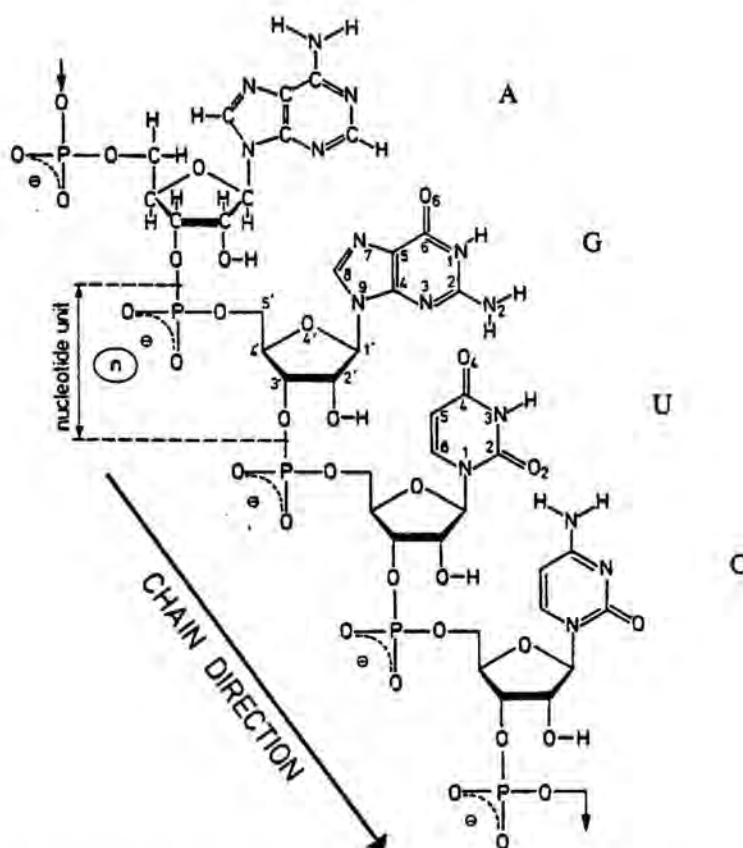
Figure 4. A fragment of a hypothetical RNA chain. The sequence of the fragment along the defined chain direction from the 5' to 3' end is: adenosine (A), guanosine (G), uracil (U), and cytosine (C). The nucleotide units are linked together by a 3',5'-phosphodiester linkage. An atom numbering scheme is indicated for the adenosine and uracil units.

reveals the presence or absence of base stacking in a compound of interest. For example, when poly(A)·ploy(U) is heated from 15° to 80° C there is a 2.5-fold increase in intensity of the uracil band at 1236 cm^{-1} and a 1.6-fold increase in intensity of the adenine band at 730 cm^{-1} (Small & Peticolas, 1971b). This is direct evidence of extensive base stacking in poly(A)·poly(U). Type 2 changes reveal information, in 600-700 cm^{-1} region of the spectrum, concerning the conformation of the furanose backbone of certain purine containing compounds. For example, the alternating copolymer poly(dG-dC) undergoes a conformational change from B DNA to Z DNA when the salt concentration is increased from 0.15M to 4 M. When this change in conformation occurs, a guanine band shifts in frequency from 680 cm^{-1} to 625 cm^{-1} (Nishimura et al.,1983; Benevedies et al., 1983; reviewed by Peticolas et al.,1987). Raman spectra representing this A to Z transition are shown in Figure 5.

Conformation-sensitive changes in the furanose-backbone-associated bands of the Raman spectrum of DNA and RNA are quite different from the changes associated with nitrogenous base bands discussed above. These bands contain information about the overall orientation of the entire phosphodiester backbone and will henceforth be referred to as furanose-phosphodiester modes. The position of these Raman bands is strongly dependent on the torsional angle delta about the C5'-C4'-C3'-O3' bond (Figure 6) (Lu et al., 1977; Brown & Peticolas, 1975). This, in turn, defines the pucker of the furanose ring expressed as the pseudorotation phase angle, P (Levitt & Warshel, 1978) (Figure 7). Inspection of Figure 7 reveals minima in the potential energy contours in two general areas of the
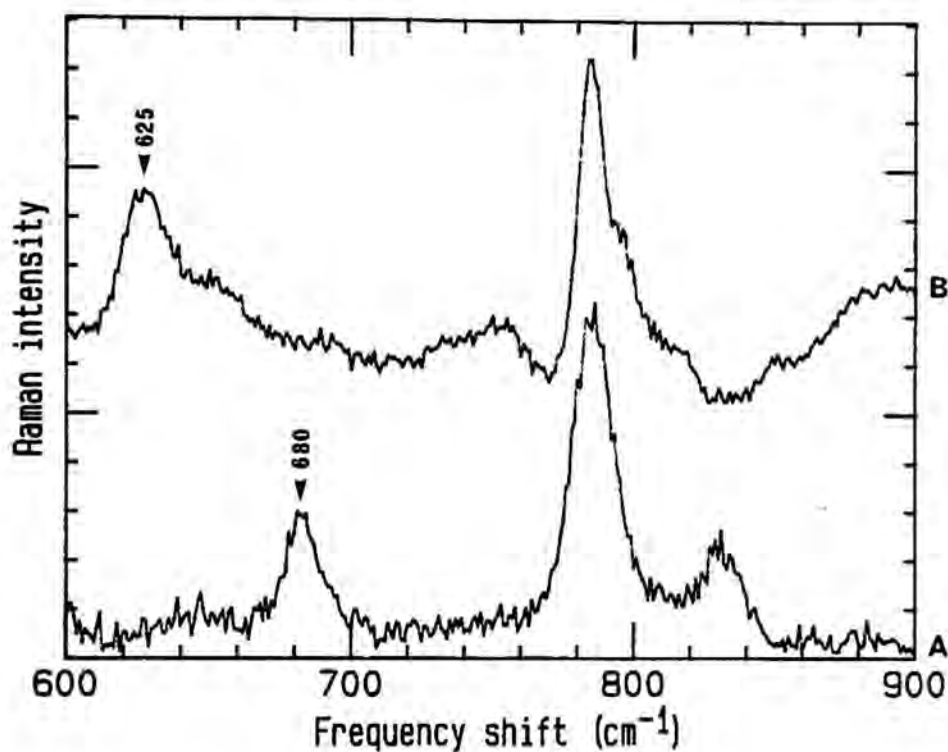
Figure 5. Characterization of the right-handed B and left-handed Z forms of the polymer poly(dG–dC)·poly(dG–dC). Spectrum A corresponds to the B form of the polymer in 0.1 M NaCl. Spectrum B corresponds to the left-handed Z from of poly(dG–dC)·poly(dG–dC) in 4 M NaCl.

a)

BASE

C5'

C1'—O

δ
150°

O3'
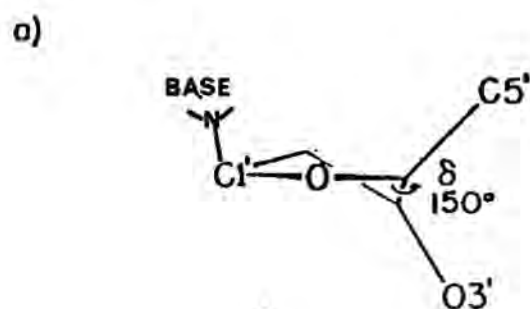
Figure 6. Furanose torsion angle δ. Angle δ directly affects furanose conformation which in turn affects the position of the furanose backbone bands in the Raman spectrum of nucleic acids.
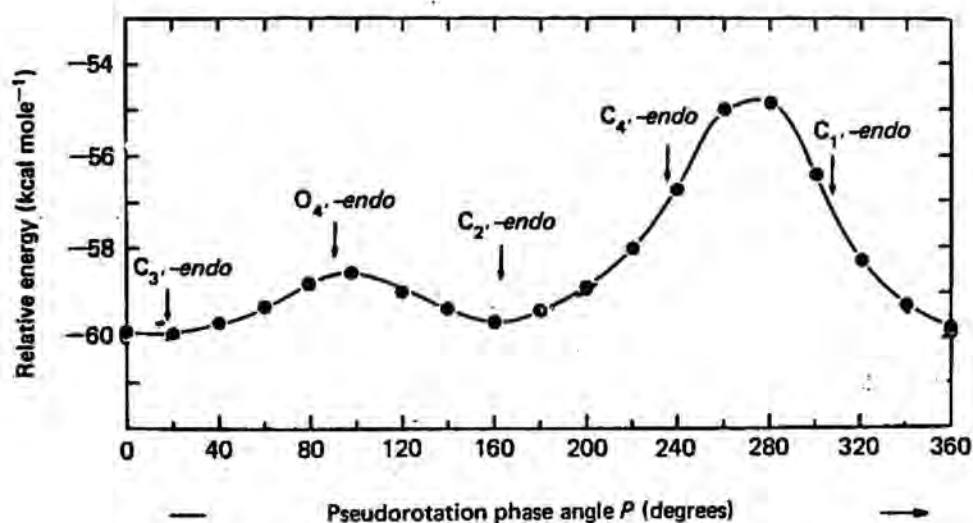
Figure 7. Variation of total energy of furanose conformations with pseudorotation phase angle P. Adapted from Levitt & Warshel (1978).

pseudorotational phase angle. The one near $P = 0 - 10°$ corresponds to the C3'-endo ring pucker and is found in A-genus nucleic acids (dsRNA and A DNA). This family of nucleic acids has a strong, sharp Raman band around 807-814 cm^{-1}. The second minimum is near $P = 160°$ and corresponds to the C2'-endo ring pucker. The C2'-endo furanose ring pucker is found in the classic model of B-genus DNA and a band at 835 cm^{-1} is observed in the Raman spectrum of DNA fibers at high relative humidity. Thus, even though the 807-814 cm^{-1} and 835 cm^{-1} bands arise from and are assigned to the antisymmetric O-P-O stretching vibration, they are closely associated with the conformation of the furanose ring.

The complexity of Raman spectra has necessitated an empirical approach to the assignment Raman bands to specific molecular groups and conformations. Studies on model compounds (Lord & Thomas, 1967; Thomas & Kyogoku, 1977; Nishimuria et al., 1978, 1984) and on DNA fibers and crystals (Erfurth et al., 1975; Thomas & Peticolas, 1983a,b; Martin & Wartell, 1982; Thomas et al., 1984) have been of great value in establishing the assignments of DNA and RNA bands. A summary of some important Raman bands of nucleic acids that are sensitive to conformation is presented in Table 1 (see Peticolas et al., 1987 for a complete review of this subject).

Since the position and intensity of Raman bands are sensitive to conformational interactions they can be used to study protein-nucleic acid binding reactions. Ligand-DNA (Manfait et al., 1982) and protein-cofactor (Yue et al., 1984) binding complexes have

TABLE I. Important Raman Bands of Nucleic Acid Components that are Sensitive to Conformation.

Frequency shift (cm^{-1})

1100	PO_2 symmetric stretch
805–815	C3'-endo ester linkage marker for furanose-phosphate chain mode in A-genus nucleic acids
835	C2'-endo ester linkage marker for furanose-phosphate chain mode in B-genus nucleic acids
682	Guanine ring breathing mode marker for C2'-endo-anti furanose-phosphate chain mode in B DNA
665	Guanine ring breathing mode marker for C3'-endo-anti furanose-phosphate chain mode in A DNA
625	Guanine ring breathing mode marker for C3'-endo-syn furanose-phosphate chain mode in A DNA
1260	Weak cytosine band in B-DNA
1265	Strong cytosine band in Z-DNA
1318	Moderate guanine band in B-DNA
1318	Very strong cytosine band in Z-DNA
1334	Moderate guanine band in B-DNA
1355	Moderate guanine band in Z-DNA
1362	Moderate guanine band in B-DNA
1418	Weak guanine band in Z-DNA
1420	Moderate guanine band in B-DNA
1426	Weak guanine band in Z-DNA

been evaluated using Raman difference spectra. Difference spectra provide information concerning which part of the ligand or cofactor interacts with the DNA or protein. For example, Yue et al. (1984) obtained the Raman spectrum of liver alcohol dehydrogenase (EC 1.1.1.1) (LADH)-NADH complex. First they obtained the spectrum of free LADH in the absence of its cofactor, NADH. Next they obtained the Raman spectrum of free NADH. Finally, they obtained the Raman spectrum of LADH with NADH bound in a 1:2 molar ratio where no excess NADH was believed to be present. The spectrum of free LADH was then subtracted from the spectrum of LADH + NADH. The result of this subtraction was the spectrum of bound NADH. Comparison of the bound NADH with the free NADH spectrum revealed significant changes in the Raman spectrum of NADH upon binding to LADH. From these changes, it was shown that both the adenine and the nicotinamide moieties of NADH were involved in binding to LADH. The $-NH_2$ groups of NADH were also shown to participate in binding to LADH but it was not possible to determine whether one or both $-NH_2$ groups were involved. Such direct evidence of binding interactions is difficult to obtain by other methods.

III. Research Goals

The goals of this research were three-fold. First, I sought to determine how the Raman spectrum of 2-5A was different from that of 3-5A. During the course of these studies each spectrum was studied for clues to why 2-5A is biologically active and 3-5A is not. This comparative study necessitated that each peak in the Raman spectrum be assigned to a particular portion of the molecule.

Work with model compounds enabled me to assign each major band in the Raman spectrum and led to the pH, temperature, and 2-5 vs 3-5 comparative study. Second, I sought to determine why different isomers of 2-5A differed in their biological activities. More specifically, why does pppA2'pA2'pA bind and activate RNase L while pA2'pA2'pA binds but does not activate RNase L? Is this difference in activity a result of the conformation of the molecule, or is it merely due to the triphosphate moiety, or do both contribute? These questions led to studies of the Raman spectra of several oligomers containing 2',5'-linkages. Oligonucleotides of different chain length, phosphodiester linkages, and 5'-terminal phosphorylation were examined. Third and perhaps the most ambitious, I sought to determine areas of the 2-5A molecule involved in binding to the monoclonal antibody 3AC9. I hoped that these model studies would provide more basic knowledge about the nature of the binding of 2-5A's to proteins. In addition, these studies would be valuable to those interested in the design and synthesis of analogues of 2-5A as potential chemotherapeutic agents. Raman spectroscopy is suited to studies of protein-nucleic acid binding reactions because it can provide information on the portions of the ligand involved in direct interaction with the protein.

IV. MATERIALS and METHODS

RAMAN STUDIES

Commercial 2',5'-linked trimer core, A2'pA2'pA, trimer 5'-monophosphate, pA2'pA2'pA, and trimer 5'-triphosphate, pppA2'pA2'pA (ammonium salts) were purchased from Pharmacia Chemical

Company (Piscataway, NJ). Synthetic 2',5'-linked trimer core and trimer 5'-monophosphate (sodium salt) were generously supplied by Dr. Paul F. Torrence (NIH). Adenosine (Sigma grade), AMP (Sigma grade), and ATP (Sigma grade), were purchased from Sigma Chemical Company (St. Louis, MO). All samples were dissolved in distilled water or in buffer containing 150 mM NaCl, 10 mM HEPES, pH 7.4. Sample concentration was estimated spectroscopically and ranged from 10-100mM. Raman experiments were carried out at 15° C except where noted otherwise. The temperature of the brass sample holder was maintained by a thermostatically controlled circulating water bath.

The Raman instrument consisted of a Coherent Innova 90 argon ion laser source operating at 514.5 nm with typically 250 mw of light power at the sample, a thermostatted brass sample holder, a 300mm focal length f 0.6 aspheric lens for light collection optics, a Spex 1403 double monochrometer with 1800 grooves/mm holographic gratings, an RCA 31034 PMT, and a Spex Datamate coupled to a Cromemco Z80 based microcomputer. Spectral bandpass was set to 6 cm-1. Data was collected at 1 cm-1 intervals at a scan rate of 1 cm-1/sec. About 15 scans were collected for each spectrum with a 2 sec per cm-1 integration time. Samples of approximately 5 microliters were held in melting point capillary tubes.

Spectra containing significant noise were smoothed using the algorithm of Savitsky & Golay (1967). Water and solvent background peaks were subtracted from spectra to satisfy two criteria. The spectrum between 1730 and 1800 cm^{-1} must be linear or free of curvature, and a linear extrapolation of this region must intersect close to baseline at 1160 to 1180 cm^{-1} (Williams, 1983).

When the nucleic acid sample was very fluorescent the spectrum of the fluorescence band could introduce considerable curvature to the baseline of the Raman spectrum (Figure 8). When this happened it became impossible to satisfy the water subtraction criteria above and a graphical solution was used. In this procedure, the fluorescence band curvature was removed by drawing a line to fit the fluorescence band (Figure 9) using a cubic spline program. After the band due to fluorescence was corrected, the spectrum of water/buffer was subtracted to meet the two criteria above (Figure 10).

A computer generated spectrum of triethyl ammonium ion (TEA) was generated using the same data handling programs used for water/buffer subtraction. First, the spectrum of triethyl ammonium bicarbonate (TEAB), pH 7.4, was obtained. Second, the spectrum of ammonium bicarbonate, pH 7.4, was obtained. Third, the spectrum of ammonium bicarbonate was subtracted from the spectrum of TEAB to generate the spectrum of TEA (Figure 11). The spectrum of TEA obtained in this manner was used to correct the spectrum of NIH pA2'pA2'pA.

To ensure that samples were pure and were not degraded by the laser beam, or by changes in pH, or by high temperatures employed in temperature experiments, samples were analyzed using C-18 reverse phase HPLC. Less than one microliter of sample was removed from each melting point capillary before and after scanning and diluted approximately 20-fold for analysis. The HPLC system consisted of a Waters model 730 data module, a Waters model 720 system controller, a Waters model 710B WISP, 2 Waters model 510
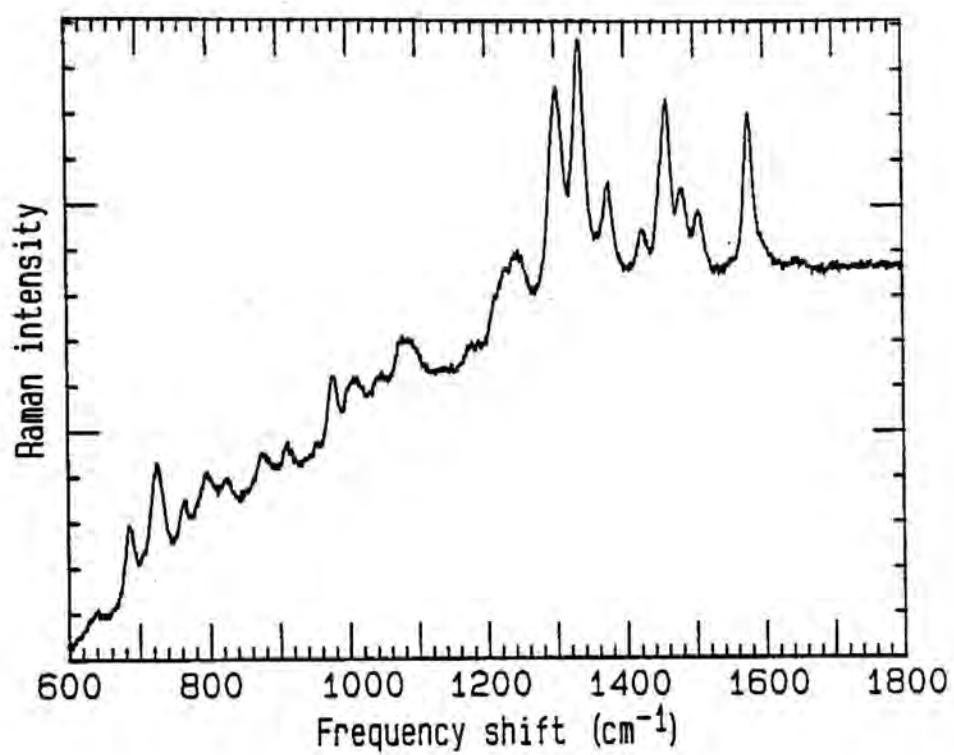
Figure 8. Raw data showing the fluorescence band in the spectrum of pA2'p(8BrA)2'pA.
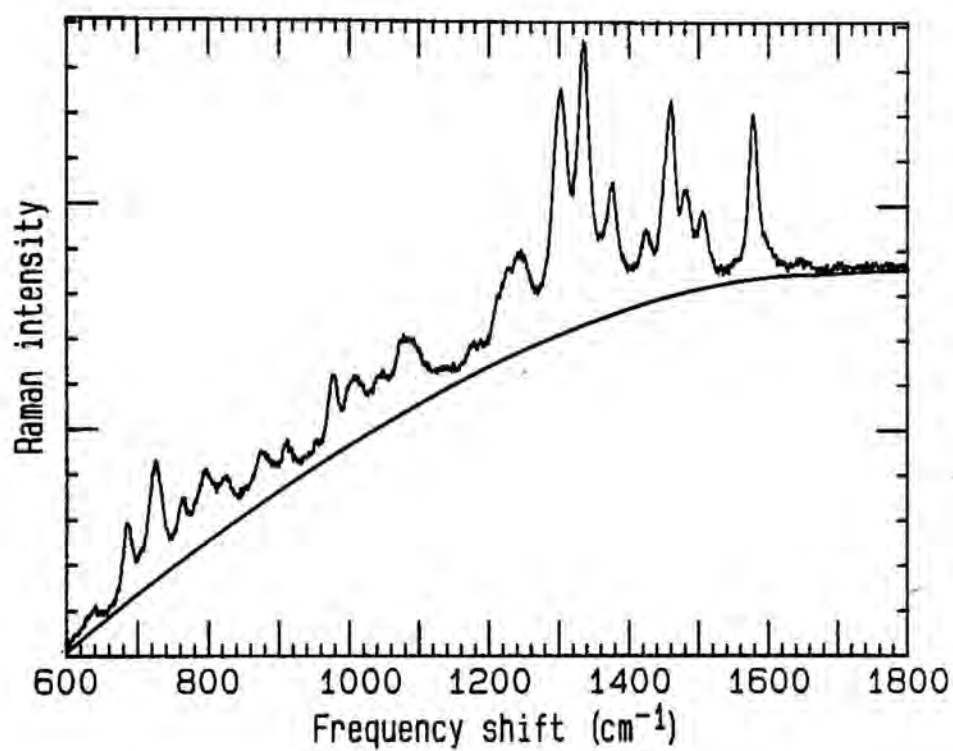
Figure 9. The spectrum from Figure 8 with the hand drawn line which was used to correct the baseline due to fluorescence.
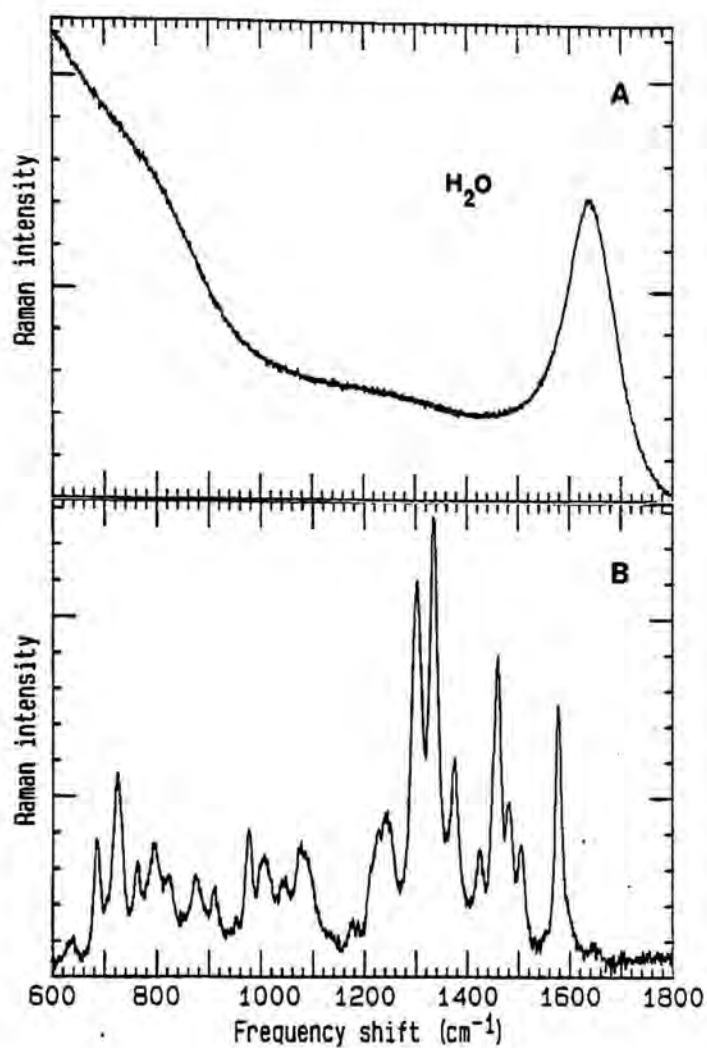
Figure 10. Corrected Raman spectrum of pA2'p(8BrA)2'pA. (a) Raman spectrum of water. (b) Raman spectrum of pA2'p(8BrA)2'pA with water subtracted.
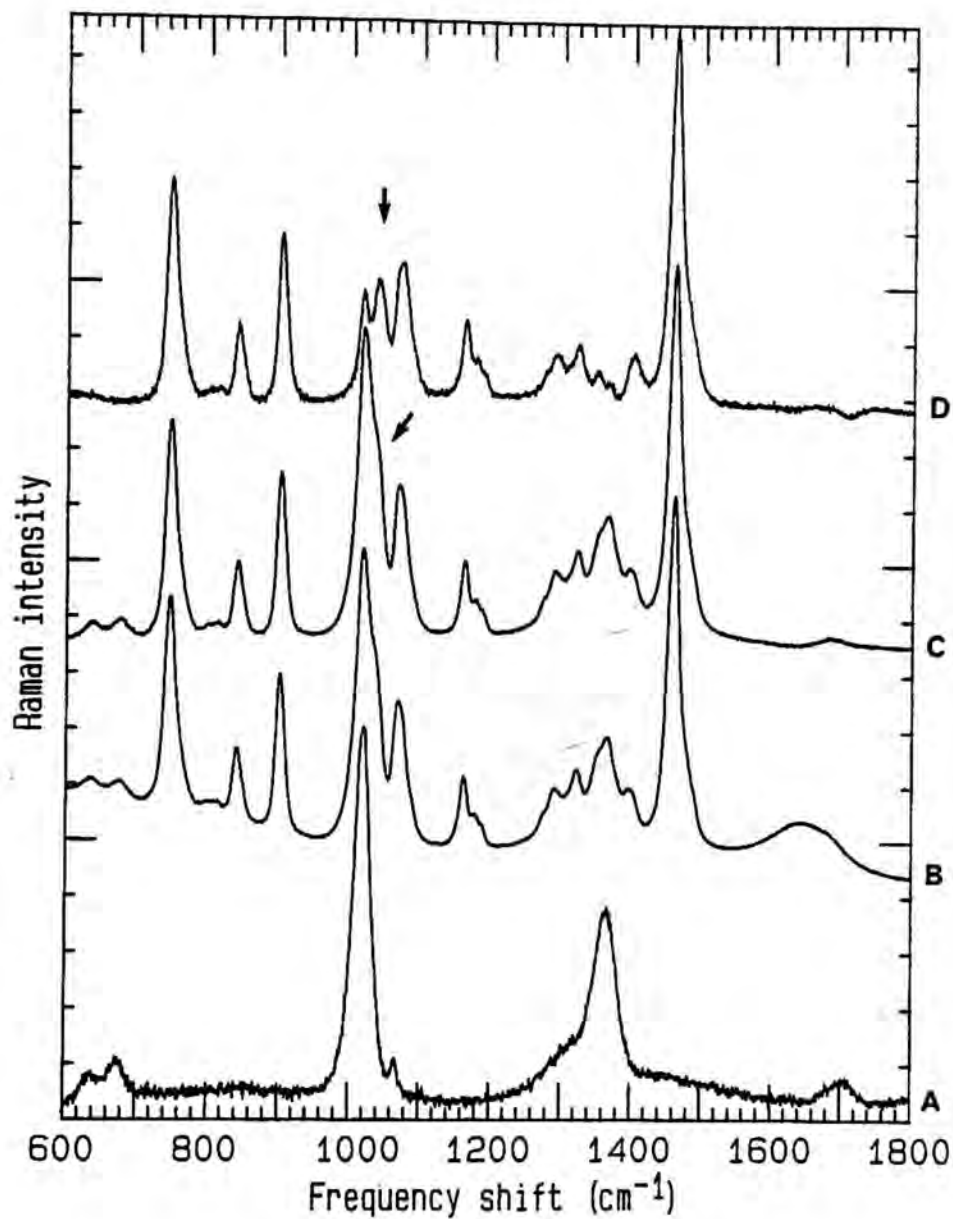
Figure 11. Computer generation of the Raman spectrum of triethyl ammonium ion. (b) Spectrum of TEAB, pH 7.4. (a) Spectrum of ammonium bicarbonate, pH 7,4. (c) Spectrum of TEAB – water. (d) Spectrum of TEAB – ammonium bicarbonate.

solvent delivery systems, and a Kratos model 769 variable wavelength
detector. Buffer A was 50 mM ammonium acetate, pH5.2, and buffer B
was 25% acetonitrile. The flow rate was 1 mL/minute. The column
was a Waters mBONDAPACK C-18 3.0 mm x 30 cm stainless steel column.
The gradient was programed as follows: 0-5 minutes, 100% A, 5-25
minutes, shallow exponential gradient (curve 07) to 25% B, and
25-35minutes, steeper exponential gradient (curve 08) to 100% B.
Absorbance was monitored at 259 mm. Average retention times in
minutes were as follows: pppA2'pA2'pA, 27.2, ppA2'pA2'pA, 24.0,
pA2'pA2'pA, 24.2, A2'pA2'pA, 35.6,A2'pA, 34.4, AMP, 9.2, adenosine,
29.9.

Sample pH was measured by insertion of a specially
constructed combination pH electrode, measuring 0.9 mm (diameter) by
6.0 cm (length) (Microelectrodes, Inc., Londonderry, NH), into the
melting point capillary. Accurate pH measurements were made on
volumes as low as two microliters and were done in duplicate. There
was no significant difference in the pH of a 5 υL sample, determined
as described above, and the pH of 1 mL of the same sample measured
in a test tube. Sample pH was changed by delivering less than 1 υL
of ice cold 0.1 N KOH to the inside of the capillary with the tip of
the pH electrode. The electrode and sample were kept on ice to
minimize possible base-mediated degradation. This procedure changed
the pH by about 0.5 units per addition step without degrading the
sample. The ionized 980 cm-1 and protonated 1095 cm-1 phosphate
peak heights were measured after each spectrum was normalized to the
729 cm-1 band of adenine using data handling programs described by
Williams(1983).

Samples scanned in D20 were lyophilized and reconstituted on ice with D20 from Sigma Chemical Company (St. Louis, MO). The sample was immediately transferred to the thermostated 15°C brass sample holder for Raman analysis.

Monoclonal Antibody Purification

Starting material was murine ascites fliud diluted 1:3 in PBS, pH 7.4. Ascites fluid was dialyzed into 20 mM Tris pH 8.5 and filtered through a 0.22 micron filter before application to a DEAE-5PW column which was used to separate monoclonal antibody from two major contaminating proteins of ascites, transferrin and albumin. Each fraction from the DEAE-5PW column was checked for immunoreactivity using an ELISA assay (Johnston et al., 1985). The immunoreactive fractions were applied to a Pharmacia Mono-P chromatofocusing column to remove the remaining transferrin from monoclonal antibody. Ampholytes introduced by chromatofocusing were removed by a gel filtration step using Pharmacia 6+12 columns in tandem. The tandem arrangement of these columns was used to accommodate the large protein load.

DEAE-5PW: The Waters HPLC system described above was used to elute monoclonal antibody from a DEAE-5PW column. The DEAE-5PW column measured 12 cm x .75 cm and was purchased from LKB, Rockville MD. The flow rate was 1.0 mL/min and 1.0 minute fractions were collected. Buffer A was 20 mM Tris·HCL pH 8.0. Buffer B was 0.250 M NaCl in 20 mM Tris pH 7.0. A 40 minute linear gradient was run. The monoclonal antibody eluted between transferrin at 20 minutes and albumin at 38 minutes, but its position was strongly dependent upon

the salt concentration of the starting material. The column was cleaned after each run by injecting 1.0 mL of 1.0M NaCl followed by a blank gradient. 20-50 mg of protein in 5.0 mL of starting buffer was loaded onto the column prior to elution.

Mono-P: An LKB HPLC system was used to elute the antibody from a Pharmacia HPLC Mono-P column (Pharmacia Chemicals AB, Sweden). Chart speed was 1.0 mm/min. Flow rate was 1.0 ml/min. Pressure was 32-38 bar. Typically, pooled DEAE fractions (5.0 ml) were diluted 1:3 in starting buffer and applied to the column. The column was washed with 3.0 ml of elution buffer. Starting buffer was 0.025 M bis-Tris, pH 6.4. Elution buffer was Polybuffer 74, pH 5.0. Both buffers were adjusted to the correct pH with HCL. The column was eluted with 40 mLs Polybuffer 74. These conditions produced a pH gradient from 6.0 to 5.0. The antibody eluted at 25-28 minutes. The column was cleaned after each application by injecting 1.0 mL of 2.0 M bis-Tris.

Superose 6 + 12: The same LKB HPLC system was used to exchange the purified antibody into 0.15 M NaCl for storage at -20° C. The sample was concentrated to a volume of 200 microliters using a Centricon filter centrifuged at 5000 RPM for 1 hour followed by a 4 minute centrifugation at 3000 RPM to deposit the sample in a collection vial. Concentrated antibody was applied to the two columns in series. The Superose 12 was placed in line first since it can withstand higher pressures than the Superose 6 column. The column was standardized with a protein mixture of ferritin,

aldolase, ovalbumin, and cytochrome C, each at a concentration of 4.0 mg/ml. It is important to have a component with color in the standard mix in order to observe the sample's introduction and band width on the column. The standard (50 νL) was injected at a sensitivity of 0.1 AUFS. Flow rate was dictated by pressure limit of the Superose packing material. These columns in tandem should never exceed 30 bar. Typical running pressure was 19 to 26 bar.

ELISA assay: Immunoreactive fractions were identified using ELISA assays developed previously (Johnston et al., 1985). Microtiter plates (Dynatech, Alexandria, VA) were coated with 0.02 νg/mL Ficoll-pA$_3$. The antibody was diluted 1:10^6 in PBS supplemented with 0.1% ovalbumin and 0.5% Tween 20 added to the wells, and incubated at 30° C for 30 minutes. Plates were washed three times with PBS-Tween 20. Peroxidase-labeled anti-mouse IgG was diluted 1:100, added to each well, and incubated at 30° C for 45 minutes. Plates were washed three times in PBS + Tween and ABTS/H$_2$O$_2$ substrate was added. The plate absorbance was obtained at 414 nm at 5 and 10 minutes.

Growth of ascites: Typically, CD2F1 mice were injected intraperitoneally with 10^7 HY21-3AC9 cells (Johnston et al., 1985). Ascites were harvested from the peritoneum from 10 to 14 days after injection. Mice were sacrificed by cervical dislocation. The ascites fluid was immediately diluted 3-fold in PBS and stored at -70° C.

SDS-PAGE procedure: Gels were run on a Mighty Small II slab gel electrophoresis, model SE 250, unit (Hoefer Scientific

Instruments, San Francisco, CA). 0.75 mm thick 10 or 12% gels were poured as described under general instructions in the SE 250 II manual. The separating gel was 5.0 cm high, the stacking gel was 2.5 cm high. Each sample was heated at 95 ° C in buffer containing 0.125 M Tris·HCL pH 6.8, 4% SDS, 20% glycerol with bromphenyl blue as the tracking dye, and 10% 2-mercaptoethanol. Electrophoresis was carried out under 22 ma constant current. Gel voltage varied from 75-90 volts at 0 time to 150-200 volts at 60- 70 minutes. The gel was stained with Coomassie Blue R-250 with gentle rocking for 30 minutes. Gels were destained in a solution containing 7 % acetic acid and 5% methanol.

Solutions:

Resolving gel buffer.......1.5 M Tris-HCl pH 8.8

Stacking gel buffer........0.5 M Tris-HCl pH 6.8

SDS........................10 % solution

Tank Buffer................0.025 M Tris pH 8.3, 0.192 M glycine, 0.1% SDS

Ammonium persulfate........10% solution

V.   Results and Discussion

V.A.   Raman Spectra of Model Compounds

Raman spectra of compounds that are the "building blocks" of 2',5'-oligoadenylates were taken so that the bands in spectra of 2-5A's could be assigned. Figure 12 depicts the structures of the model compounds that were studied. Inspection of Figure 12 reveals the systematic "building" of the 2-5A molecule from the heterocyclic base to the nucleoside and finally the nucleotide.

Major differences in the Raman spectra of purine and adenine result from the presence of an exocyclic N6 amino group attached to the C6 carbon of adenine (Figure 13). The ring breathing band at 800 cm^{-1} in purine is shifted to 729 cm^{-1} in adenine. Another major difference in the spectra is the strong 1254 cm^{-1} band in adenine. This band is assigned to the N-H bending of the exocyclic amino group of the adenine molecule (Tsuboi et al., 1973). The triplet peaks at 1285, 1310, and 1360 cm^{-1} in purine are absent in adenine. Instead, the characteristic 1308, 1338, and 1378 cm^{-1} triplet bands of adenine are present in this area of the spectrum. These peaks have been assigned to the N7-C8-N9 part of the adenine molecule (Lord et al., 1967) and are probably shifted relative to purine because of differences in vibrational coupling caused by the N6 amino group. This illustrates how a relatively small change in a molecule, such as the addition of an amino group, can effect a large change on the vibrational energy levels of the molecule. Since purine and adenine are not very soluble in water,

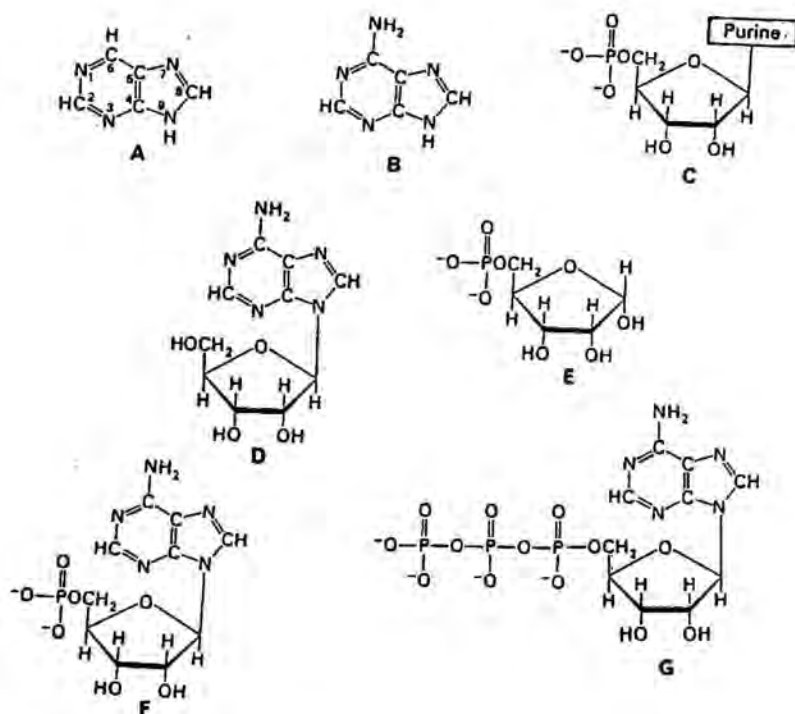**Figure 12.** Structures of model compounds. (a) purine, (b) adenine, (c) purine riboside, (d) adenosine, (e) ribose 5'-phosphate, (f) AMP, (g) ATP.
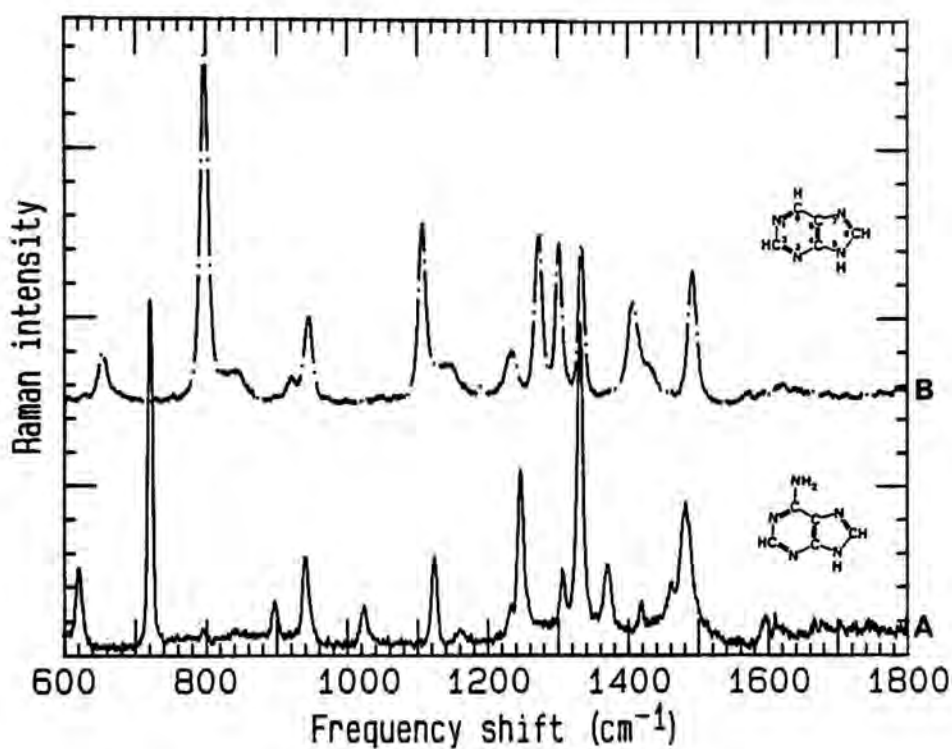
Figure 13. Raman spectra of (a) adenine and (b) purine. Samples were powder with 0.15 M NaCl buffered with 10 mM HEPES at pH 7.4 layered on top to act as a heat sink. The laser beam was defocused and laser power reduced to 100 mw at the laser source.

scans were performed on powder samples as described under Materials and Methods. Although the intensity of the peaks may differ, many of the same peaks are observed in the Raman spectra of the more soluble model compounds described below.

The addition of ribose to purine and adenine gives purine riboside and adenosine (Figure 14). The corresponding spectral changes occur for at least two reasons: 1. The spectra are those of nucleosides dissolved in water, and 2. Changes in vibrational coupling result from the N9-C1' adenine-ribose glycosidic linkage. The change in vibrational coupling is most evident in the 1200-1400 cm^{-1} region of the Raman spectra. The triplet found in the purine riboside spectrum is replaced by a broad doublet in the spectrum of adenosine (Figure 14b). There is also a new 1590 cm^{-1} band which has been assigned to the N3-C4-C5 area of the base (Baret et al.,1979) (see Table II).

Two new bands that are ribose modes appear in the purine riboside spectrum at 860 cm^{-1} and 1460 cm^{-1} (Peticolas et al., 1979). These are the only two modes of ribose that are clearly identifiable using normal mode analysis. These bands are also evident in the Raman spectrum of ribose 5'-phosphate (Figure 15). The strong band at 980 cm^{-1} in this spectrum is due to the 5'-terminal phosphate and will be discussed below. The 800-900 cm^{-1} bands are due to the phosphate ester stretching mode (Shimanouchi et al.,1964; Brown et al., 1975; Eyster et al., 1974; Van Zandt et al.,1977a,b). Specifically, if R_1 is a ribose ring attached to the phosphate at the 5' position and R_2 is either a hydrogen or another ribose ring, the 800-900 cm^{-1} bands are due to the $\{R_1-(PO_2^-)-O-R_2\}$
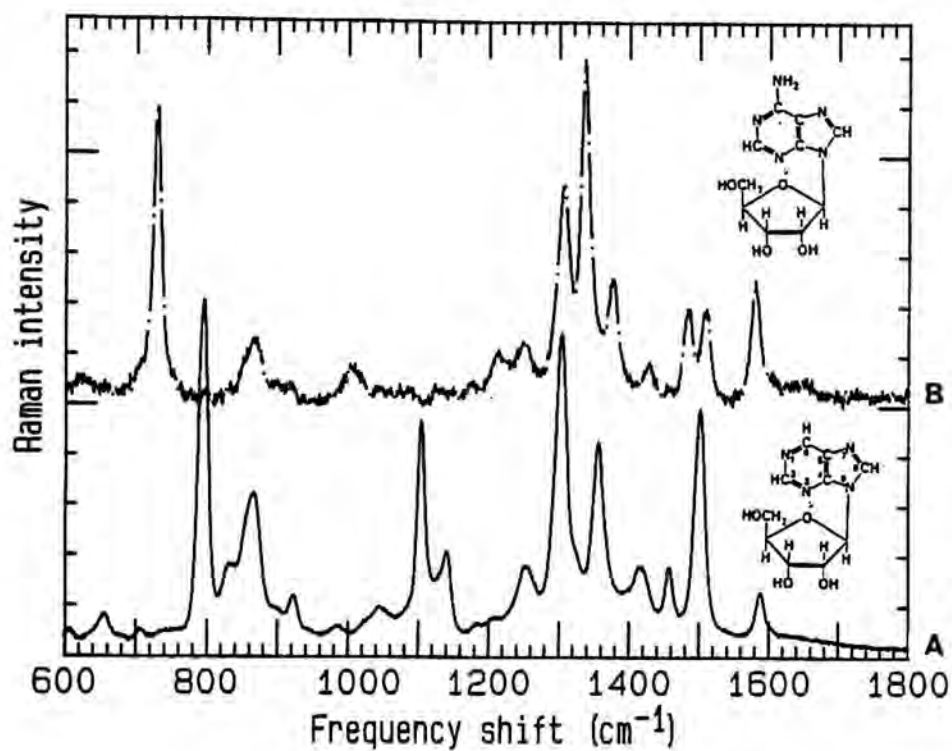
Figure 14. Raman spectra of (a) purine riboside and (b) adenosine in 0.15 M NaCl buffered with 10 mM Hepes, pH 7.4.
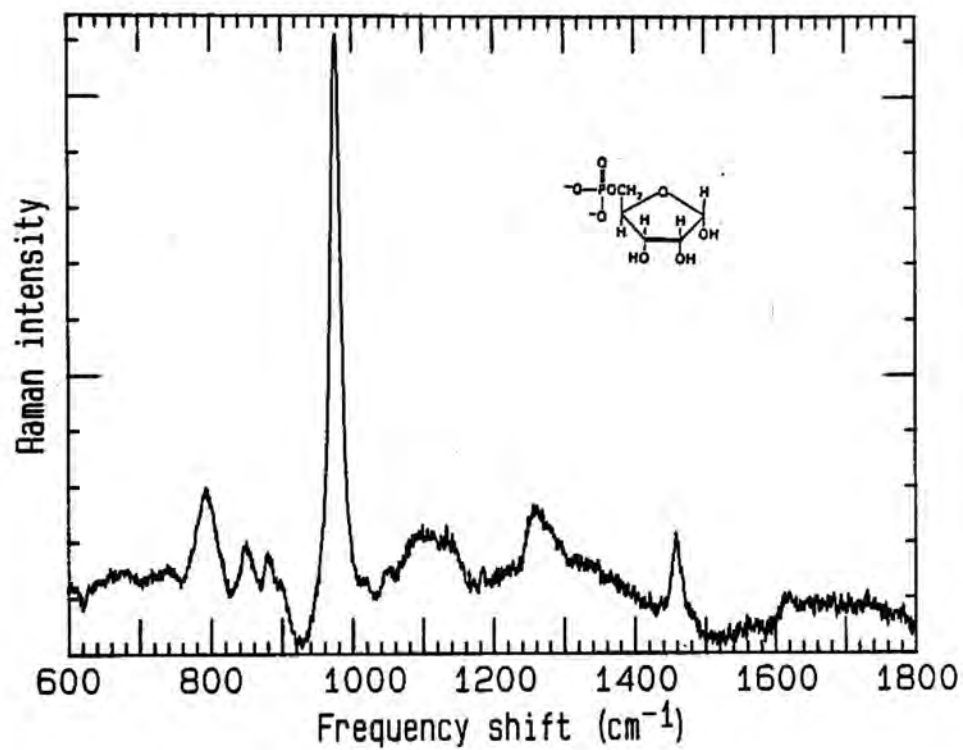
Figure 15. Raman spectrum of ribose-5-phosphate in water pH 7.0.

chain. This vibration has been shown to be conformation-dependent in DNA, RNA, and aggregates of GMP and will be discussed further below.

The frequency of the bands in the Raman spectrum of adenosine (Figure 14b) are the same as those observed in purine riboside but the bands have different widths and intensities. The 1460 cm^{-1} band in the spectrum of adenosine is weak but observable and the 860 cm^{-1} band has no shoulder but is a rather broad peak. The 1480 cm^{-1} band seen in the spectrum of adenine is split into two bands in adenosine at 1480 and 1510 cm^{-1}, presumably due to vibrational coupling through the N9-C1' glycosidic bond. The 1580 cm^{-1} band seen in the Raman spectrum of purine riboside is also present in adenosine (see Table II). A 1650 cm^{-1} band that is related to the C5-C6-NH$_2$ area of the molecule (Tsuboi et al., 1973) and a broad peak at 1220 cm^{-1} are also observed. The ring breathing mode at 729 cm^{-1} is somewhat broadened and the band at 640 cm^{-1} is reduced sharply in intensity.

In summary, the addition of ribose to the adenine base results in a compound that has two new bands due to ribose at 860 and 1460 cm^{-1}, and two new base bands at 1510, and 1220 cm^{-1}. This general pattern of intensities and band frequency is observed in all of the adenine containing compounds discussed below.

The model compounds are completed by the addition of phosphate groups to the 5'-terminus of the molecule. The Raman spectra of AMP and ATP are depicted in Figure 16b and 16c, respectively. Adenosine (Figure 16a) is shown for comparison. The 1150-1800 cm^{-1} region of these spectra are very similar and contain
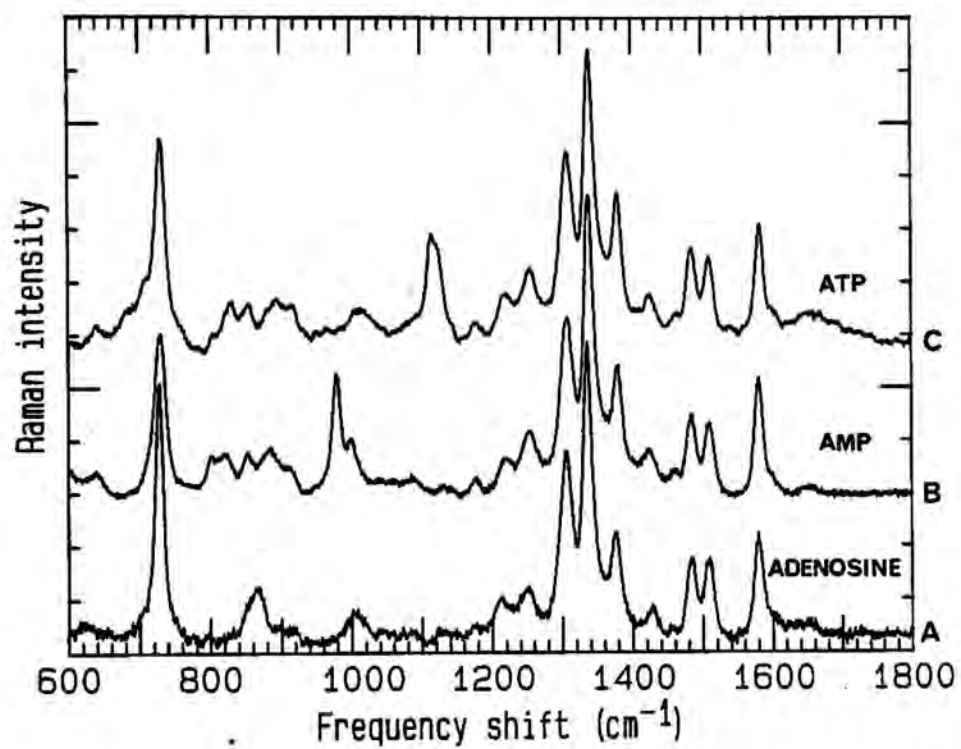
Figure 16. Raman spectra of (a) adenosine, (b) AMP, and (c) ATP in 0.15 M NaCl buffered with 10 mM HEPES, pH 7.4.

bands discussed above. The striking difference in the two spectra occurs at 1125 and 980 cm^{-1} and results from the 5'-triphosphate and 5'-monophosphate, respectively (Rimai et al., 1969). The AMP spectrum is strongly differentiated from the polyphosphates ADP and ATP by the presence of the symmetric phosphate stretch for the ionized form, PO^-_3, at 980 cm^{-1} and protonated form at 1082 cm^{-1}. In ATP, the ionized form has a band at 1113 cm^{-1} while the protonated form has a band at 1126 cm^{-1} (Rimai et al., 1969). These pairs of ionized and protonated lines are probably associated with the symmetric stretch involving the O=P=O group in the polyphosphates. However, these are vibrational modes of the chain as a whole, i.e. they are linear combinations of displacements involving all the groups. It is therefore understandable that the effect of the loss of·the terminal proton is less for ATP than it is in AMP and accounts for the difference in the frequency observed for the ionized species for AMP (980 cm^{-1}) and ATP (1113 cm^{-1}) (Lord & Thomas, 1967; Rimai et al., 1969). The frequency of the protonated form remains relatively constant for AMP and ATP at about 1090 cm^{-1}. This can be explained if these vibrations involve mainly the P=O bond. The motion of this vibration would correspond to the displacements of the P atoms against the O atoms and therefore is not especially sensitive to the number of groups involved.

The 729 cm^{-1} band in the spectrum of ATP contains a shoulder (Figure 16c). This shoulder is observed at 680 cm^{-1} in ATP, 710 cm^{-1} in ADP (not shown) and is nonexistent in AMP. Since this peak is absent in AMP and decreases in frequency with the number of phosphate groups, it is tentatively assigned to the polyphosphate

chain by Rimai et al., (1969). The occurrence of this peak and its assignment is discussed below in the section entitled "Linkage Isomers".

The phosphodiester modes in AMP and ATP are shifted lower in frequency relative to those in adenosine and are found in the 800-900 cm^{-1} region of the spectrum (Figure 16b,16c). AMP has bands at 800, 820, 850, and 880 cm^{-1} while ATP has bands at 800, 830, 850 and 880 cm^{-1}. Some of these bands probably represent different populations of ribose pucker that arise because of variations in the overall geometry of the furanose-phosphodiester linkages. Their significance will be discussed below in the section entitled "Conclusions".

V.B.1. General characteristics of Raman spectra of 2-5A.

The structure of 2',5'-oligoadenylate is depicted in Figure 17. Numerous similarities exist between the Raman spectrum of each model compound (adenosine, AMP, and ATP) and the Raman spectrum of 2',5'-oligoadenylates (A2'pA2'pA, pA2'pA2'pA, and pppA2'pA2'pA) (Figure 18). These spectra contain bands that originate from vibrational modes of the 5'-monophosphate (980 cm^{-1}) (Figure 18c, 18d), the 5'-triphosphate (1125 cm-1, Figure 18e, 18f), the phosphodiester backbone (800-880 cm-1), and the adenine bases (729 & 1200-1600 cm-1). Thus, the major differences in the Raman spectra of A2'pA2'pA, pA2'pA2'pA and pppA2'pA2'pA result from differences in the 5'-terminus and the ribose-phosphodiester backbone.

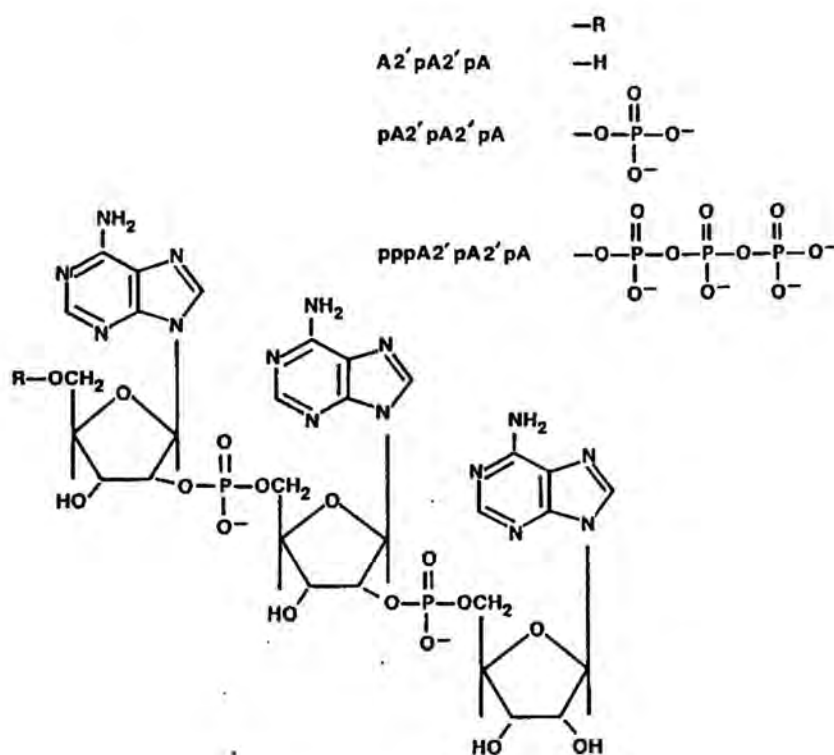The major Raman active modes for model compounds and

Figure 17. The structure of 2-5A trimers. R=H, trimer core; R=PO$_4$, trimer 5'-monophosphate; R=PO$_{10}$, trimer 5'-triphosphate.
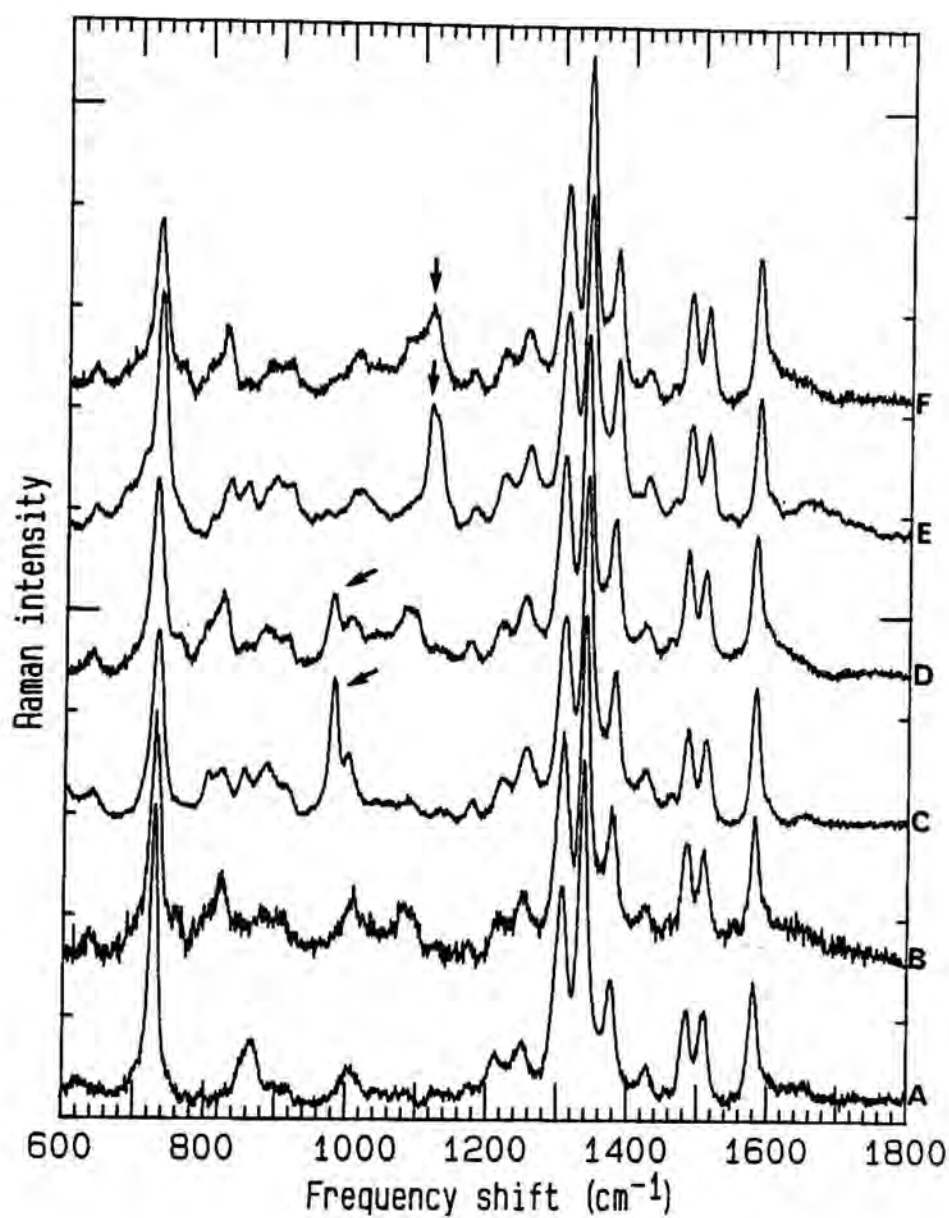
Figure 18. Raman spectra of 2',5'-oligoadenylates in water pH 7.3. Model compounds are shown for comparison. (a) adenosine, (b) A2'pA2'pA, (c) AMP, (d) pA2'pA2'pA, (e) ATP, (f) pppA2'pA2'pA.

2',5'-oligoadenylates at pH 7.3 are summarized in Table II. Ring
vibrations were identified by comparison with the frequencies
reported for nucleotide monomers (Lord & Thomas, 1967; Fodor et al.,
1985; Rimai et al.,1969) and polynucleotides (Baret et al.,1979).
Backbone vibrations were identified by comparison with normal
coordinate calculations (Brown & Peticolas, 1975; Shimanouchi et
al., 1964; Lu et al., 1975). These results show excellent
correlation with previously published data on A3'pA3'pA and
polyriboadenylic acid (Small & Peticolas, 1971; Prescott et
al.,1974).

V.B.2. Adenine Related Modes.

Modes above 1240 cm^{-1} arise from vibrations of adenine bases
(Table II). Minor differences between the observed Raman frequency
of base bands in the spectra of model compounds and 2-5A may arise
from coupling through the N9-C1' bond. Bands at 1308, 1340, 1378,
1422-1428, 1482-1484, 1510-1515, and 1580-1585 cm^{-1} have been
identified previously as adenine ring modes (Tsuboi et al.,1973).
Peaks at 630-640 and 729 cm^{-1} also arise from the adenine ring,
although the width of the 729 cm^{-1} peak may be slightly effected by
the molecules' state of 5'-phosphorylation (Rimai et al., 1969).

Preliminary studies suggested that a 1455 cm^{-1} band in 2',5'
trimer 5'-monophosphate, pA2'pA2'pA, (NIH source), originated from
the base moieties (Johnston et al.,1985). This preliminary
assignment was based upon the position of the band, its occurrence
in adenosine modified at the C8 position with bromine (spectrum not
shown), and the claimed purity of the sample. However, this 1455

Table I. Raman active modes for model and 2',5'-linked compounds.

Observed Raman frequency shift (cm⁻¹)ᵃ						Calculated frequency shift (cm⁻¹)ᵇ	Potential Energy Distributionᶜ
adenosine	A2'pA2'pA	AMP	pA2'pA2'pA	ATP	pppA2'pA2'pA		
1650		1650		1650			$C=N(19)$ $C-C(25)$ $C-N(23)N-C=(19)$
1582	1580	1580	1578	1585	1580	1581	$C5C4(48) - C4N3(31)$
1512	1510	1510	1510	1515	1510	1531	$C5C4(25) - C2N3(23)$
1486	1480	1482	1480	1487	1480	1468	$\delta C2H(29)-N9C8(19) + \delta C8H$
1458	1460	1460	1458	1462	1460	1464	ribosyl CH_2 bendingᵈ
1428	1422	1422	1422	1422	1425	1689	$C4N(44) - \delta C8H(15)$
1378	1378	1378	1378	1380	1380	1351	$C-N(50)C=C(16)$
1340	1340	1340	1340	1340	1340	1329	$N7C5(39) + C8N7(12)$
1308	1310	1308	1305	1305	1310	1309	$N9C8(30) + N3C2(14) + \delta C8H(14) - \delta C2H$
1254	1254	1254	1254	1254	1254	1424	$N1C6(31) + C6N6'(26)$
1214	1220	1220	1218	1220	1222	1218	adenine ring bending
1178	1180	1180	1180	1180	1178	1171	$N1-C2-N3(25)$ $N1-C2(23)$ $C2=N3(14)$ $N6-C6=N1(14)$
				1113	1115	1125	$PO_3^=$ 5'-triphosphateᵉ

Table I. (Con't)

Observed Raman frequency shift (cm^{-1})[a]						Calculated frequency shift (cm^{-1})[b]	Potential Energy Distribution[c]
adenosine	A2'pA2'pA	AMP	pA2'pA2'pA	ATP	pppA2'pA2'pA		
	1085		1075		1080		O-P-O symetric diester stretch[d]
1005	1010	1000	1010	1015	1010		adenine torsion
		980	980				PO$_3$" 5' monophosphate[e]
			918	918	918		not assigned
	880	882	895	892	890		not assigned
865							not assigned
		854		855	850		asymetric O-P-O[d], backbone[e]
	825	822	825	830	825		not assigned
		802	802	805	802		symetric O-P-O[d]
	780		795		780		C4-N9-C1'(16) C1'O5'(11)
729	729	729	729	729	729	681	δN7C8N9(19) - N9ribose(14) + δC5N7C8(12) + δC4N9C8(11)
630	638	640	638	640	640		backbone-A bending

[a] Frequency shifts experimentally observed in this report.
[b] Frequency shifts assigned by normal mode analysis by Fodor et al. (1985) and/or Baret et al. (1979)
[c] Potential enegery distributions based on normal mode analysis by Fodor et al. (1985) and/or Baret et al. (1979), except where noted otherwise.
[d] Assignment from Thomas et al., (1983).
[e] Assignment from Rimai et al. (1969).

cm^{-1} band was found to originate from a triethyl ammonium ion residue from the purification of the compound and was identified as such by the methods detailed below.

First, the 1455 cm^{-1} peak was identified as a strongly polarized band. A polarizing filter was inserted in the light path between the sample and the monochrometer, allowing collection of Raman spectra in which light that was parallel or perpendicular to the electronic vector of the laser beam was selectively allowed to pass into the monochrometer for data collection. The spectra were normalized as discussed under Materials and Methods and peak heights were measured. A ratio of each peak height in the perpendicular to that in the parallel spectrum was calculated. Comparison of the band ratios in the two spectra allowed the assignment of symmetric and asymmetric vibrational bands in the Raman spectrum. Symmetric bands have a dichroic ratio of < 1.0 while asymmetric bands are > 1.0.

The dichroic spectra of the NIH pA2'pA2'pA are depicted in Figure 19. In the perpendicular scan (Figure 17a), the symmetric base ring breathing bands at 729 cm^{-1} and the phosphate modes at 823, 980, and 1080 cm^{-1} are absent. Most other peaks were decreased in intensity relative to that observed in the parallel scan. However the 1455 cm^{-1} band increased in intensity relative to the parallel scan (Figure 19b). The ratio of these band intensities was 1.3 and therefore, the 1455 cm^{-1} peak is a strongly polarized band. This result implies that the 1455 cm^{-1} band observed in the NIH samples results from an asymmetric vibration. Since most base modes are expected to be symmetric this was an unusual result that
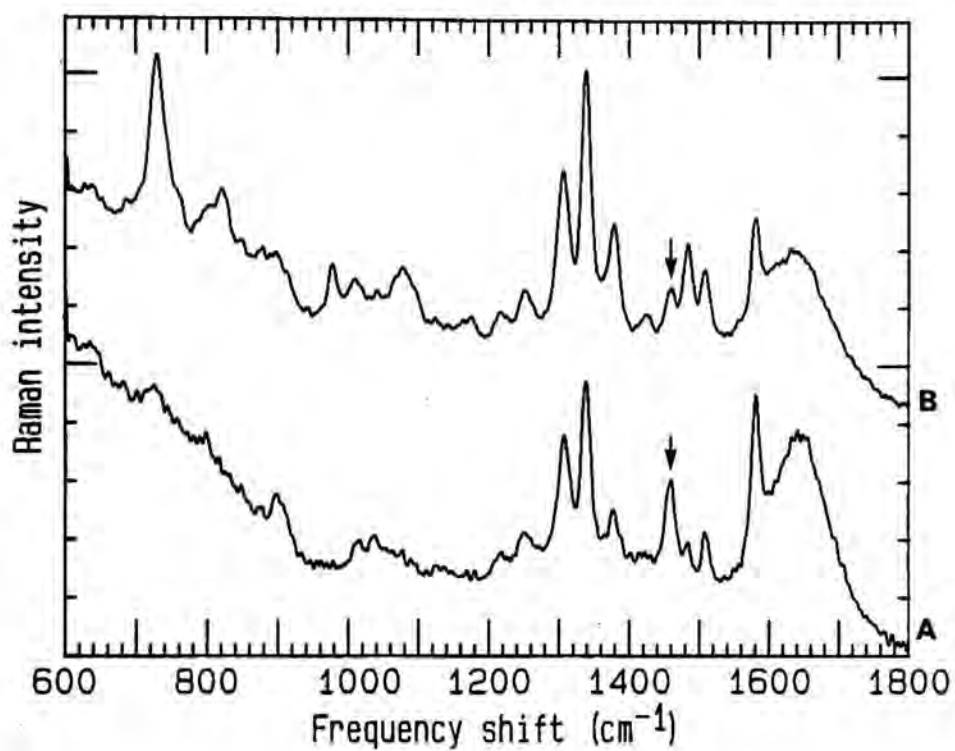
Figure 19. Parallel and perpendicular scan of pA2'pA2'pA (triethyl ammonium salt) in 0.15 M NaCl buffered with 10 mM HEPES pH 7.4. (a) perpendicular scan (b) parallel scan.

cast doubt on the assignment of the 1455 cm^{-1} band as a base vibrational mode. The asymmetry of the mode suggested that it may originate from a contaminant.

A review of the procedure for synthesis of the NIH pA2'pA2'pA revealed the possibility that the sample may have been contaminated with triethyl ammonium bicarbonate (TEAB) during its purification. A sample of TEAB for Raman analysis was obtained from the laboratory of Dr. Paul Torrence. The Raman spectrum of TEAB was compared with the Raman spectrum of NIH pA2'pA2'pA (Figure 20). Inspection of these two spectra indicate the strong possibility of TEAB contamination. TEAB has strong peaks at 765, 840, 900, and 1455 cm^{-1}. Inspection of the spectrum of NIH pA2'pA2'pA (Figure 20b) reveals peaks in every one of these areas. Peaks in the TEAB spectrum from 1000-1200 cm^{-1} result from the bicarbonate portion of the molecule that was presumed to be volatilized during vacuum evaporation. Therefore these peaks would not be expected in a contaminated sample that had been subjected to vacuum evaporation. The spectrum of TEAB was modified as discussed under Materials and Methods to generate a computer corrected spectrum of the triethyl ammonium portion of the molecule (see Figure 11). The resulting spectrum of TEA was then subtracted from the NIH pA2'pA2'pA to generate a corrected spectrum (Figure 21b). The resulting corrected spectrum was compared to the spectrum of a commercially available ammonium salt of pA2'pA2'pA (Figure 21c.) Peaks in the NIH sample of pA2'pA2'pA at 765, 840, 900 and 1455 cm^{-1} were eliminated from the spectrum. No new, negative or shifted peaks were observed. This result strongly suggested that the contaminant responsible for
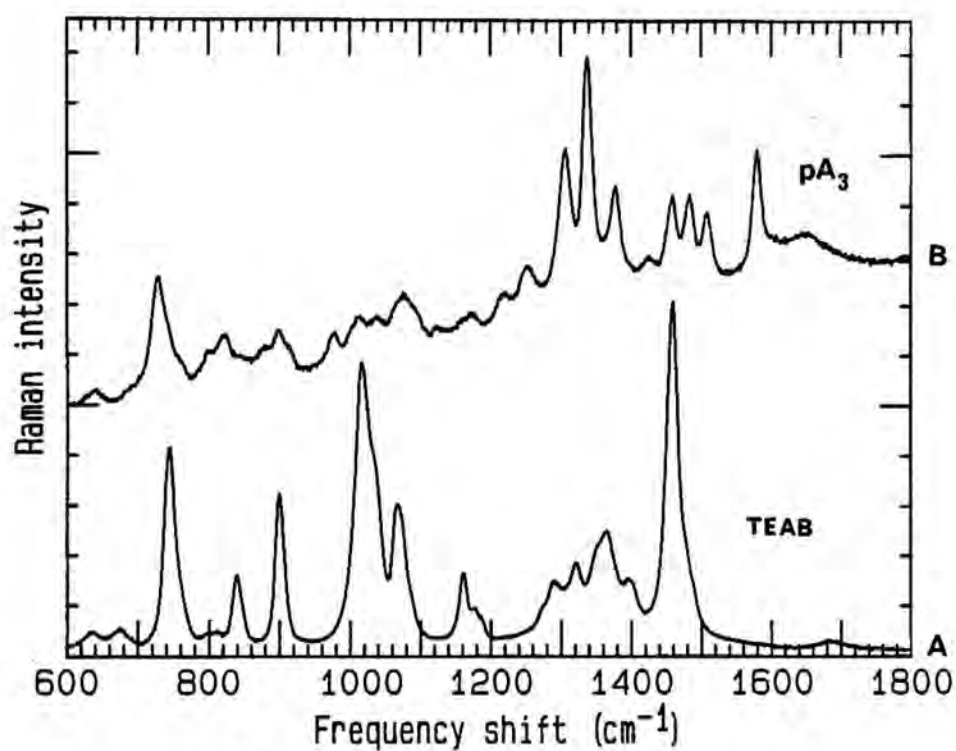
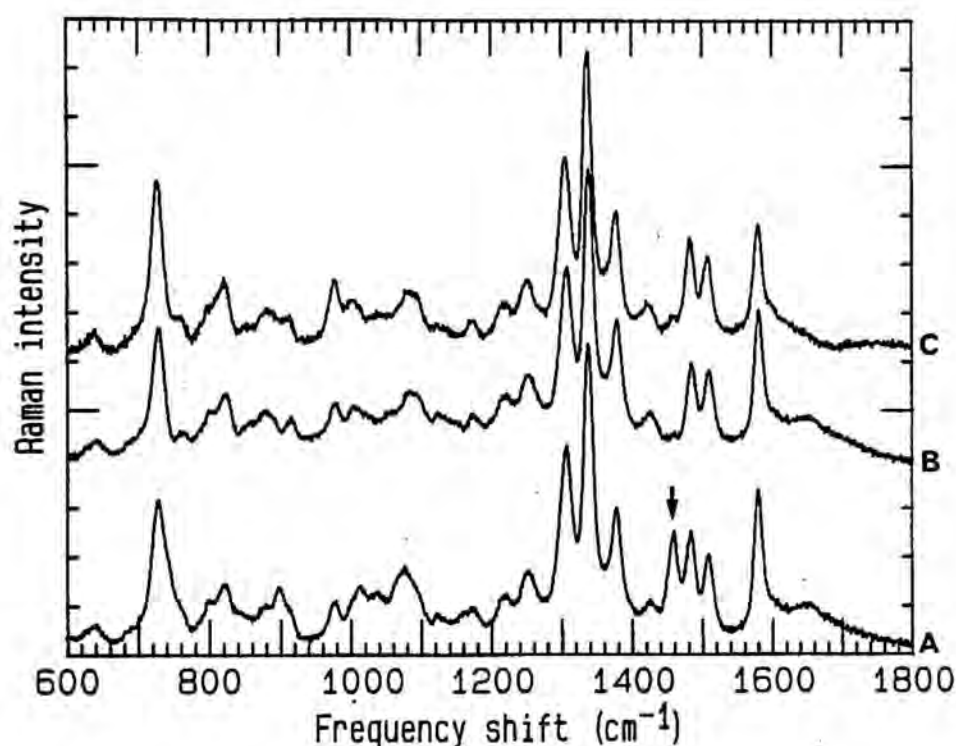**Figure 20.** The Raman spectrum of (a) TEAB pH 7.5 and (b) pA2'pA2'pA in water pH 6.8.

Figure 21. Subtraction of the Raman spectrum of TEAB from
pA2'pA2'pA. (a) TEA salt of pA2'pA2'pA (NIH) pH 6.8 in 0.15 M NaCl
buffered with 10mM HEPES, (b) Raman spectrum of pA2'pA2'pA (spectrum
(a)) with TEA subtracted as described under Materials and Methods,
(c) pA2'pA2'pA in water, pH 7.3 commercial source.

the 1455 cm^{-1} peak was TEA.

To verify this finding, a portion of the NIH sample was exchanged from the TEA salt to the ammonium salt as described under Materials and Methods. The resulting spectra contained no 1455 cm^{-1} peak (Figure 22b).

The above experiments provide substantial proof that at least a portion of the original NIH sample of pA2'pA2'pA was a triethyl ammonium salt and not a sodium salt as it was reported to be. In pH experiments with NIH pA2'pA2'pA, the intensity of the 1455 cm^{-1} mode was followed as a function of pH. As expected, the intensity did not change between pH 3 and 8, indicating that the band was not ionizable and further supporting the assignment of the 1455 cm^{-1} band to contaminating TEA (Figure 23).

V.B.3. pH Sensitive Modes.

The effect of pH on the Raman spectra of AMP and pA2'pA2'pA were compared to verify assignments of certain bands in pA2'pA2'pA and to explore the environment of the 5'-terminal phosphate of pA2'pA2'pA. The 2-5A molecule contains several groups that are ionizable between pH 3 and 8. At low pH the N3 position of the adenine ring becomes protonated and positively charged. The 5'-terminal phosphate groups also ionize between pH from 2 to 9.

The adenine base of both AMP (Figure 24) and pA2'pA2'pA (Figure 25) becomes protonated at low pH. This results in a large change in the 1300-1400 cm^{-1} region of the Raman spectrum. The region of the molecule responsible for these changes is assigned to the C=C (1378 cm^{-1}) N3C2 (1308 cm^{-1}) and N1C6 (1338 cm^{-1}).
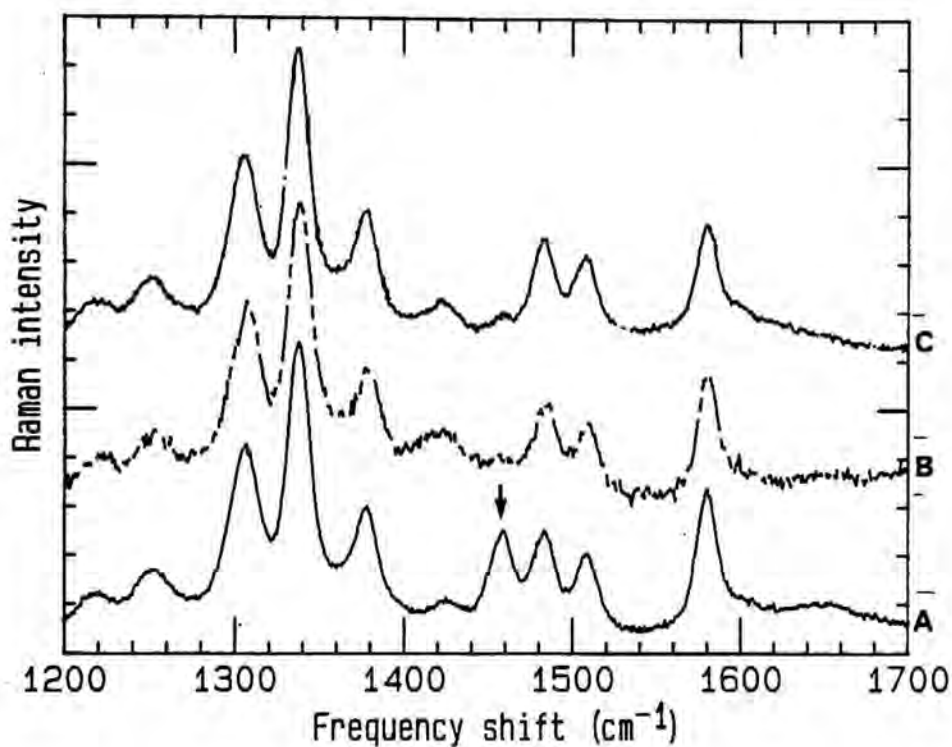
Figure 22. Windowed Raman spectrum of the base modes of pA2'pA2'pA. (a) original sample of pA2'pA2'pA in 0.15 M NaCl buffered with 10mM HEPES pH 6.8, (b) pA2'pA2'pA exchanged to the ammonium salt pH 7.3, (c) pA2'pA2'pA in water pH 7.3, commercial source.
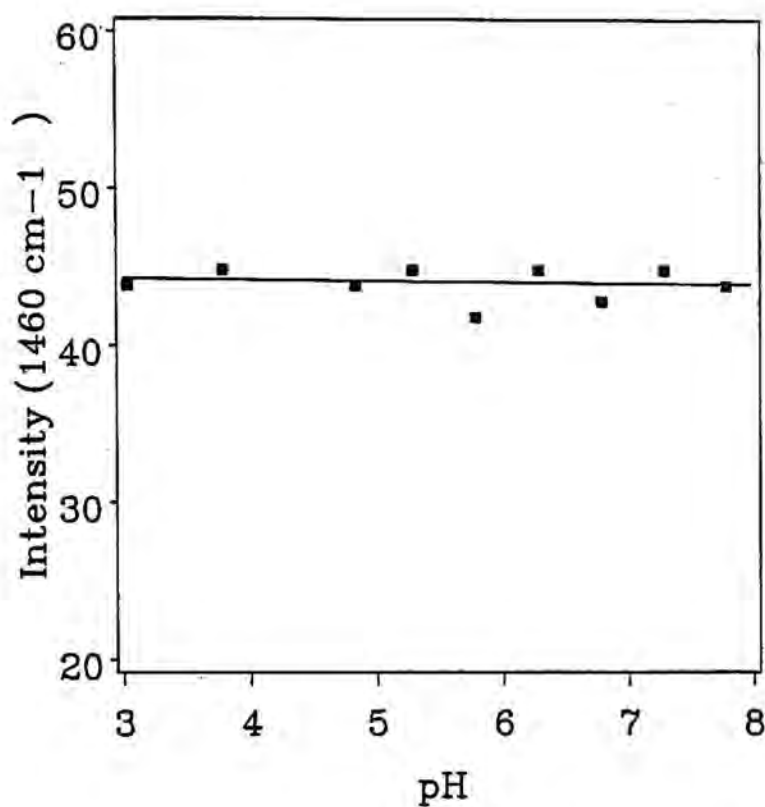
Figure 23. Effect of pH on the 1460 mode of pA2'pA2'pA. Normalized Raman intensity of the 1460 band vs pH ( ).
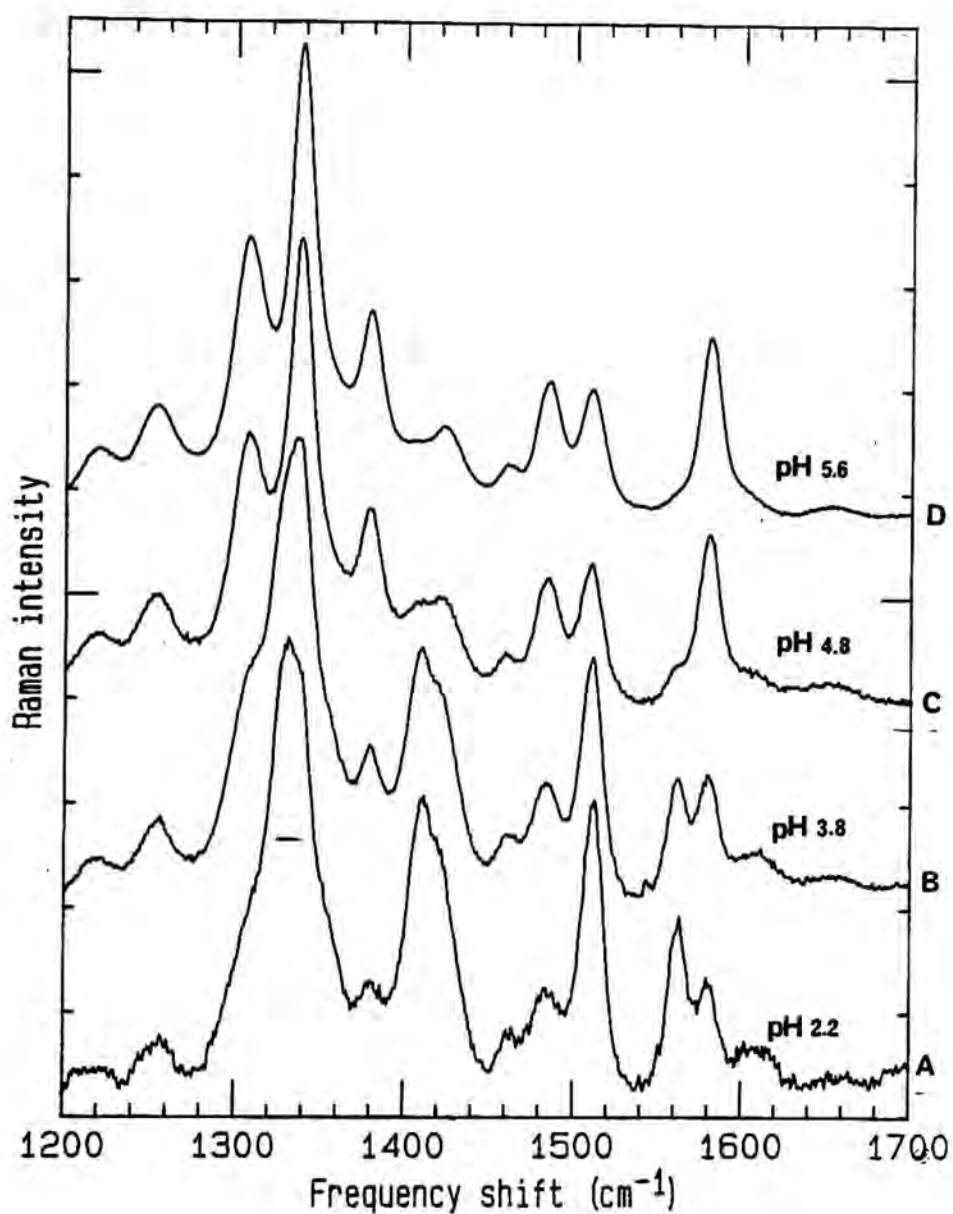
Figure 24. Effect of pH on the base modes of AMP. Windowed Raman spectrum of AMP in water pH (a) 2.2, (b) 3.8, (c) 4.8, (d) 5.6.
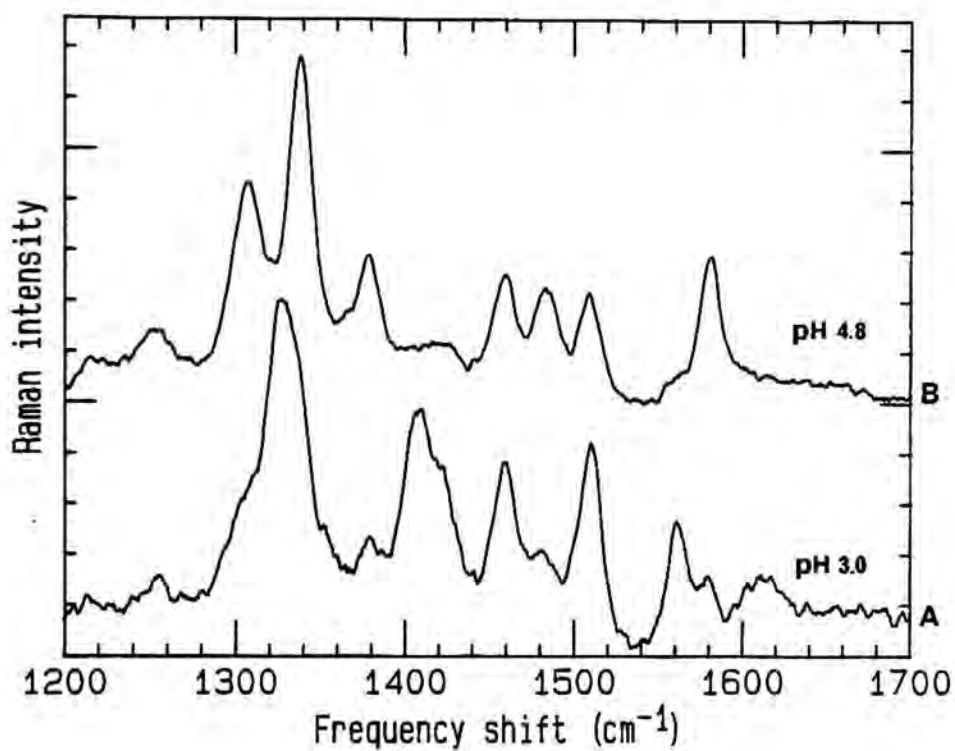
Figure 25. Effect of pH on the base modes of pA2'pA2'pA. Windowed
Raman spectrum of pA2'pA2'pA in water pH (a) 3.0, (b) 4.8

These peaks arise from areas of the base very near the region of the ring undergoing protonation. The normal mode band assignments in Table II are in good agreement with these observations.

The positions of phosphate modes in the Raman spectra of 5'-phosphorylated 2',5'-oligoadenylates were made by comparison with Raman spectra of AMP, ATP, and A2'pA2'pA and previously reported spectra of nucleotides (Rimai et al., 1969; Yue et al., 1986). Bands arising from vibrations of the 5'-monophosphates at 980 cm^{-1} and from the triphosphates at 1125 cm^{-1} were observed in AMP and ATP and in 2',5'-oligoadenylates. The effect of pH on the ionization state of pA2'pA2'pA, as reflected by the 980 cm^{-1} (ionized) and 1084 cm^{-1} (protonated) phosphate bands, was investigated to determine the pK_a of the 5'-terminal phosphate. An altered pK_a may indicate that the 5'-terminal phosphate of pA2'pA2'pA interacts with other portions of the 2-5A molecule through 5'-terminal phosphate group hydrogen bonding. The pH was varied from 2.0 to 9.0 for AMP and from 3 to 8 for pA2'pA2'pA. Spectra were normalized to the 729 cm^-^{1} adenine base band which is not affected in intensity or frequency by changes in pH from 5 to 7 (Rimai et al., 1969) or from <3 to >5 (Lord & Thomas, 1967). AMP and pA2'pA2'pA Raman spectra are depicted in Figure 26 and Figure 27, respectively. Expanded scale spectra were also plotted to clearly visualize the characteristic 980 cm^{-1} $PO_3^=$ modes of AMP and pA2'pA2'pA (Figure 28, 29). The 980 cm^{-1} peak in the trinucleotide spectrum is less intense than the corresponding peak in AMP. This results from the higher ratio of 5'-phosphates to purine bases in AMP.

A plot of the normalized Raman intensity of the 980 cm^{-1}
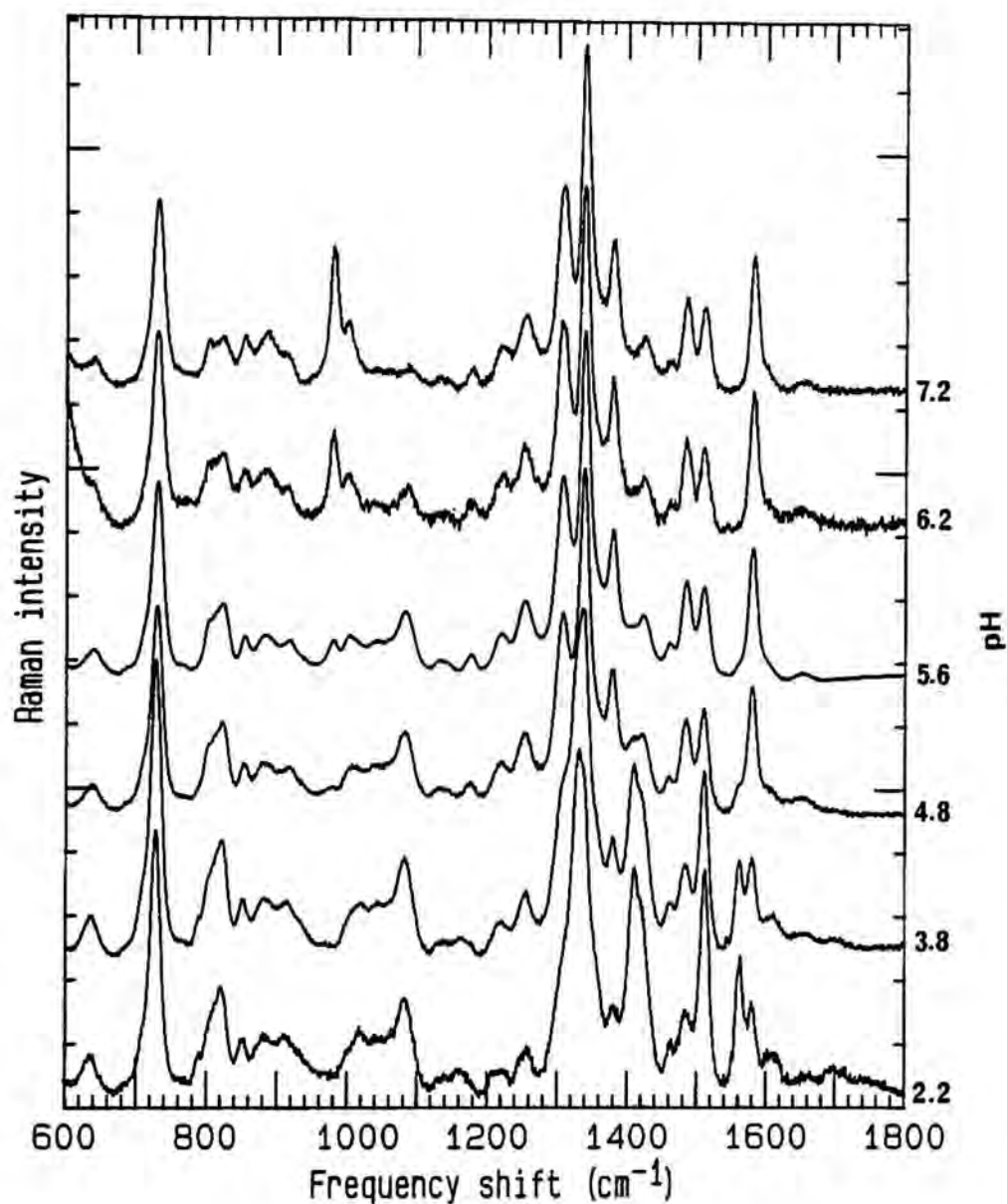
Figure 26. Effect of pH on the vibrational modes of AMP. Raman spectra of AMP in water pH (a) 2.2, (b) 3.8, (c) 4.8, (d) 5.6, (e) 6.2 (f) 7.2.

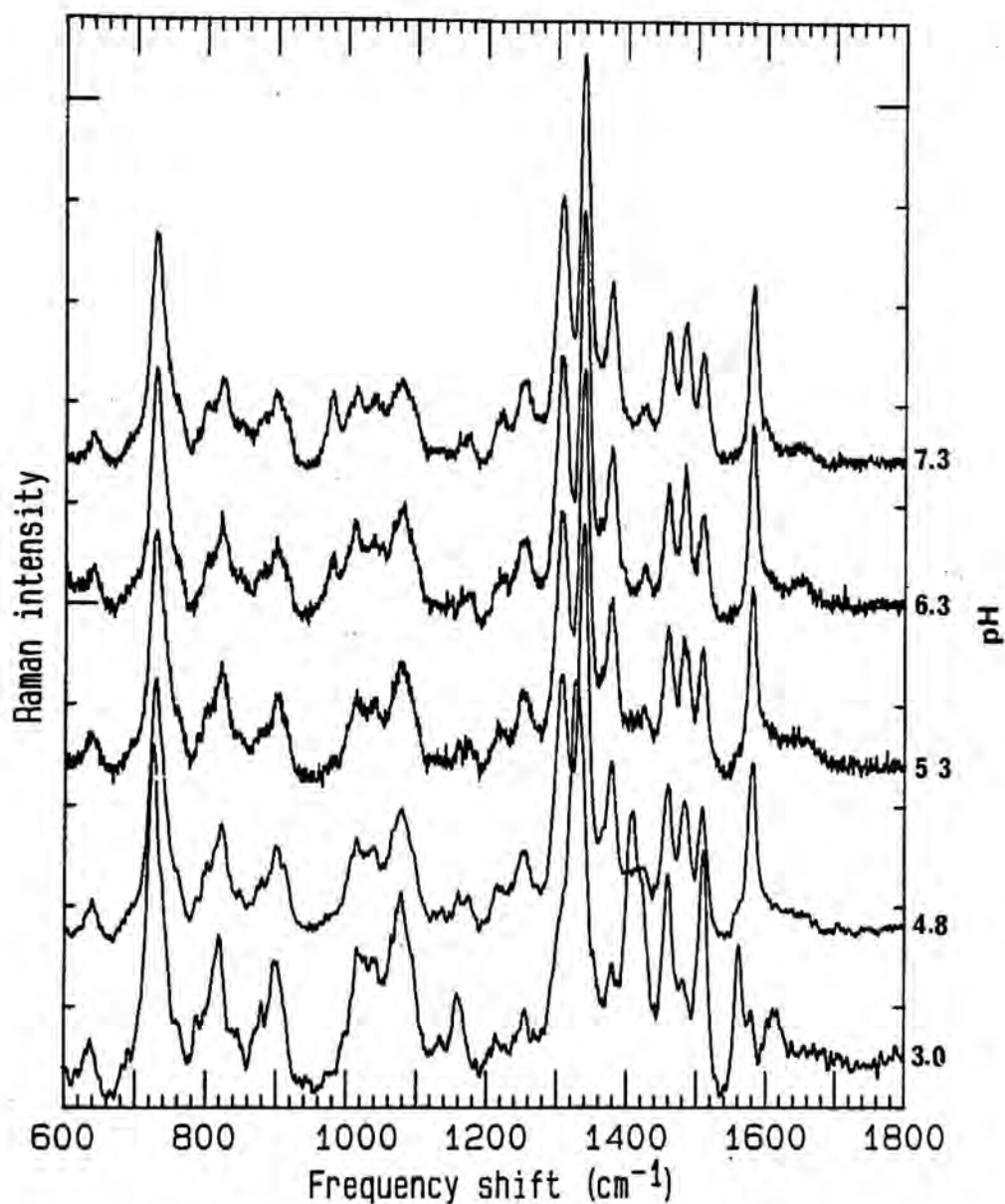**Figure 27.** Effect of pH on the vibrational modes of pA2'pA2'pA.
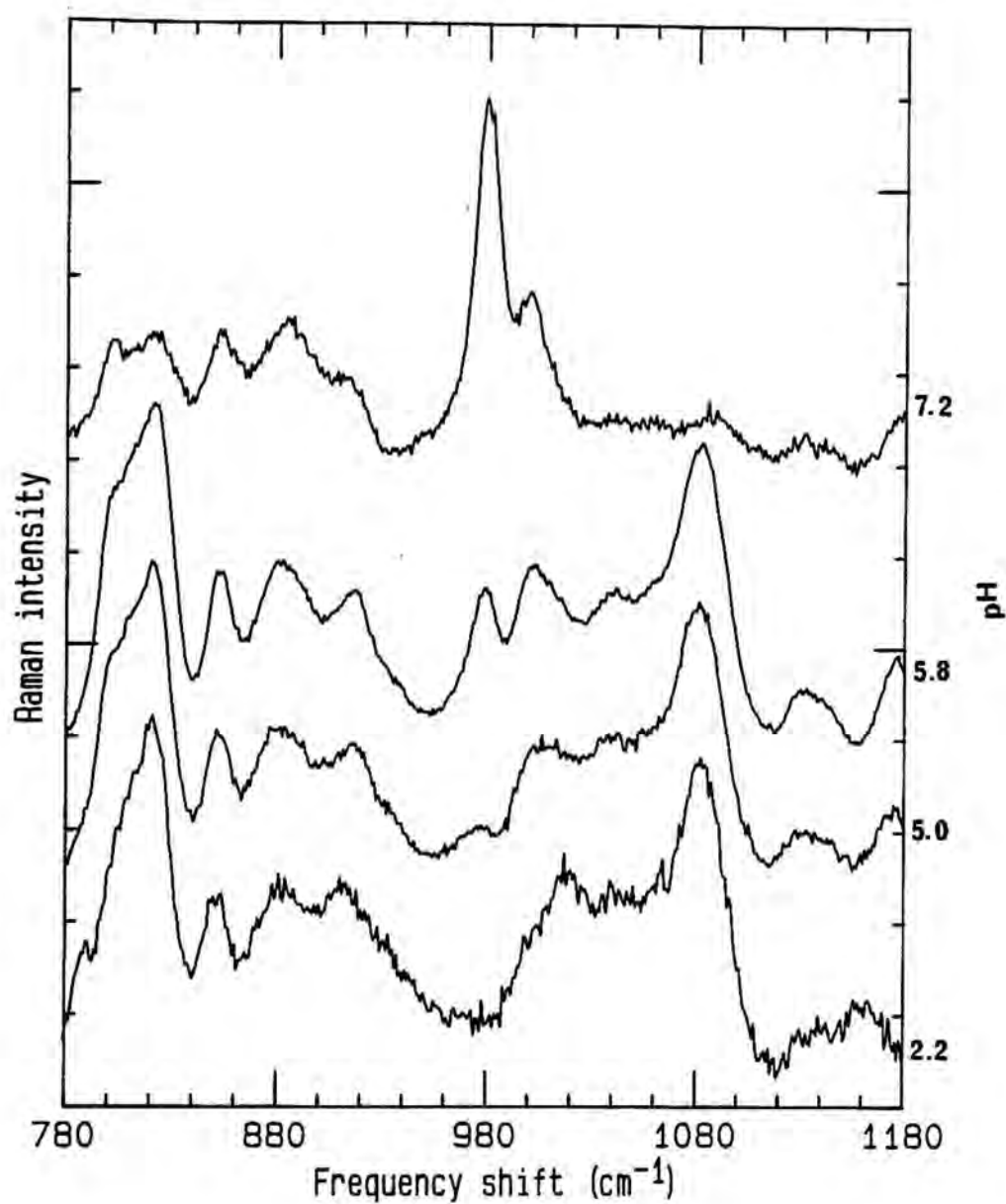Raman spectra of pA2'pA2'pA in water at pH 3.0, 4.8, 5.3, 6.3, 7.3.

Figure 28. Effect of pH on the phosphate modes of AMP. Windowed Raman spectra of AMP in water at pH 2.2, 5.0, 5.8, 7.2.
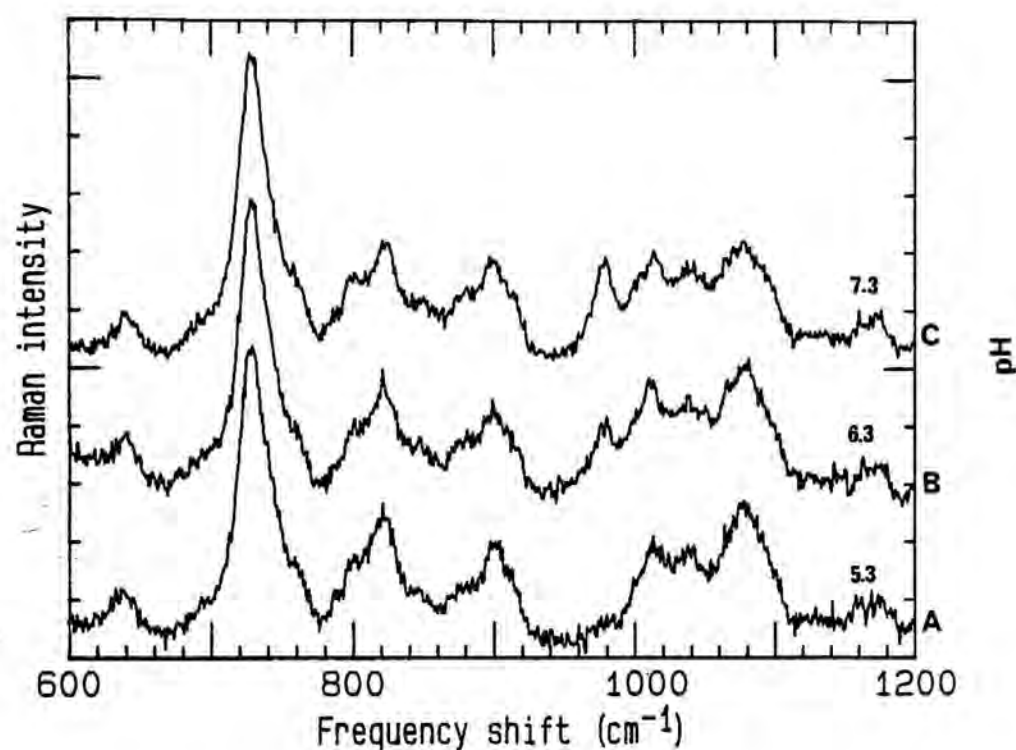
Figure 29. Effect of pH on the phosphate modes of pA2'pA2'pA. Windowed Raman spectrum of pA2'pA2'pA in water pH (a) 5.3 (b) 6.3 (c) 7.3

(ionized) and 1084 cm^{-1} (protonated) bands was constructed for AMP (Figure 30) and for pA2'pA2'pA (Figure 31). The pH range of the AMP experiment allowed a precise determination of the pK_a of AMP. A straight line was drawn from the midpoint of the titration curve to the x-axis. This is where the ionized and protonated band lines cross within experimental error for AMP (Figure 30). The apparent pKa of AMP was estimated to be 6.05. The pH range of for the pA2'pA2'pA experiment was not as large as for AMP to avoid base mediated hydrolysis of valuable 2-5A samples. The pK_a of pA2'pA2'pA was estimated by drawing a vertical line from the point at which the ionized and protonated band lines crossed to the x-axis and was determined to be 6.1 (Figure 31).

The results of these experiments suggest that the 5'-terminal phosphate of pA2'pA2'pA behaves just as the 5'-terminal phosphate of AMP in a concentrated solution. This suggests that the 5'-terminal portion of the 2-5A molecule does not participate in any stable solution interactions under these experimental conditions.

V.B.4 Deuteration Effects.

The spectra of trimer monophosphate, pA2'pA2pA, in H_2O and in D_2O were compared to verify certain band assignments in pA2'pA2'pA and to explore the environment of the exocyclic amino groups of 2-5A (Figure 32). The timing of this experiment was critical in order not to confuse the spectra with C-8 and C-2 deuteration of the adenine base. Exchange of the C8 and C2 protons of the adenine base is much slower than exchange of the ribose hydroxyls and the exocyclic amino group of adenine (Thomas et al.,

Figure 30. Normalized Raman intensity vs pH for the phosphate modes of AMP. (a) ionized 980 cm^{-1} ($\square$); (b) protonated 1080 cm^{-1} ($\triangle$).
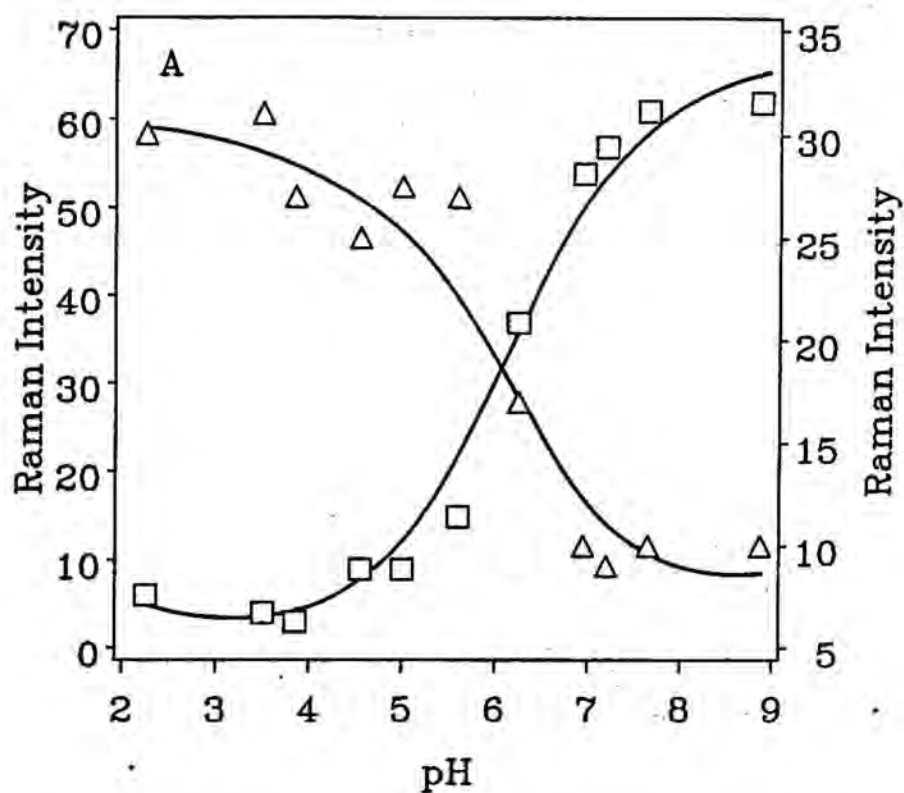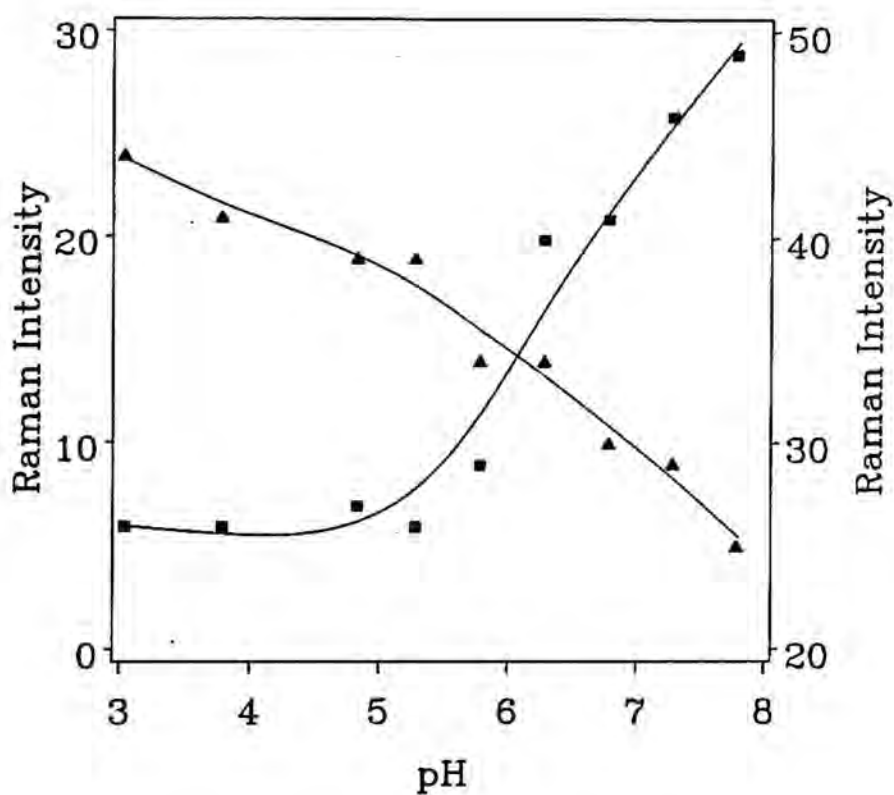
Figure 31. Normalized Raman intensity vs pH for the phosphate modes of pA2'pA2'pA. (a) ionized 980 cm^{-1} (■); (b) protonated 1080 cm^{-1} (▲).
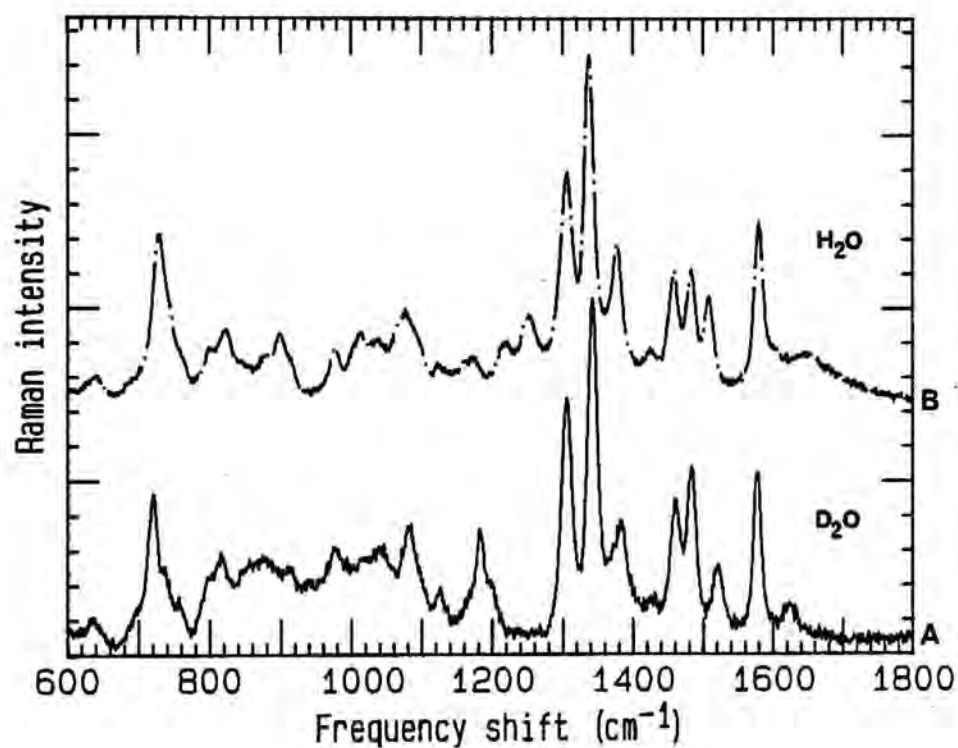
Figure 32. The Raman spectrum of pA2'pA2'pA in (a) D_2O pH 6.6 and (b) in H_2O pD 6.2. pH was estimated by spotting a small amount of sample on pH paper.

1975). After 5 hours at 80° C, approximately 67% of AMP C-8 hydrogens are exchanged. C-2 exchange is even slower (Elvidge et al.,1971). The samples used in these experiments were reconstituted at 4° C and then immediately transferred to the Raman sample holder thermostated at 10° C. The low temperature of reconstitution and the immediate, low temperature Raman scans probably prevented the exchange of C-8 and C-2 protons in these experiments.

A minor band at 1650 cm^{-1} in H$_2$O was shifted down in frequency to 1625 cm^{-1} in D$_2$O. Since the six membered ring of adenine is aromatic, this band may be related to the high frequency ring modes that arise from substituted benzenes (Fodor et al., 1985). The band at 1254 cm^{-1}, assigned to the exocyclic N6 amino group of the adenine bases by Tsuboi et al.(1973), is not present in D2O, indicating that this band assignment is correct for the 2',5'-oligoadenylates.

Deuteration resulted in the appearance of two new bands at 1182 and 1200 cm^{-1}. The 1182 cm^{-1} mode has been assigned previously to the ND2 scissor by Tsboi et al. (1973). The 1200 cm^{-1} band probably arises from adenine, since it also appears when AMP is deuterated (Yue et al., 1986). Most bands above 1300 cm^{-1} also shifted down slightly in frequency as a result of changes in vibrational coupling. However, the band at 1505 cm^{-1} shifted up in frequency to 1520 cm^{-1}. The reason for this shift is not readily apparent especially since this band is assigned to the C2-N3-C4-C5 area of the adenine base. Since the Raman spectrum provides no other evidence, i.e. the increase in intensity of a band at 1465 cm^{-1}, of C-2 exchange it is hard to account for this shift in

frequency. The shift may result from different vibrational coupling due to deuteration of the amino hydrogens of C6. Numerous changes in the 700-900 cm^{-1} region of the spectrum, containing ribose and phosphate bands, were also observed.

The results for the deuteration experiment suggest that the exocyclic nitrogens of pA2'pA2'pA are free of any stable solution interactions, i.e. hydrogen bonding. This is consistent with the postulate that the exocyclic amino groups of 2-5A are in same environment as the $-NH_2$ groups of AMP. Another sensitive way to assess the "environment" of the adenine bases in 2-5A would be to perform C-8 deuteration experiments. C-8 exchange rates would be expected to depend upon the details of molecular structure and conformation in the vicinity of the exchangeable groups. Therefore, comparative rate determinations on AMP, 3-5A, and 2-5A would provide a basis for the further evaluation of the secondary structure in 2-5A.

V.B.5. Assessing Secondary Structure

Raman hyperchromism is observed in the spectra of ordered structures such as poly rA when the bases unstack at high temperature. Bands in the Raman spectra of poly rA and A3'pA3'pA at 729, 1308, and 1510 cm^{-1} increase upon melting at 90°C (Prescott et al., 1974). Raman spectra of pA2'pA2'pA at 16-90° C were obtained to assess the secondary structure of pA2'pA2'pA (Figure 33, ammonium salt; Figure 34, TEA salt). First, it is important to note that Raman spectra normalized to either the 1095 cm^{-1} O-P-O band or the 1338 cm^{-1} adenine band were identical. The 1095 cm^{-1} band has been

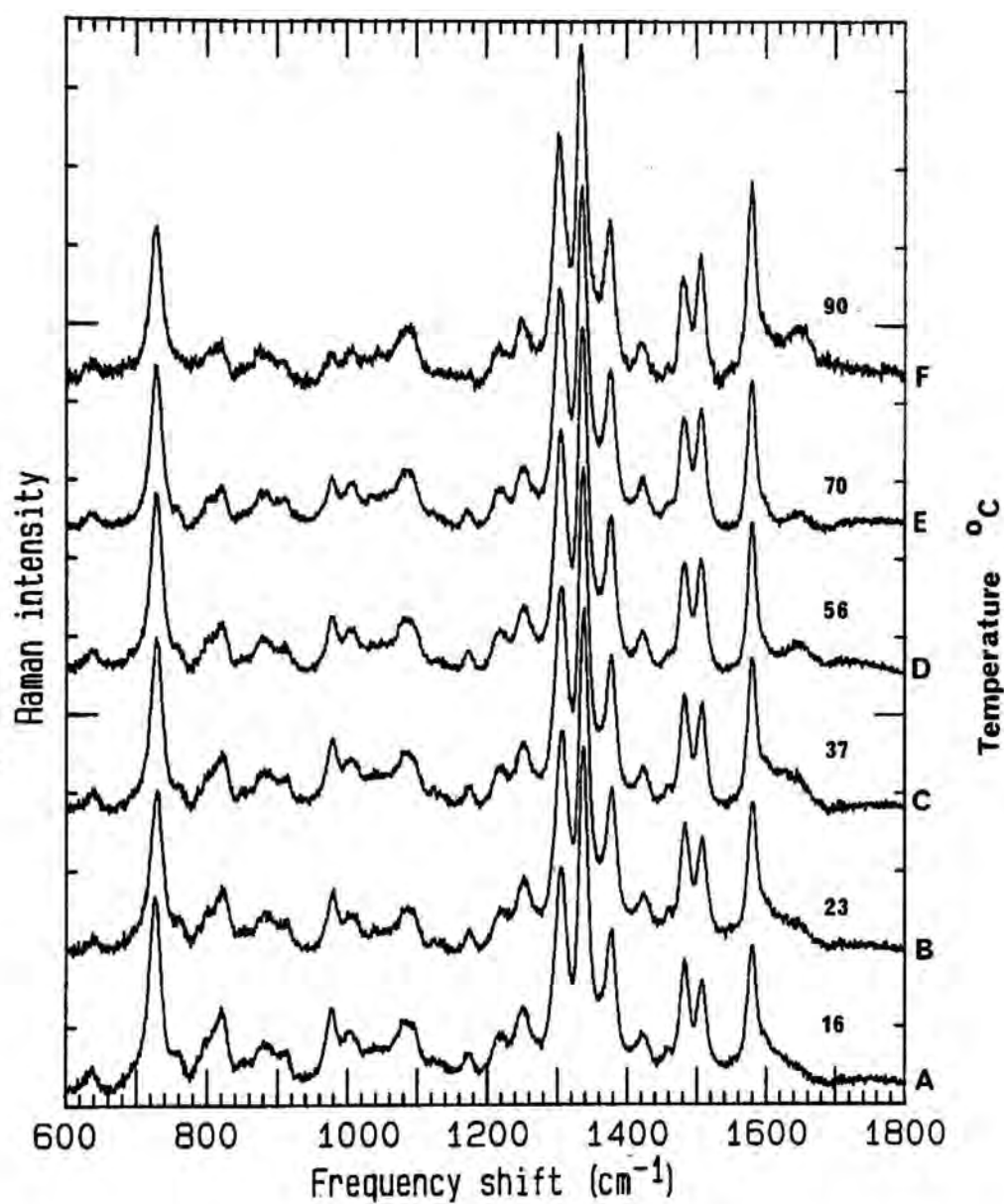**Figure 33.** Effect of temperature on the Raman spectrum of pA2'pA2'pA. The Raman spectrum of pA2'pA2'pA in water, pH 7.3, at (a) 16, (b) 23, (c) 37, (d) 56, (e) 70, and (f) 90 degrees C.
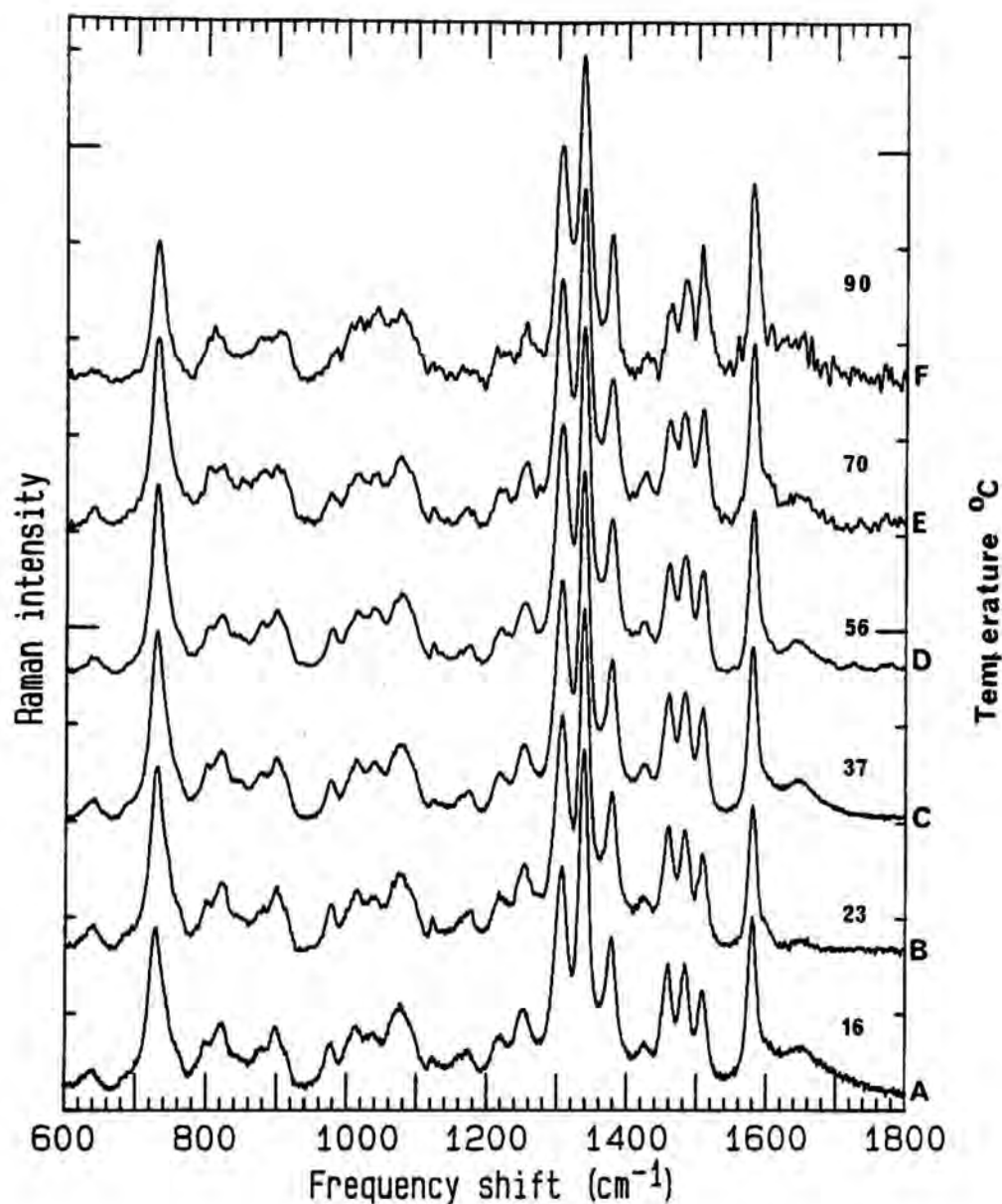
Figure 34. Effect of temperature on the TEA salt of pA2'pA2'pA.
The Raman spectrum of pA2'pA2'pA, TEA salt in 0.15 M NaCl buffered
with 10 mM HEPES, pH 6.8 , at (a) 16, (b) 23, (c) 37, (d) 56, (e)
75, and (f) 90 degrees C.

used by many investigators to normalize spectra of nucleic acids. However, caution must be used since this band is very sensitive to pH. We observed no change in the relative intensity of either of these bands with temperature, indicating that the 1338 cm^{-1} band may also be a good band to normalize to under these circumstances.

Raman intensities of various bands in the normalized spectra of AMP, A3'pA3'pA and pA2'pA2'pA were measured and plotted as a function of temperature. Four pertinent observations were made. (i) Intensities of lines in the spectrum of pA2'pA2'pA at 1308, 1378, and 1510 cm^{-1} increased 21, 16, and 33% respectively (Figure 35). Intensities of the 1308, 1378, and 1510 lines in the spectrum of AMP increased 15, 18, and 46% respectively (Figure 36a). Intensities of the 1308, 1378, and 1510 lines in the spectrum of A3'pA3'pA increased 15, 19 and 46% respectively (Figure 36b). Changes in these spectra were linear with increasing temperature. (ii) The intensities of the 1308, 1378, and 1510 cm^{-1} bands in the spectra of AMP and pA2'pA2'pA at 16° C were similar (Figure 18). (iii) The intensities of the bands at 1308, 1378, and 1510 cm^{-1} in the spectra of pA3'pA3'pA were slightly decreased with respect to the same bands in AMP, which is consistent with observations made by Prescott et al. (1974). (iv) The 814 cm^{-1} line in the Raman spectrum of A3'pA3'pA at 20°C shifts to 798 cm^{-1} at 90°C and has been used as a measure of "disorder" (lack of secondary structure) in this and other 3',5'-linked RNA's (Prescott et al., 1974). No shift of the 823 cm^{-1} line in the spectrum of pA2'pA2'pA was observed at 90°C.

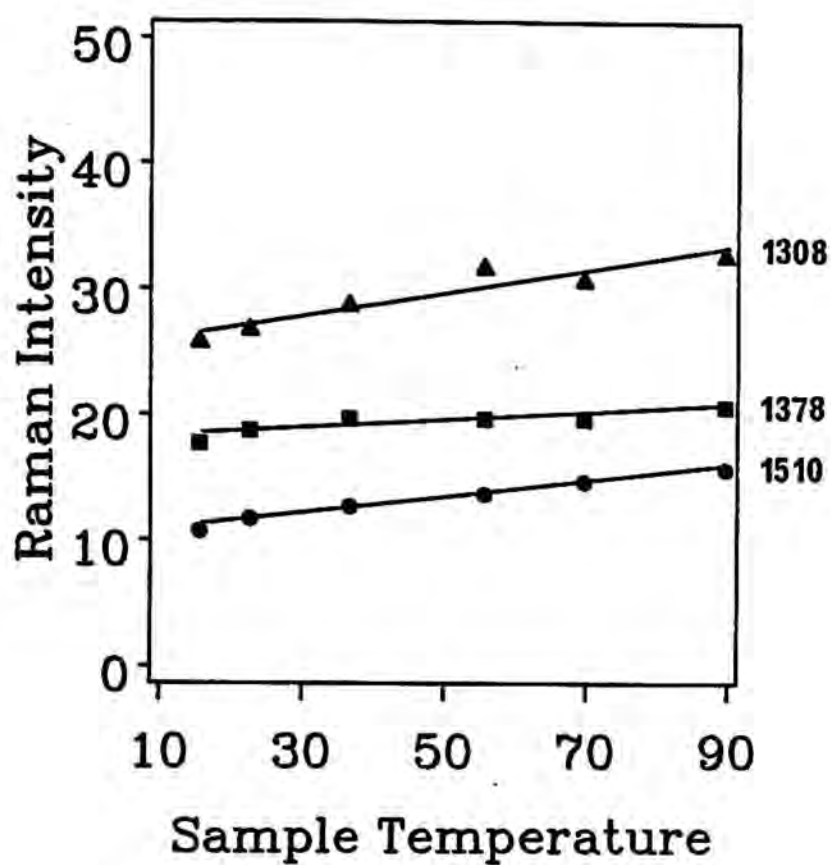For observations (i) and (ii) above, both the commercial

Figure 35. Raman intensity vs temperature of the ammonium salt of pA2'pA2'pA in water, pH 7.4.
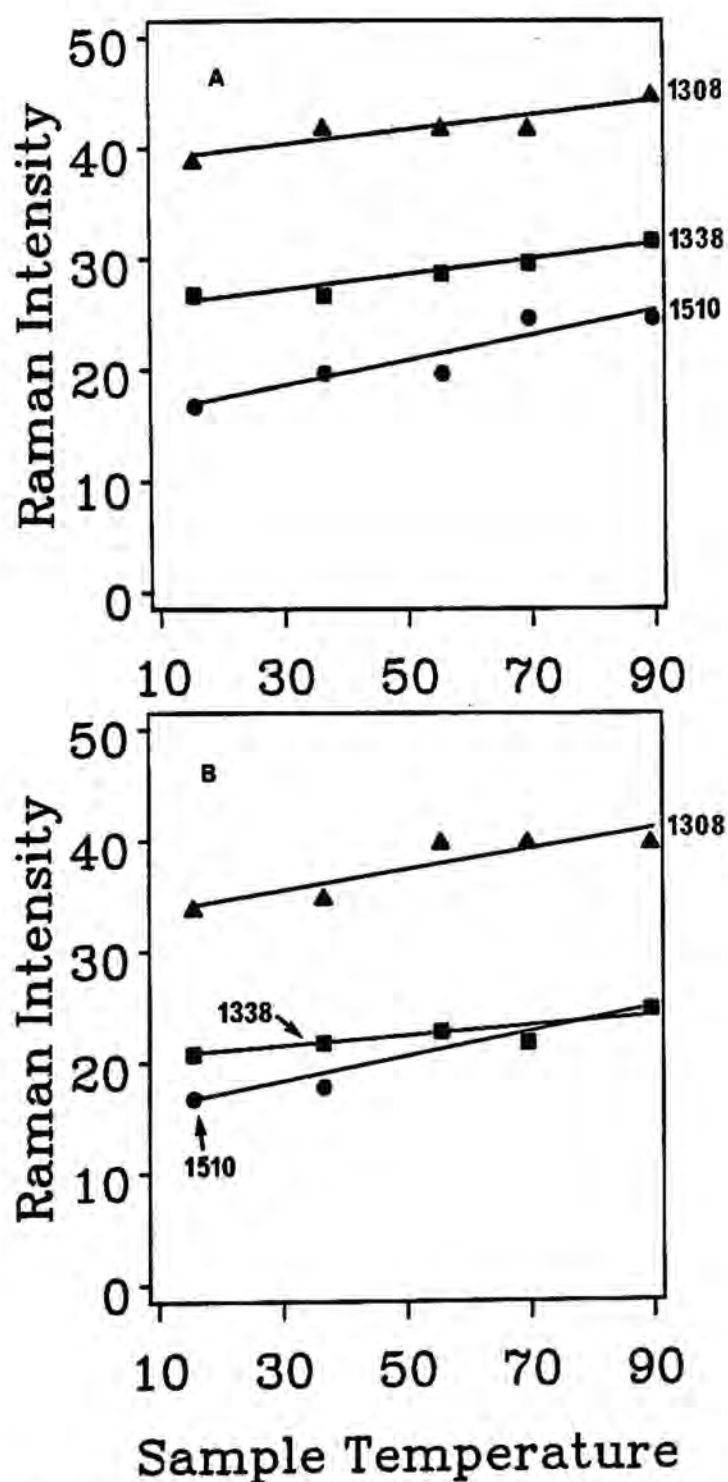
Figure 36. Raman intensity vs temperature of (a) AMP in 0.15 M NaCl, pH 7.4 and (b) A3'pA3'pA in 0.15 M NaCl buffered with 10 mM HEPES pH 7.4.

ammonium salt and the NIH TEA salt of 2-5A were compared and gave essentially identical results.

The spectrum of the TEA salt of 2-5A in methanol was obtained to further assess secondary structure. Methanol would be expected to disrupt solvation interactions between water molecules and 2-5A and thereby disrupt hydrogen bonding and secondary structure. Only minor changes in the Raman spectrum were observed. This result supports the hypothesis that 2-5 A does not contain significant base stacking in solution (Figure 37). Temperature experiments with AMP and A3'pA3'pA revealed linear changes in band intensity with increasing temperature. A3'pA3'pA and pA2'pA2'pA had similar high temperature spectra compared to the nucleotide monomer AMP which supports the conclusion that trimers, both 2',5'- and 3',5'-linked, have very little base stacking in solution.

Previously published physicochemical studies have been inconclusive with respect to the conformation of 2',5'-linked oligoadenylates in solution. Studies using CD to estimate base stacking reveal that hypochromicity of 2',5'-oligoadenylates was higher than that of the corresponding 3',5'-oligoadenylates (Sawai, 1983; Doornbos et al., 1981, 1983). This result suggests that 2',5'-oligoadenylates possess more base stacking than 3',5'-oligoadenylates. In contrast, comparison of the CD spectra of 2-5A and 3-5A tetramer, pentamer, and hexamer at 20° C shows that epsilon for 3',5'-oligoadenylates increases with increasing chain length, but it remains constant for 2',5'-oligoadenylates of increasing chain length. The conclusion was that stacking in 2',5'-oligoadenylates is weaker than in 3',5'- oligo(A)'s (Hirao et
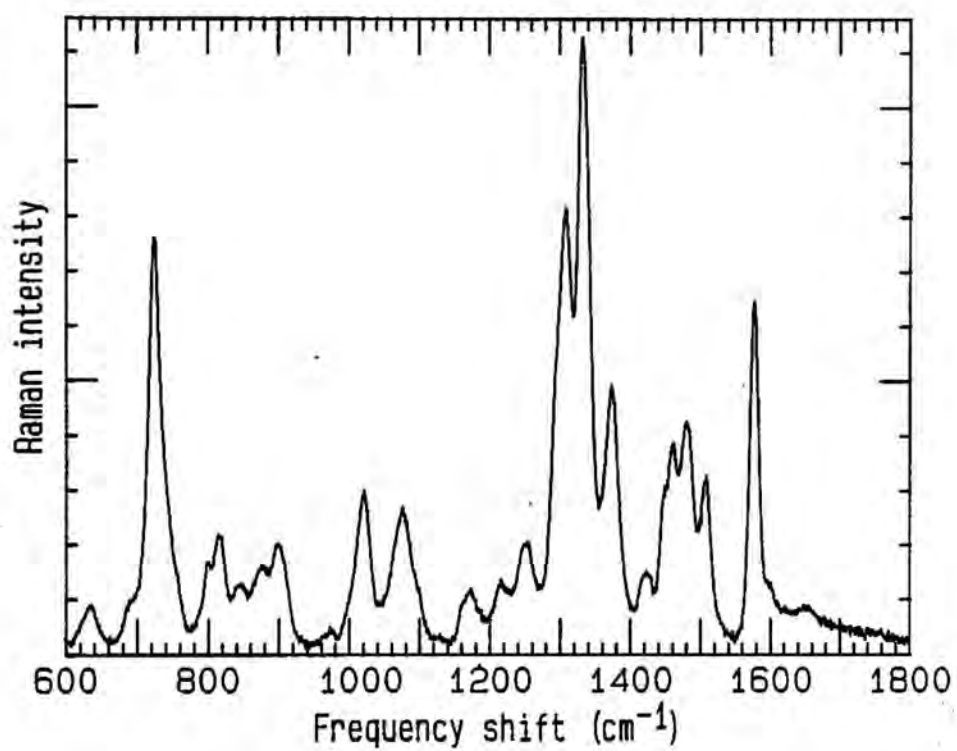
Figure 37. The Raman spectrum of pA2'pA2'pA, TEA salt, in methanol.

al., 1983; Dhingra & Sarma, 1978). X-ray analysis of the structure of crystals of A2'pC implied that a very compact right handed helix can exist; intramolecular O4' ribose-adenine stacking (rather than intermolecular base stacking) was proposed (Parthasarathy et al., 1982).

Bands in the spectra of pA2'pA2'pA and AMP that would be expected to be sensitive to base stacking, including bands at 1308, 1378, and 1510 cm^{-1}, have comparable intensities. In contrast, Prescott et al (1974) in a comparison of A3'pA3'pA and AMP concluded that 3-5A core contained base stacking. Comparable intensities for AMP and pA2'pA2'pA suggests that there is little or no base stacking in 2-5A. Further, the linear increase in the relative intensities of bands at 823, 1308, 1338 and 1510 cm^{-1}, as temperature is increased from 16 - 90°C (Figure 35), suggests that the 2-5A molecule is undergoing a change in structural equilibrium that may not be related to base stacking. A comparable study was performed on A3'pA3'pA and AMP which gave similar results (Figure 36). The Raman spectra of nucleic acid polymers with secondary structure such as poly(rA) and poly(A)·poly(U) (Small & Peticolas, 1971) or GpC (Prescott et al., 1974) revealed a sharp break point in a plot of temperature vs Raman intensity as the polymer melted. Such was not the case for AMP, pA2'pA2'pA, or A3'pA3'pA.

V.C. Raman Spectra of Isomers of 2',5'-oligoadenylaytes

V.C.1. Linkage Isomers

Spectra of pA2'pA2'pA, A3'pA3'pA A2p'A2'pA, and pA3'pA3'pA were examined to investigate the importance of the 2',5'-

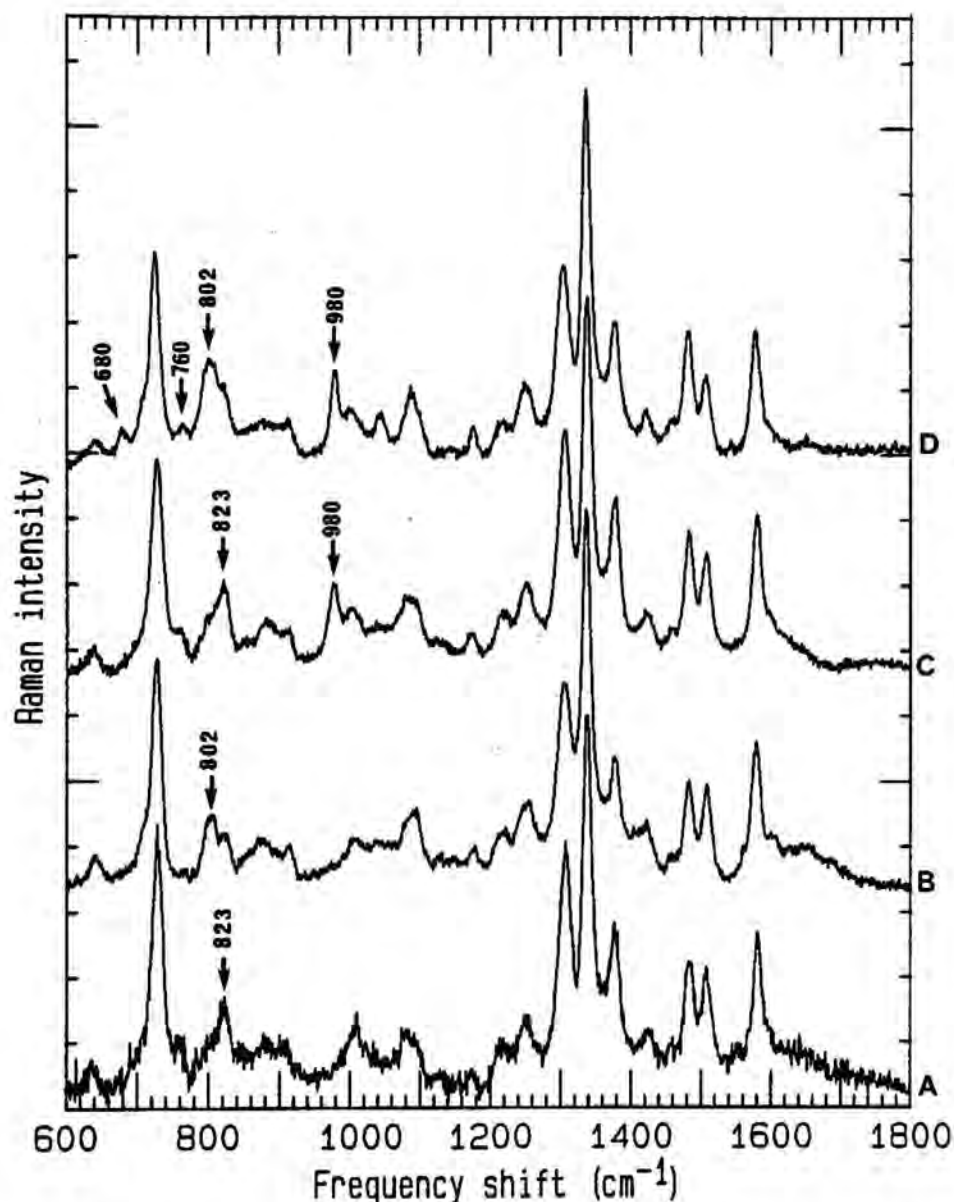**Figure 38.** Comparison of the Raman spectra of 2',5'- and 3',5'-oligoadenylates. (a) A2'pA2'pA in water pH 7.3, (b) Ap3'pA3'pA in water ph 7.3, (c) pA2'pA2'pA, ammonium salt, in water, pH 7.3, (d) pA3'pA3'pA, sodium salt, in 0.15 M NaCl buffered with 10 mM HEPES pH 7.4.

phosphodiester bond on Raman active modes. In general, the spectra of the 3',5'-linked and the 2',5'-linked oligoadenylates were very similar. For example, the $PO_3^=$ mode at 980 cm^{-1} (Rimai et al., 1969) was observed for both pA2'pA2'pA and pA3'pA3'pA (Figure 38c,d). pA3'pA3'pA had low intensity but well-resolved bands at 680 and 760 cm^{-1} (Figure 38d); these modes appeared as shoulders on the 729 cm^{-1} band of pA2'pA2'pA (Figure 38c). The ratio of the intensities at 1510 cm^{-1} and 1482 cm^{-1} was smaller in 3-5A than in 2-5A (Figure 38c,d).

The major difference between A2'pA2'pA and A3'pA3'pA was in the frequency of the furanose-phosphodiester marker bands found in the 800-825 cm^{-1} region of the spectrum (Figure 39). The Raman spectrum of 3',5'-linked trimer core, A3'pA3'pA, revealed the presence of a strong furanose-phosphodiester mode at 802 cm^{-1} and a relatively weaker mode at 820 cm^{-1}. 2',5'-Oligoadenylates contained both of these furanose-phosphodiester bands but the band at 823 cm^{-1} was stronger and sharper relative to the 820 cm^{-1} band of 3-5A. The form of 2',5'-oligoadenylate which is capable of activating the cellular endonuclease, pppA2'pA2'pA, had the sharpest band at 823 cm^{-1} (Figure 39e).

pA3'pA3'pA but not A3'pA3'pA has weak but well-resolved bands at 680 and 760 cm^{-1} that were significantly less discernable in both pA2'pA2'pA and A2'pA2'pA (Figure 39). These bands are also not present in poly(rA) (Prescott 1974). Ramai et al. (1969) assigned bands at these positions to the polyphosphate chain at the 5'-terminus of ADP and ATP because they were absent in AMP (see Figure 16). This assignment does not explain our results since
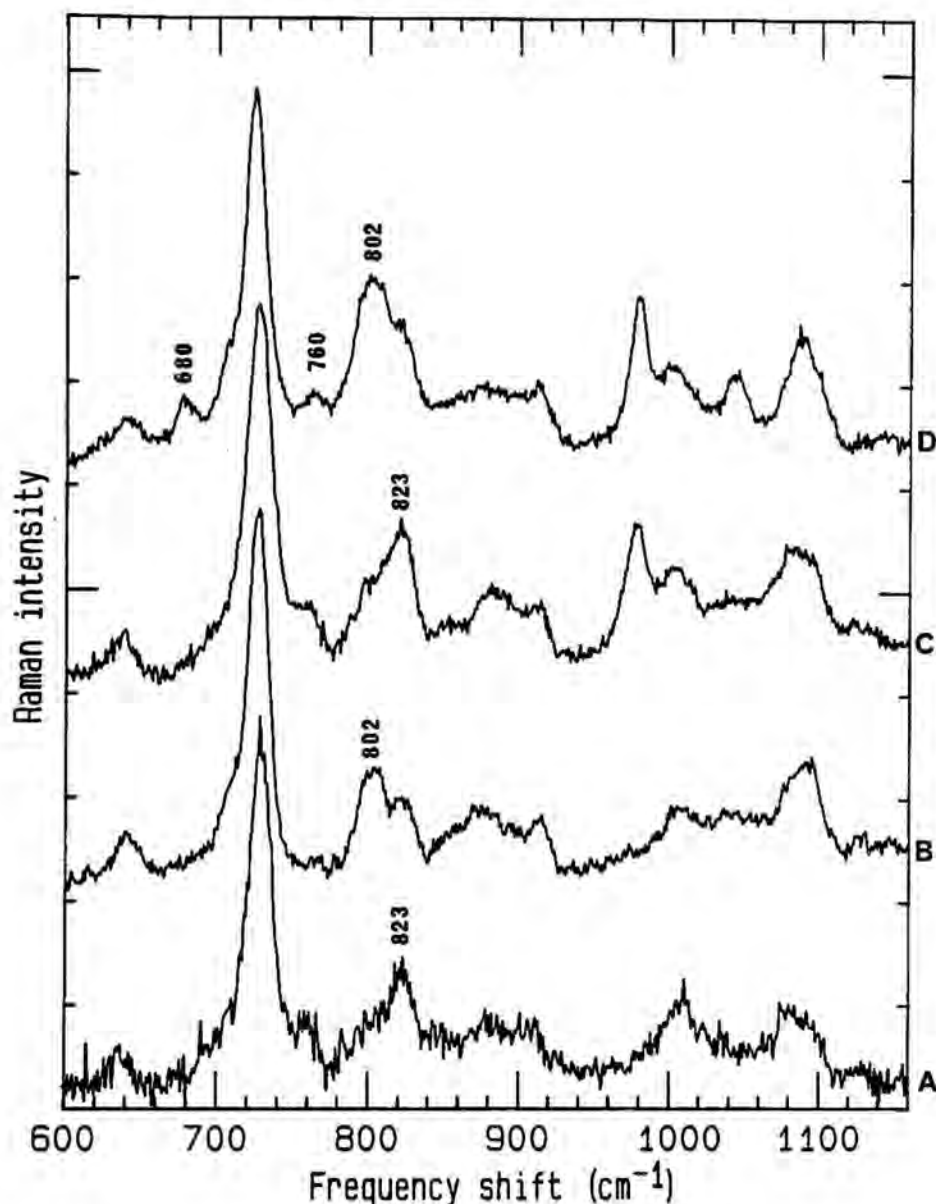
Figure 39. Windowed Raman spectra from Figure 38 comparing the base, ribose, and phosphate modes of 2',5' and 3',5'-oligoadenylates. (a) A2'pA2'pA in water pH 7.3, (b) A3'pA3'pA in water ph 7.3, (c) pA2'pA2'pA, ammonium salt, in water, pH 7.3, (d) pA3'pA3'pA, sodium salt, in 0.15 M NaCl/10 mM HEPES pH 7.4.

pA3'pA3'pA does not contain polyphosphate. Preliminary studies of pA3'pA2'pA and pA2'pA3'pA have provided further clues to the nature of the 680 and 760 cm^{-1} bands in oligonucleotides (Figure 40a,b). When the first ribose is 3',5'-linked, as in pA3'pA2'pA, both the 680 and 760 cm^{-1} bands are present (Figure 41c), as observed with pA3'pA3'pA (Figure 41d). However, when the first linkage is 2',5'-linked, as in pA2'pA3'pA (Figure 41b), the Raman spectrum appears similar to pA2'pA2'pA (Figure 41a), which lacks well-resolved bands at 680 and 760 cm^{-1}. These results imply that the 680 and 760 cm^{-1} bands in oligonucleotides may arise from a phosphate group at the 5'-terminus of certain oligonucleotides. Changes in backbone parameters such as the glycosyl torsion angle, which may accompany differences in the phosphodiester linkage, may account for the observed difference between 2',5'- and 3',5'-linked oligonucleotides.

V.C.2. Chain Length Oligomers

The Raman spectra of the "family" of cores, dimer, trimer, and tetramer in saline HEPES pH 7.4, were obtained (Figure 42). The dimer and trimer cores do not bind RNase L very efficiently but the tetramer core is reported to bind RNase L with only 10-fold less activity than its corresponding 5'-monophosphate, pA2'pA2'pA2'pA (Torrence et al., 1983). It is thought that the longer chain is capable of slipping into the binding site as a result of having the minimum, pA2'pA2'pA, structure. The spectrum of tetramer core (Figure 42c) shows intensity differences in the base modes of the spectrum that were reported previously to be sensitive to base
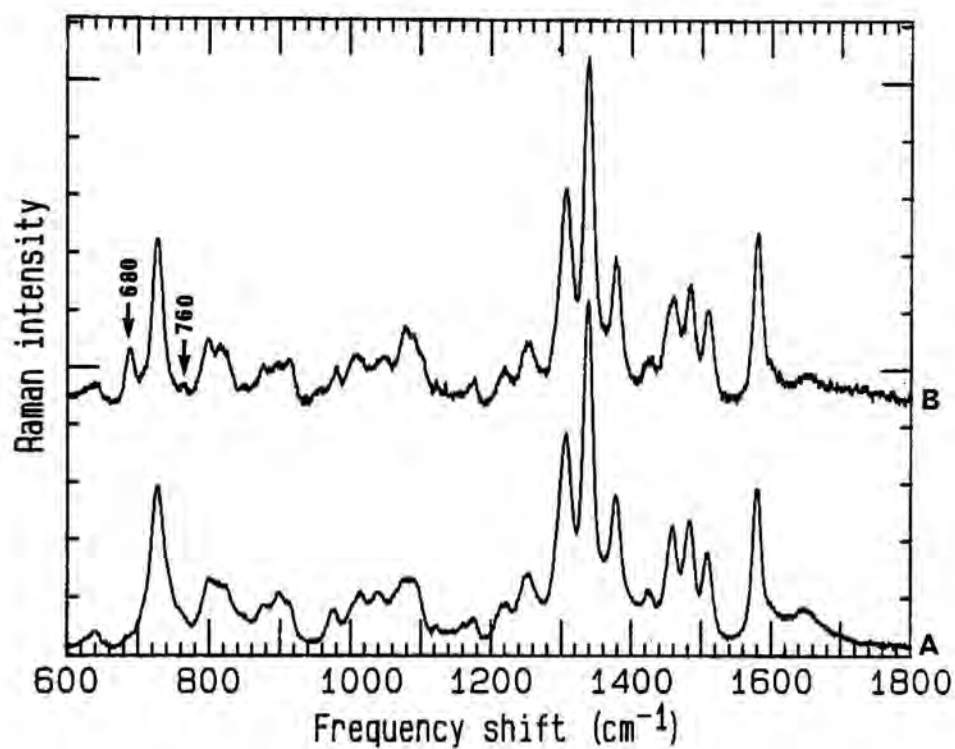
Figure 40. Raman spectra of the linkage isomers pA2'pA3'pA and pA3'pA2'pA, TEA salts, in 0.15 M NaCl buffered with 10 mM HEPES pH 6.8. (a) pA2'pA3'pA (b) pA3'pA2'pA.
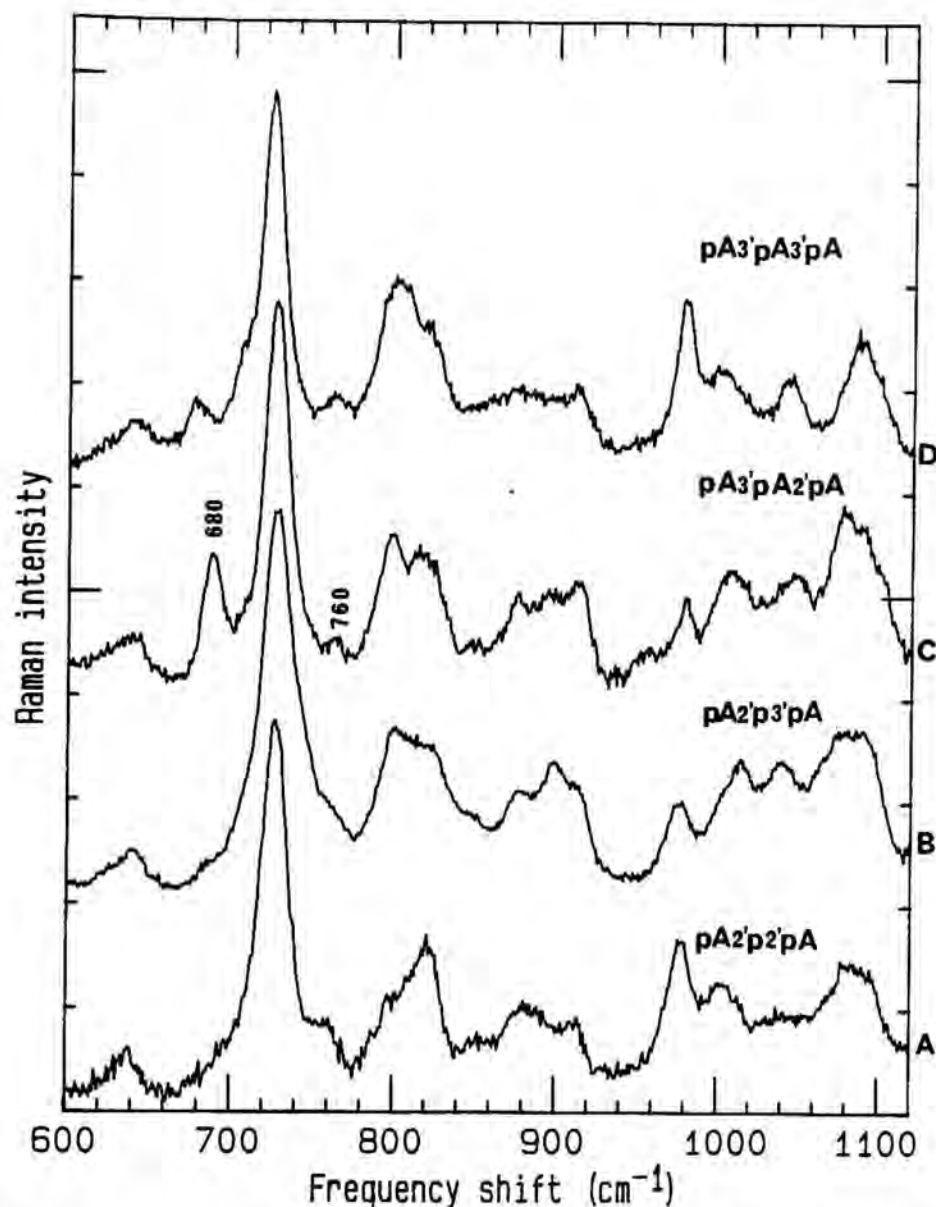
Figure 41. Windowed Raman spectra from Figure 40 comparing the base, ribose, and phosphate modes of pA2'pA3'pA and pA3'pA2'pA in 0.15 M NaCl/10 mM HEPES pH 6.8. Windowed spectra of pA2'pA2'pA and of pA3'pA3'pA are shown for comparison. (a) pA2'pA2'pA, ammonium salt, in water, pH 7.3 (b) pA2'pA3'pA in saline HEPES pH 6.8 (c) pA3'pA2'pA in saline HEPES pH 6.8 (d) pA3'pA3'pA in saline HEPES pH 7.3.
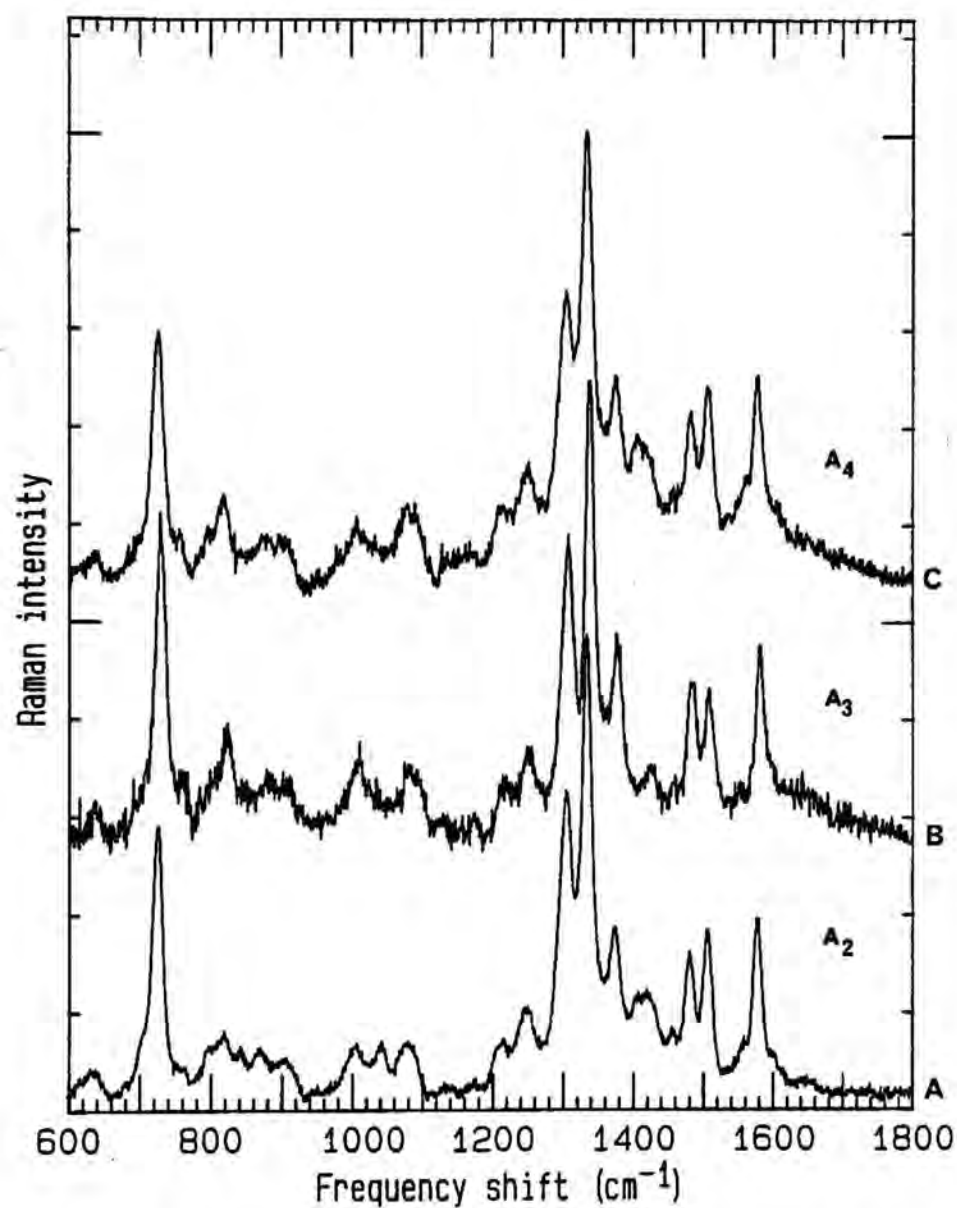
Figure 42. Raman spectra of A2'pA, A2'pA2'pA, and A2'pA2'pA2'pA.

(a) A2'pA in 0.15 M NaCl/10 mM HEPES pH 6.8 (b) A2'pA2'pA in water

pH 7.3 (c) A2'pA2'pA2'pA in 0.15 M NaCl/10 mM HEPES pH 6.8.

secondary structure found in tetramer core that may facilitate its ability to bind RNase L. The chain length isomers also differ slightly in the intensity of the 802 cm^{-1} shoulder intensity that arises from the backbone-ribose modes. The significance of the ribose-backbone modes are discussed under Conclusions.

The addition of 5'-phosphate to the chain length isomers results in dimer, trimer, and tetramer 5'-monophosphates. As mentioned above, these monophosphates are 10-100 times more active than the corresponding cores in antagonizing the action of pppA2'pA2'pA (Torrence et al., 1983). In this family, elongation of the oligonucleotide chain does not lead to a substantial increase in 2-5A antagonistic activity (Torrence et al.,1983). The Raman spectra of the 5'-phosphorylated 2-5A's were virtually identical and support the chain length/activity correlation (Figure 43). Small differences are noted in the ribose backbone region, 800-850 cm^{-1} and in the O=P=O symmetric stretch at 1090 cm^{-1}. The differences in the 1090 cm^{-1} region of pA2'pA2'pA2'pA probably result from differences in sample pH. These pH differences are evident by the weak intensity of the 980 cm^{-1} band and the increased intensity of the 1090 cm^{-1} band. Both of these bands are sensitive to pH (see the section entitled pH sensitive modes).

V.C.3. 8-Bromo isomers of pA2'pA2'pA

In light of the unusual biological activity of one of the bromine containing isomers of 2-5A, the solution spectra of three brominated isomers was examined. The Raman spectra of 8-bromoadenine, and 8-bromoadenosine were compared to the Raman
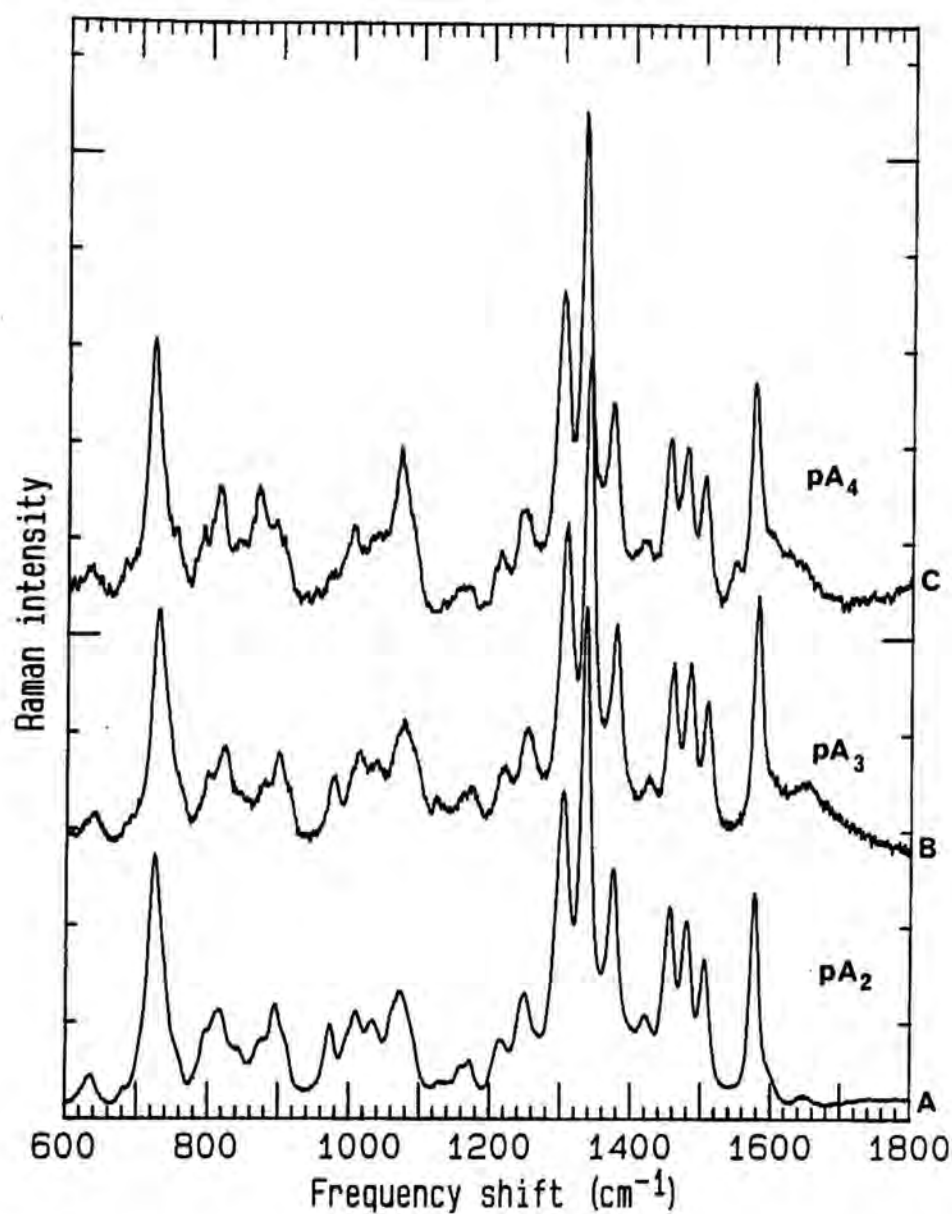
Figure 43. Raman spectra of 2-5A dimer, trimer, and tetramer monophosphates, TEA salt, in saline HEPES pH 6.8. (a) pA2'pA (b) pA2'pA2'pA (c) pA2'pA2'pA2'pA

spectrum of adenine (Figure 44) in order to determine the effect of bromination at C-8 on these compounds.

There are many differences in the spectra of adenine and 8-bromoadenine (Figure 44a,b). The four most substantial differences are as follows: First, the 729 cm^{-1} band in adenine shifted up in frequency to 758 cm^{-1}. Second, the intensity of the 1254 cm^{-1} band in 8-bromoadenine was increased relative to that observed in adenine. This mode was assigned by Tsuboi et al (1973) to the exocyclic N6 amino groups of adenine. Third, the base modes in the 1200-1400 cm^{-1} region changed in frequency. Fourth, a doublet band at 1440-1460 cm^{-1} appeared in the 8-bromoadenine spectrum. This area is assigned to the C8H stretching vibration of adenine (Fodor et al., 1985 and references therein).

The Raman spectra of the nucleosides were also compared. Virtually every part of the 8-bromoadenosine spectrum is different from adenosine (Figure 44c,d). The ring breathing band at 729 cm^{-1} in adenosine is shifted up to 765 cm^{-1} in 8-bromoadenosine. The ribose backbone bands at 860 cm^{-1} in adenosine are split into complex triplets extending from 850 to 950 cm^{-1} in the spectrum of 8-bromoadenosine. The N6 amino group bands at 1254 cm^{-1} in adenosine is shifted to a very intense doublet at 1220 cm^{-1} in 8-bromoadenosine. The base modes from 1280-1420 cm^{-1} in 8-bromoadenosine are different in intensity and position compared to adenosine. There is a strong band at 1460 cm^{-1} in 8-bromoadenosine that is in the region assigned to the C8 substitution of the adenine base. And finally, the 1580 cm^{-1} band in adenosine is split into two bands at 1580 and 1610 cm^{-1}.
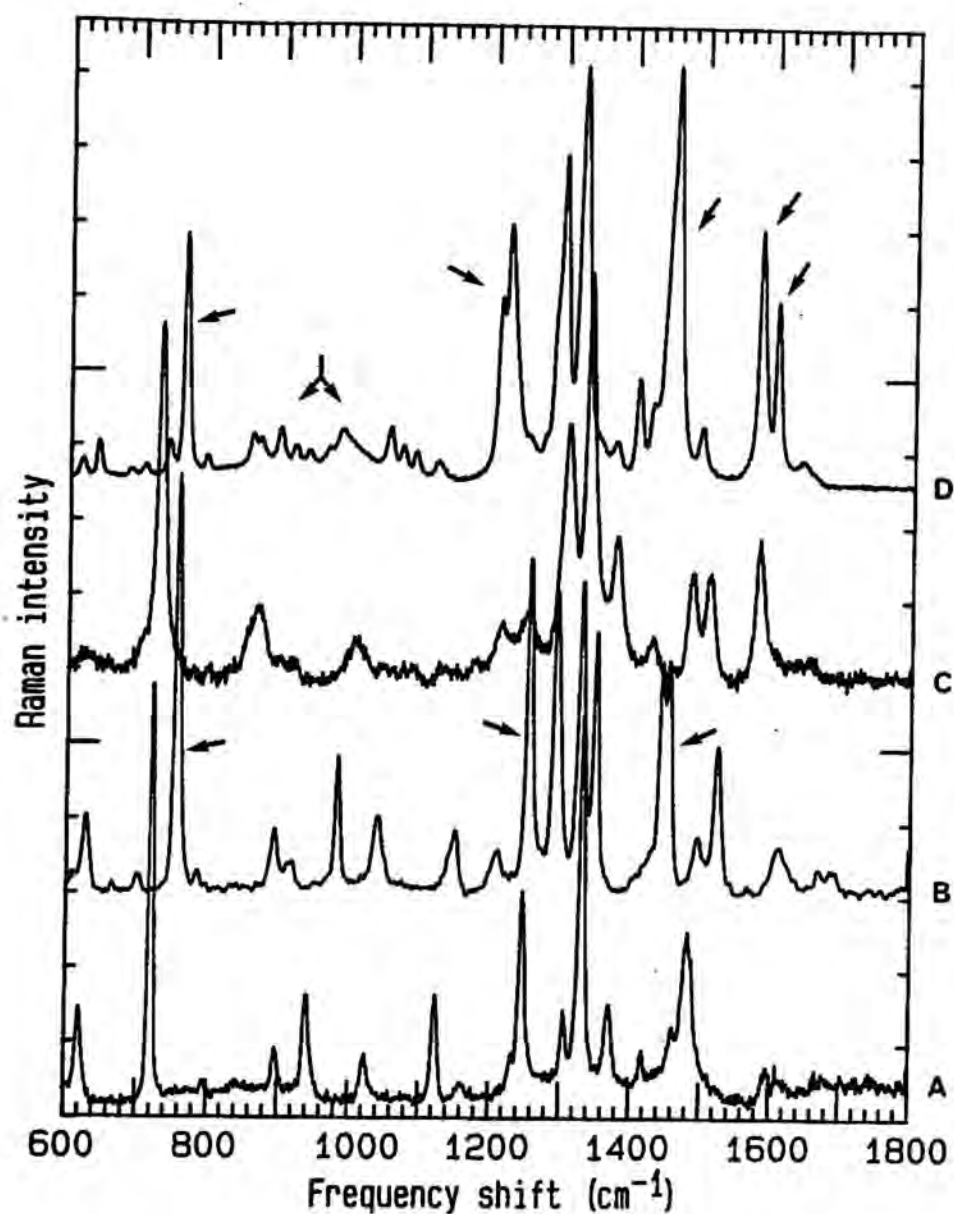
Figure 44. Raman spectrum of (a) adenine powder (b) 8-bromoadenine powder (c) adenosine (d) 8-bromoadenosine 0.15 M NaCl buffered with 10 mM HEPES was layered on top of the powder sample to act as a heat sink.

The Raman spectrum of pA2'p(8BrA)2'pA, pA2'(8BrA)2'p(8BrA), and p(8BrA)2'pA2'pA are depicted in Figure 45a,b. These are complex spectra that are significantly different from the spectra of pA2'pA2'pA (see Figure 38c). However, four areas of these spectra contain interesting information that may reveal clues to understanding the unexpected ability of pA2'(8BrA)2'p(8BrA) to bind RNase L. (i) In each brominated analogue of 2-5A, the characteristic adenine ring breathing band at 660-780 cm^{-1} is split. This probably arises from the dual populations of adenine and 8-bromoadenine rings within each molecule. The ring bands of p(8BrA)2'pA2'pA and pA2'(8BrA)2'pA are split in the same manner resulting in a new breathing mode at 685 cm^{-1} in addition to the band at 729 cm^{-1} (Figure 45a,c). The biologically active pA2'p(8BrA)2'p(8BrA) shows a different pattern of splitting with the new breathing mode at 760 cm^{-1} (Figure 45b) in addition to the 729 cm^{-1} band. This shift from 729 to 760 is similar to the one observed for adenine (729 to 758 cm^{-1}) and adenosine (729 to 765 cm^{-1}). (ii) The 1254 cm^{-1} band assigned to the exocyclic N6 amino group of adenine (Tsuboi, 1973) is shifted to 1240 cm^{-1} and markedly sharper in the spectrum of the biologically active analogue, pA2'p(8BrA)2'p(8BrA). (iii) The characteristic adenine triplet at 1308, 1338, and 1378 cm^{-1} is shifted and changed in intensity in pA2'p(8BrA)2'p(8BrA) compared to the other two 8-bromo isomers and pA2'pA2'pA. (iv) The intensity of the 1460 cm^{-1} band is different in all three spectra but the most conspicuous change in intensity and band pattern occurs from 1420-1520 cm^{-1}. Peaks at 1480 and 1510 cm^{-1} in pA2'pA(8BrA)2'pA and p(8BrA)2'pA2'pA are reduced to
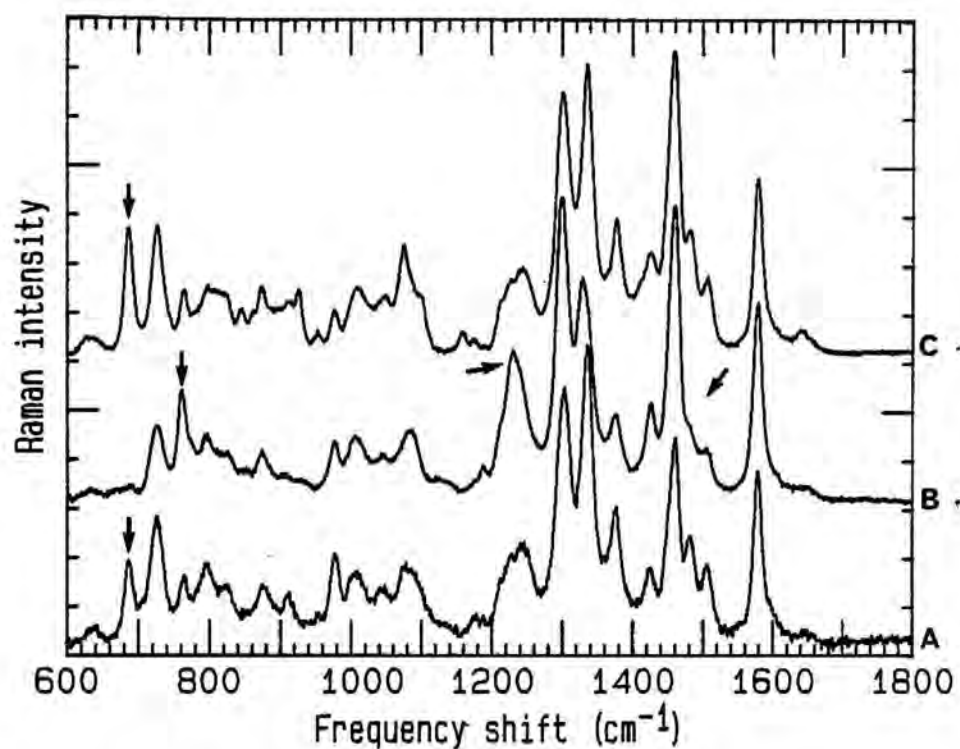
Figure 45. Raman spectra of the 8-Bromo isomers of 2',5'-oligoadenylates in 0.15 M NaCL buffered with 10 mM HEPES pH 7.3. (a) $pA2'pA^{8Br}2'pA$ (b) $pA2'A^{8Br}2'pA^{8Br}$ (c) $pA^{8Br}2'pA2'pA$.

shoulders in the 1460 cm^{-1} peak in the spectrum of the biologically active pA2'(8BrA)2'p(8BrA).

Earlier studies on 2-5A's implicated the first base as important in binding to RNase L, but suggested that the middle base is not important for either binding or activation (reviewed by Torrence 1985). In light of this, it is not surprising that p(8BrA)2'pA2'pA does not bind RNase L. On the other hand, it is not clear why pA2'p(8BrA)2'pA does not bind RNase L since the middle base is not reported to be important in this interaction. Bromination of the middle base may disrupt the conformation of the molecule in a region important for binding. Because of the considerable complexity of the ribose-phosphodiester backbone region of these spectra, little information concerning backbone orientation or ribose pucker can be obtained. However, the results summarized above demonstrate that the Raman spectra of the biologically active pA2'p(8BrA)2'p(8BrA) (Torrence et al., 1987) possesses distinct differences from the spectra of the two non-biologically active counterparts. These include a higher frequency for the adenine ring breathing mode (760 cm^{-1}), and an increase in intensity and shift of the 1254 cm^{-1} band that arises from the exocyclic amino groups. Therefore, the biologically active analogue has structural features that distinguish it from the inactive analogues by Raman spectroscopy. The details of these structural differences can not yet be clearly defined, but may be related to the overall geometry of the adenine ring and/or the environment of the exocyclic amino groups. The relationship of these structural changes to differences in biological activity is purely speculative.

For example, one may speculate that differences between the Raman spectrum pA2'p(8BrA)2'p(8BrA) and the other two brominated analogues result from stable solution interactions, i.e. hydrogen bonding of the exocyclic N6 amino groups of the former. A hydrogen bonding interaction is postulated because the 1254 cm^{-1} band assigned to the C6 amino group of adenine is changed both in intensity and in frequency. This could explain the shift to 760 cm^{-1} ring breathing band and the change in bands at 1308, 1378, 1510 cm^{-1}. If the molecule has inter- or intra-molecular hydrogen bonding then base-base interactions (stacking) may also occur. This proposed base stacking may not affect the intensity of bands sensitive to base stacking in 3',5'-linked nucleic acids. However, the observation that the stacking sensitive bands are different in pA2'(8BrA)2'p(8BrA) relative to other brominated analogues suggests that base-base interactions may be present.

Biological studies suggest that the syn or anti conformation of the third base may determine whether the isomer of 2-5A is capable of activating RNase L since bromination at the C8 position of adenine probably forces the base into a syn conformation. Bromination of the last two bases may force an overall conformation that is similar to that induced by the 5'-terminal triphosphate of pppA2'pA2'pA. This would explain why pA2'(8BrA)2'p(8BrA), a monophosphate, can inhibit protein synthesis in cell free extracts (Torrence et al., 1987).

V.D. Raman Studies on Protein-Nucleic Acid Interaction

V.D.1. Purification of the monoclonal antibody 3AC9

The method used to purify a protein used for Raman (or any) binding studies must be chosen to give the highest purity while subjecting the protein to mild purification conditions. The conventional methods available for the purification of antibodies are of four general types:

i. Affinity chromatography using protein A Sepharose. This method is normally suitable when the monoclonal antibody is of the IgG class and contamination by other (i.e. host proteins) IgG is not critical. Murine IgG_1 binds poorly to protein A but yields can be increased by binding at high pH.

ii. Affinity chromatography using immobilized antigen. This method is suitable when pure antigen is available and the Ab-Ag dissociation constant is not very low or very high.

iii. Ion exchange. This method is suitable when no pure antigen is available, when the monoclonal antibody is sensitive to elution conditions such as salt concentration or pH, when the monoclonal antibody is required pure of all contaminating Ig, or when the antibody does not bind to Protein A, or when large scale production is intended.

iv. Gel filtration. This method is used in combination with other techniques or when the antibody is of the IgM class.

New advances in high performance liquid chromatography (HPLC) and the availability of new ion exchange resins that provide for the efficient and mild extraction of biologically active

proteins allowed employment of HPLC columns for the purification of the mouse monoclonal antibody 3AC9 from murine ascites fluid.

Starting material containing the antibody was murine ascites fluid diluted 1:3 in PBS, pH 7.4. A typical sample contained 20-50 OD_{280} units. The starting material was dialyzed into 20 mM Tris pH 8.5 (buffer A). Typical application volume to the DEAE 5PW column was 5-10 mL of desalted ascites fluid filtered through a 0.22 micron filter. The sample was applied to the column through port three of the M-6000 A Waters HPLC pump followed by a 5 minute isocratic wash with buffer A. The column was eluted with a gradient to 250 mM NaCl pH 7.0 (Figure 46). In one preparation where 38.24 OD units of ascites was applied to the column, 35.6 OD units were recovered from the column giving a 93.1% recovery of applied material. A small portion, 0.893 OD units, did not interact with the column and was recovered in the flow through. A total of 2.1 OD units of material was recovered from the column in a clean up gradient. A gel of the protein at this stage of purification revealed a high molecular weight contaminant which was subsequently identified as transferrin.

Fractions from the DEAE 5PW gradient were tested for immunoreactivity using an ELISA assay as described under Materials and Methods. Immunoreactive peaks were pooled and applied to a Pharmacia chromatofocusing column. This column was eluted with a polybuffer74 pH gradient (from pH 6 to pH 4) which only eluted the monoclonal antibody (Figure 47). Recovery from the Mono-P step was 65 %. This step removed the transferrin but introduced ampholytes from the polybuffer 74 which into the sample. The presence of these ampholytes interfered with the migration of the protein on the PAGE
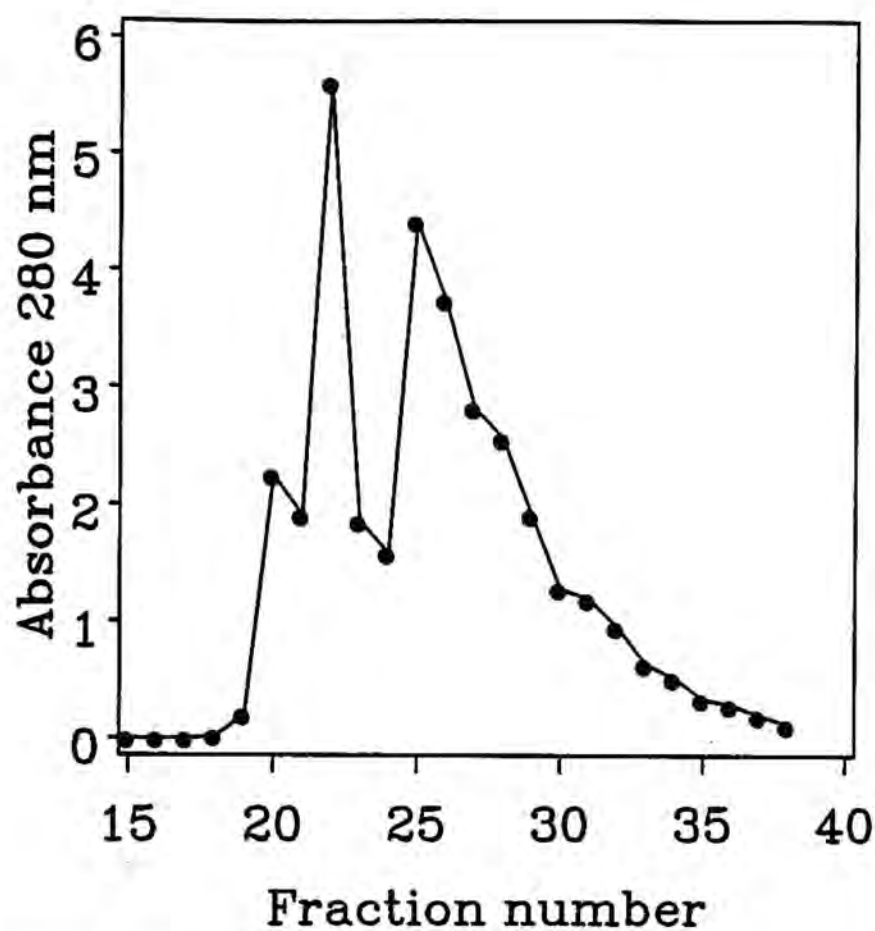
Figure 46. A_{280} profile of the DEAE 5-PW HPLC column.

(a) transferrin (b) IgG (c) albumin
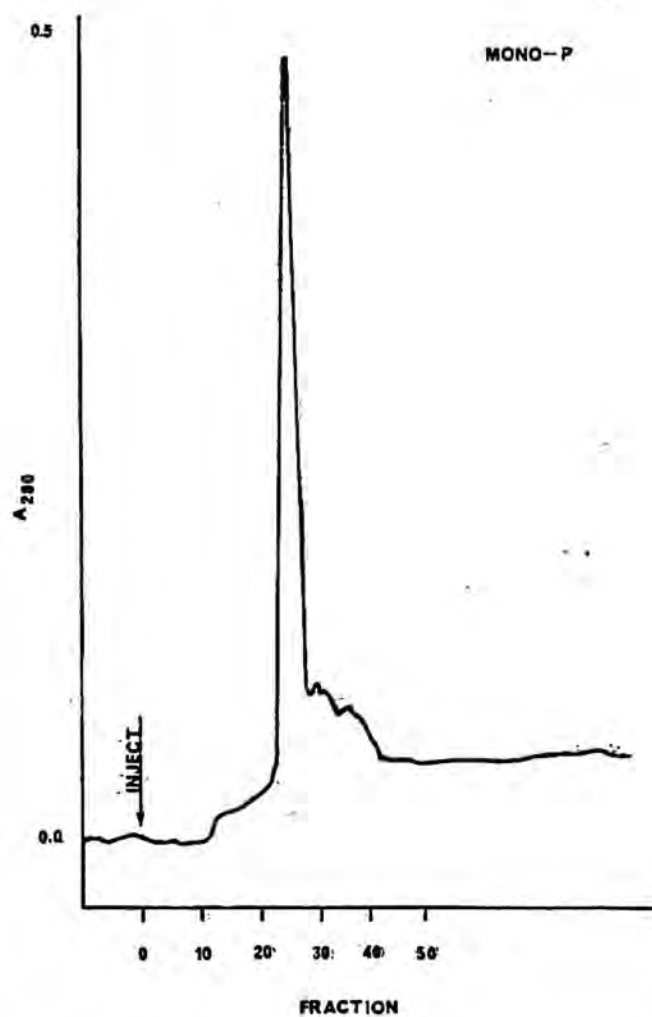
Figure 47. A_{280} profile of the Mono-P chromatofocusing column.

gels used to assess purity. The ampholytes were removed by
chromatography of the peak fractions through tandem Pharmacia
Superose 6+12 gel filtration columns. No detectable material was
lost on the gel filtration columns. The peak fractions were pooled
and concentrated prior to storage at -20° C. The procedure detailed
above resulted in the purification of about 1mg of IgG from 35 OD
units of starting material.

The results of this purification method demonstrate that
substantially purified IgG monoclonal antibody can be rapidly and
efficiently separated from murine ascites using anion exchange HPLC
with a linear sodium phosphate gradient, pH 8.5 to 7.0. Highly
purified monoclonal antibody was then obtained after a second step
that employed a chromatofocusing column eluted with a pH gradient of
pH 6 to pH 5. Removal of the ampholytes that were introduced in the
second step was accomplished using two tandem Superose gel
filtration columns of different pore sizes. Because of the high
protein loads that were applied to each column, a combination of
methods were required to obtain antibody of high purity (Figure 48).

V.D.2. Raman Studies of Protein Nucleic Acid Interactions.

Study of binding interactions between proteins and nucleic
acids require that the Raman instrument be capable of resolving a
nucleotide spectrum at concentrations as low as 2-5 mM. Since this
concentration range represents the low end of the instrument's
sensitivity, considerable effort was made to ensure that the
instrument was operating a peak efficiency. The optics were
aligned, the holographic gratings were changed to 600 groove/cm,
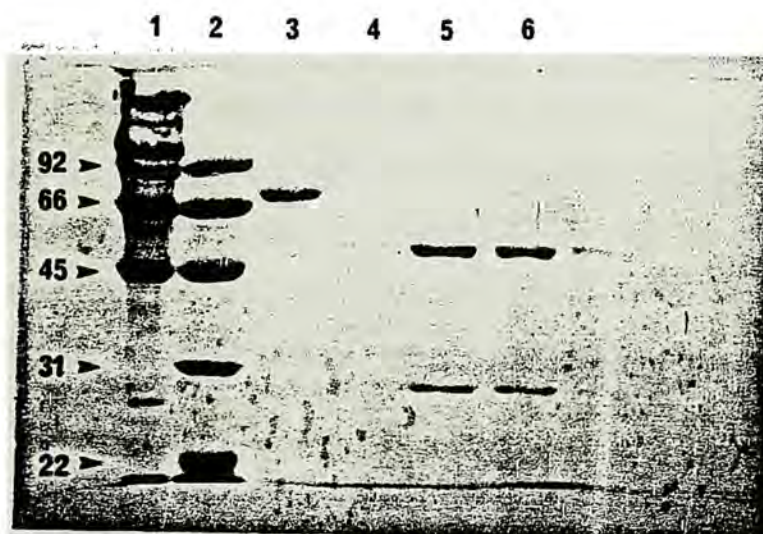
Figure 48. 12% SDS PAGE gel of the purified HY21-3AC9 monoclonal antibody.

Lane 1, High molecular weight standard; Lane 2, Low molecular weight standard; Lane 3, Transferrin removed by the Mono-P step; Lane 4, blank; Lane 5, HY21-3AC9 Monoclonal antibody; Lane 6, HY21-3AC9 Monoclonal antibody.

and a reticon detector was installed because of its superior dynamic range of response when compared to a conventional photomultiplier tube. The diode array detector is at least 10 times more sensitive to light. The laser line was changed after experiments revealed less of a problem with fluorescence at 488 vs 514 nm. Once the instrument was converted to a configuration that gave the highest sensitivity, control experiments were initiated.

First, the Raman spectrum of 50 mM AMP was obtained (Figure 49). When the spectrum of 2.0 mM AMP was scanned, several problems were encountered. First, the scan time required to obtain a spectrum of this dilute sample was on the order of several hours. This required modification of software controlling the reticon detector. Second, poor humidity control of the instrumentation room and a small amount of water in the nitrogen to the detector led to icing and a loss of resolution. An in-line water trap was installed on the nitrogen line which appeared to solve the problem. A spectrum of 2.0 mM AMP was obtained (Figure 50).

It was our intention to use the same strategy employed by Yue et al (1984, 1986) in their studies of LADH and NADH. In these studies the Raman spectra of free protein, LADH, and of free cofactor, NADH were obtained. Next, the enzyme cofactor complex was formed by mixing the protein and ligand together in a known molar ratio. The spectrum of bound NADH was obtained by subtracting the spectrum of free LADH from the spectrum of bound LADH.

A control experiment using AMP and nonspecific rabbit IgG was performed as a negative control. It was important to exhibit the capability to resolve dilute nucleotide spectra from the much
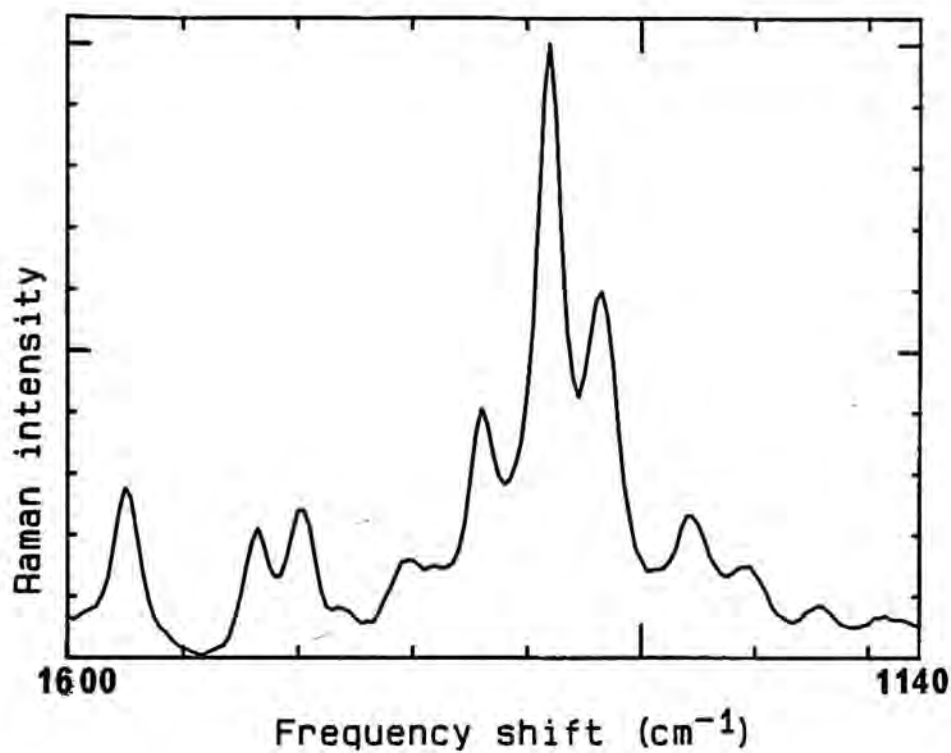
Figure 49. Raman spectrum of 50 mM AMP in 0.15 M NaCl pH 7.3. The spectrum was obtained at 15° C with 488 nm radiation, 200 mW power at the sample, a reticon detector, and 600 groove/cm holographic gratings.
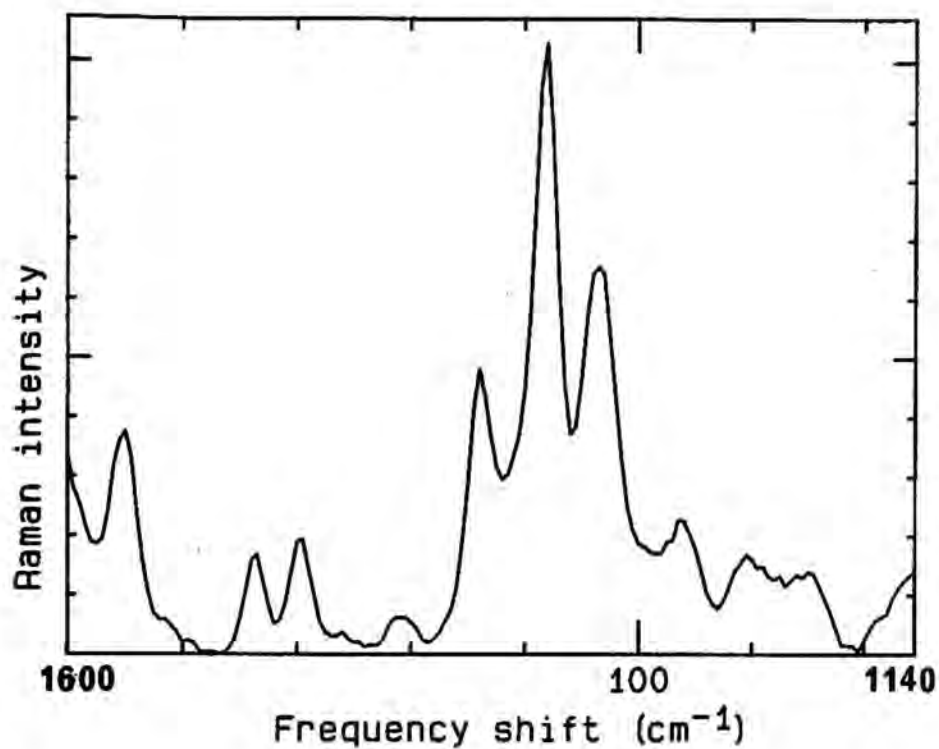
Figure 50. Raman spectrum of 2.0 mM AMP (free AMP) in 0.15 M NaCl.
The spectrum was obtained at 15° C with 488 nm radiation, 200 mW
power at the sample, a reticon detector, and 600 groove/cm
holographic gratings.

higher intensity protein signal. Spectra of free AMP (Figure 50) and of free rabbit IgG (Figure 51) were obtained. The bound rabbit IgG spectrum was obtained by mixing protein and nucleotide in a 1:2 molar ratio (Figure 52). Reconstitution conditions were carefully controlled. Buffers of the same ionic strength and pH were used to dissolve the samples before mixing. Next, the spectrum of free IgG was subtracted from the spectrum of bound IgG. Even with scan times up to 30 hours (Figure 53) a spectrum of 4.0 mM bound AMP could not be resolved. Six of these experiments were completed with various instrumentation and sample changes with similar results. The IgG protein signal was apparently too strong relative to the signal from the dilute nucleotide to allow completion of these experiments. That is, the signal to noise ratio for the nucleotide spectrum was too small. However, in the course of these experiments, significant progress was made with the instrumentation and software that ultimately resulted in an enhanced capability to obtain high quality Raman spectra of nucleic acid solutions with the visible laser.

The experiments detailed above should be readily accomplished with a UV laser. Less concentrated samples are required and, by employing the resonance Raman effect, the adenine bases can be selectively excited and thus minimize contributions from the protein. The capability to selectively excite nucleic acid bases is the great power of the resonance Raman method.
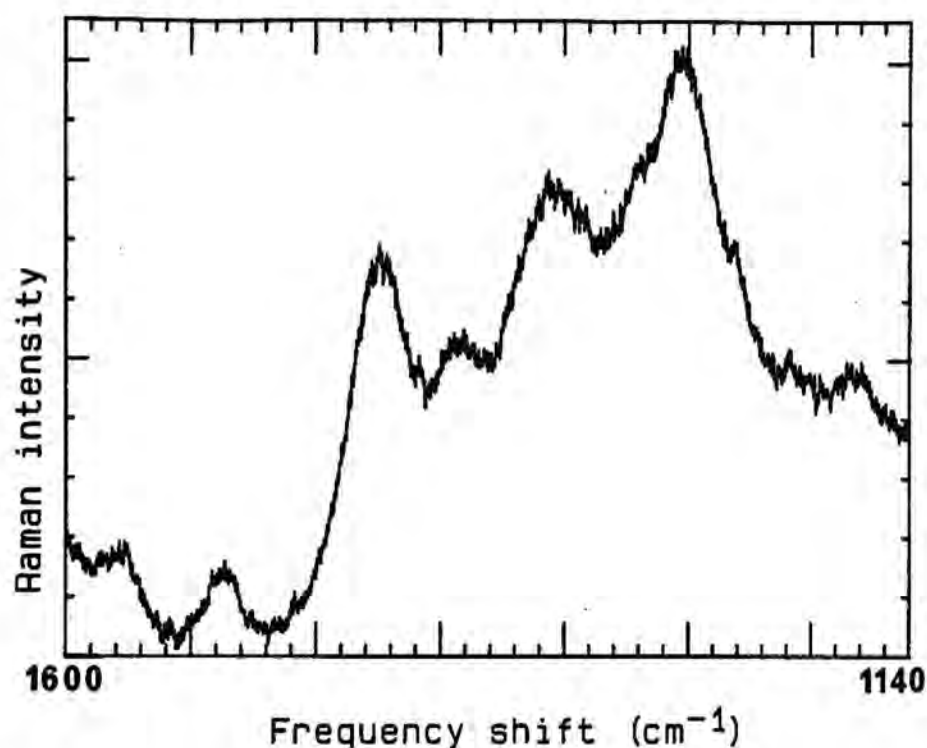
Figure 51. Raman spectrum of rabbit IgG (free IgG) in 0.15 M NaCl pH 7.3. The spectrum was obtained at 15° C with 488 nm light, 200 mW power at the sample, a reticon detector and 600 groove/cm holographic gratings.
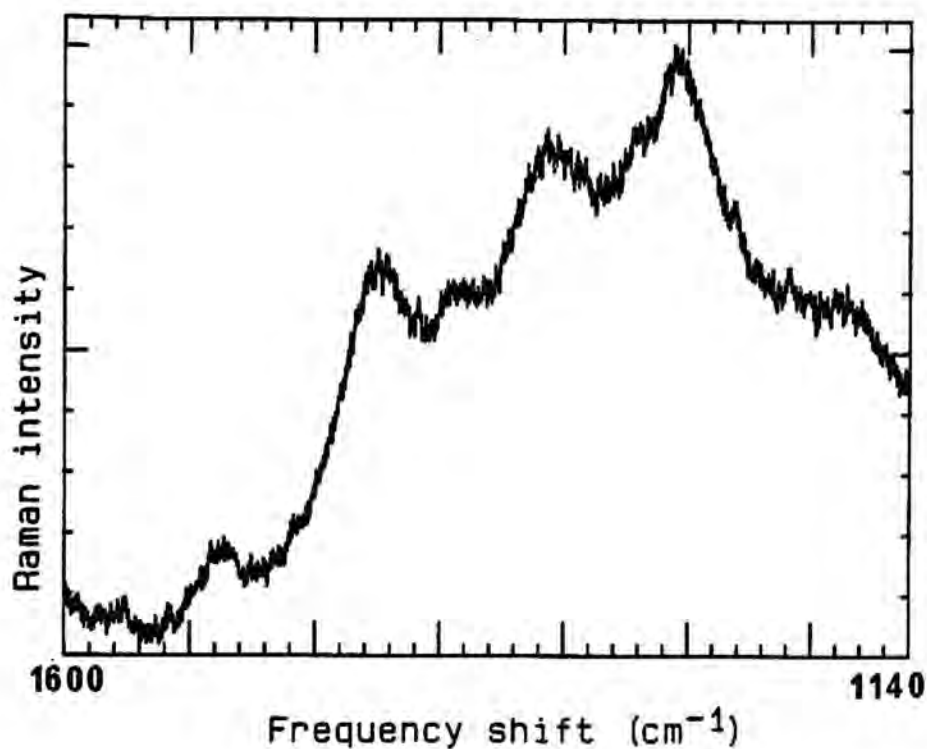
Figure 52. Raman spectrum of 2.0 mM rabbit IgG in solution with 4.0 mM AMP (bound IgG). The spectrum was obtained in 0.15 M NaCl at 15° C with 488 nm radiation, 200 mW power at the sample, a reticon detector, and 600 groove/cm holographic gratings.
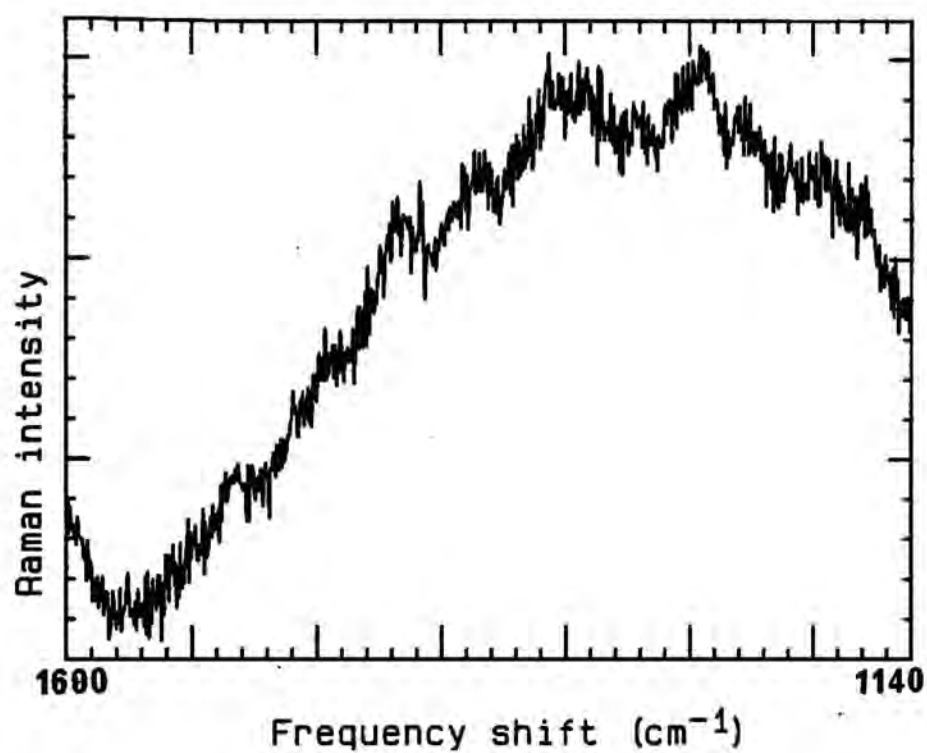
Figure 53. Difference spectrum of bound IgG - free IgG.

VI. Conclusions

A systematic approach that utilized published normal mode analysis (a method for calculating the positions of the bands in the vibrational spectrum) and model compounds was used to identify the positions of prominent base and ribose phosphate backbone peaks in the Raman spectrum of 2-5A (see Table II). Inspection of the structure of 2-5A (Figure 17) suggested experiments that could isolate portions of the molecule and provide information about the 2-5A molecule relative to model/control compounds.

The 5'-terminus of 2-5A was examined in pH experiments and found to have about the same pKa as AMP. This observation supported the hypothesis that the 5'-terminal phosphate of 2-5A in concentrated solution does not participate in stable solution interactions. The pH experiments also provided information about protonation of the adenine bases in 2-5A at pH 3.8. The Raman spectra of AMP and pA2'pA2'pA were similar at low pH indicating that the bases in the two compounds probably are in a similar environment in solution. The exocyclic N6 amino group of 2-5A is exchangeable in D_2O to ND_2 under mild conditions. The exchange experiment in which 2-5A was reconstituted in D_2O was designed to examine the C6-NH_2 portion of the molecule. The results suggested that the exocyclic amino groups of adenine in 2-5A are in an environment similar to that of AMP (Wartell et al., 1986).

Next, 2-5A was subjected to temperature studies in an effort to provide information about possible base stacking. A linear change in the intensities of several Raman bands reported to be sensitive to base stacking was observed suggesting that 2-5A has

little if any ordered stacking interaction in solution. Support for this hypothesis is also provided by the spectrum of 2-5A in methanol, a solvent that should disrupt secondary structure. Only small changes in the spectrum of pA2'pA2'pA in methanol were observed.

The study was completed by analysis of the Raman spectra of isomers of 2-5A. These spectra provided information about possible correlations between the Raman spectra and biological activity. Additional information about the identity of the Raman bands in the 2-5A spectrum was obtained by the analysis of the spectra of mixed linkage isomers and chain length isomers. A possible basis for the unusual activity of pA2'p(8BrA)2'p(8BrA) was also proposed. Specifically, the spectra indicated that the biologically active molecule was structurally distinct from the two inactive analogues analyzed.

The assignments reported here will be useful in studying the interaction of 2',5'-oligoadenylates with proteins. To that end, preliminary Raman experiments designed to investigate the interaction of 2-5A with gamma globulins were attempted. However, the spectra of AMP in the presence of non-immune gamma globulin lacked the necessary detail to permit analysis. The interaction of anti-2-5A antibodies and/or RNase L with 2-5A may be best approached using resonance Raman spectroscopy where the bands arising from the bases may be amplified relative to protein bands and where sample concentration can be dramatically lower.

The most informative portions of the Raman spectrum of pA2'pA2'pA were the phosphodiester-ribose pucker bands discussed in

the linkage isomers section. These spectra provided a possible answer as to why pppA2'pA2'pA is able to bind and activate RNase L, while pA2'pA2'pA only binds RNase L. The significance of phosphodiester-ribose pucker vibrational modes is discussed below.

Raman spectroscopy has been used previously to identify the overall geometry of the phosphodiester backbone of nucleic acids. This overall geometry is related to the pucker of the furanose ring. The Raman bands that arise from the backbone are often referred as markers for certain furanose ring puckers, i.e. C3'-endo marker band. A-genus DNA which contains a C3'-endo furanose conformation has a strong sharp band in the 807-815 cm^{-1} area (Erfurth et al., 1972; Erfurth et al., 1975; Goodwin & Brahms, 1978). Raman spectra of B and C-genus DNA has weak, broad bands at 835 and 875 cm^{-1}, respectively (Brown & Peticolas., 1975; Lu et al., 1975). For ribonucleotides, the Raman ribose C3'-endo marker bands are shifted up about 7 cm^{-1} to 814-822 cm^{-1} (Erfurth et al., 1972; Erfurth et al., 1975; Goodwin et al., 1978; Hartman et al., 1973; Peticolas & Tsuboi, 1979). Marker modes have been shown to exist in low temperature Raman scans of mononucleotides (Small & Peticolas, 1971), and in U3'pA, G3'pC an dT3'pdT (Thomas & Peticolas, 1983). Based on these results Peticolas et al. (1983) proposed that the position of the ribose marker mode for ribonucleotides in the 814-822 cm^{-1} range depends on the coupling through the 5'-ribose ester linkage. Assignment of the 823 cm^{-1} line in the spectrum of 2-5A as a phosphodiester backbone mode seems reasonable (Figure 54). Wartell and Harrell (1986) recently reported that an extra 823 cm^{-1} backbone band was required to reproduce the 800-850 cm^{-1} region of
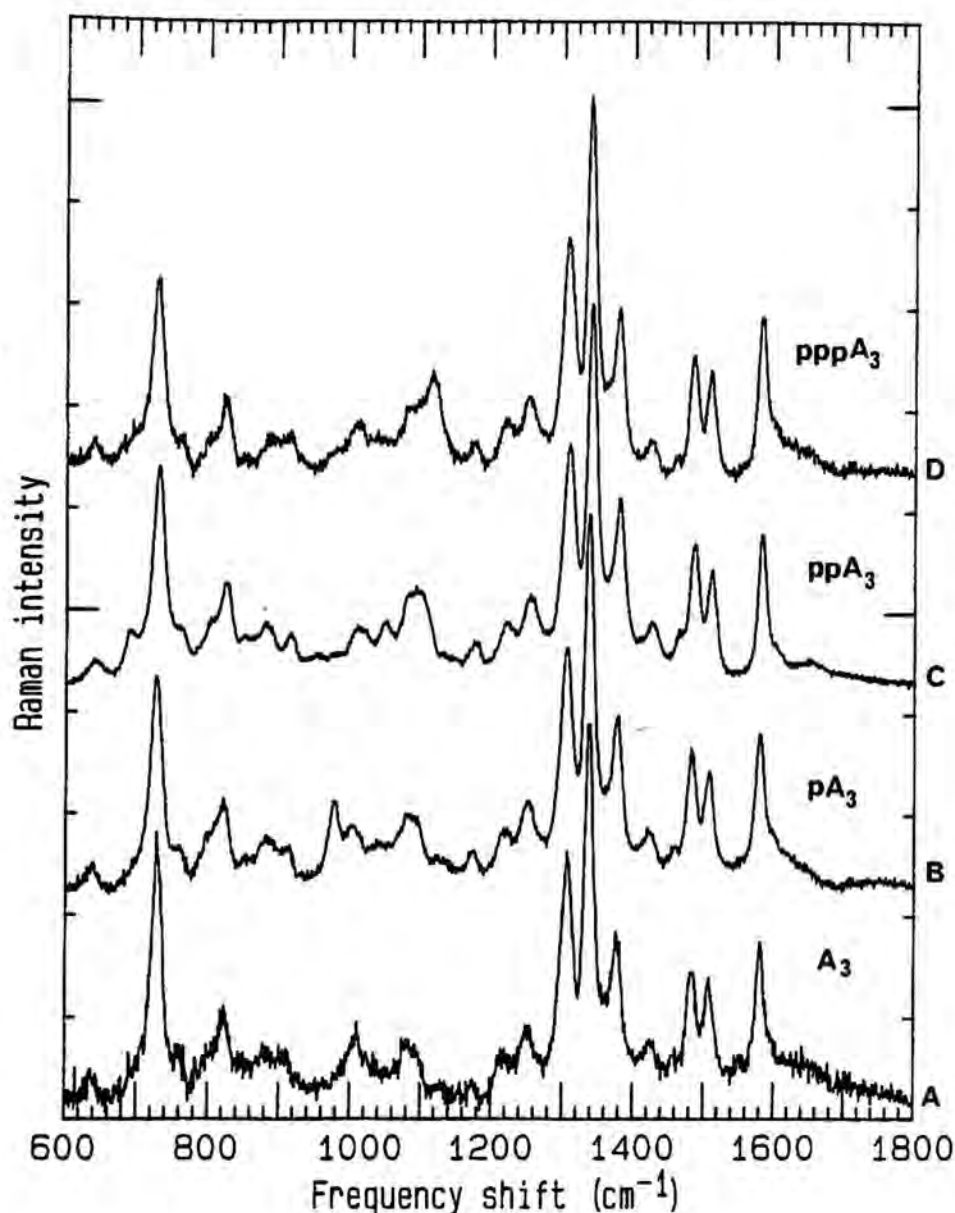
Figure 54. Raman spectra of 2-5A trimer core, monophosphate, diphosphate, and triphosphate. (a) A2'pA2'pA in water, pH 7.3 (b) pA2'pA2'pA ammonium salt, in water, pH 7.3 (c) ppA2'pA2'pA in saline HEPES pH 6.8, TEA salt (d) pppA2'pA2'pA ammonium salt, in water, pH 7.3.

poly[d(A-T)].poly[d(A-T)] by curve fitting procedures. The relationship, if any, of this band to the clearly visible 823 cm^{-1} band in the Raman spectra of 2-5A's is not yet known.

NMR studies have indicated that the ribose pucker of A2'pA2'pA is mixed at 20° C while the deoxy analogue, (3'dA)2'p(3'dA)2'p(3'dA), is almost exclusively C3'-endo at 20° C (Doornbos, et al., 1981,1983). If a mixed population of ribose puckers is observed by NMR, on a time scale of 10-6 sec, then Raman spectroscopy, on a time scale of <10-13 sec, should identify these populations of ribose pucker.

The major band at 823 cm^{-1} and the minor band at 802 cm^{-1} are assigned to phosphodiester-backbone vibrations in 2-5A's. These bands may reflect the relative predominance of one ribose pucker type over the other since the position of the backbone marker has been shown to be sensitive to the furanose pucker (Thomas & Peticolas, 1983). Further, the broadness or sharpness of the 823 cm^{-1} band may be influenced by furanose pucker or by changes in other torsion angles (Figure 54). One could speculate that the C2'-endo marker and the C3'-endo marker in the Raman spectra of 2',5'-oligoadenylates are shifted to the same frequency and that the peak at 823 cm^{-1} represents the sum of these two (or more) bands. If the two furanose marker bands are indeed shifted to the same frequency, then the shape of the band at 823 cm^{-1}, broad or sharp, may represent the relative predominance of one ribose pucker type over the other. In this case, the biologically active molecule, pppA2'pA2'pA, has a more defined ribose pucker, since the band at 823 cm^{-1} is substantially sharper than in the spectrum of

pA2'pA2'pA, (Figure 55). If the CD of the deoxy analogue of 2-5A is correct then a Raman spectrum of the compound could be used to confirm the position of the C3'-endo marker band in 2-5A. Another possibility is that the band at 823 cm^{-1} represents a sum of furanose puckers that occur within the C3'-endo family. If this is the case, then the biologically active pppA2'pA2'pA has a predominant member of this family of puckers (Figure 55). In either case, the Raman spectra demonstrate that the phosphodiester backbone and possibly the furanose pucker in the biologically active pppA2'pA2'pA differs from that found in non-biologically active forms of 2-5A and in 3',5'-oligoadenylates.

Further information on the structure of 2-5A's could be provided by obtaining the Raman spectrum of crystals of a compound such as A2'pG which has a known crystal structure determined by X-ray diffraction. Comparison of the Raman spectra of such a compound in its crystalline and solution states would provide direct evidence for the solution conformation of the dinucleotide. These experiments could be extended to 2-5A once several obstacles are overcome. First, high quality crystals of 2-5A must be obtained. Second, the x-ray structure of 2-5A must be solved. Third, the Raman spectra of 2-5A crystals must be obtained and compared to its solution spectrum. This would provide valuable information about the general structure of 2-5A and 2',5'-linked nucleic acids in general.

2',5'-Oligoadenylates probably present unique conformational properties that are important in binding and activating RNase L.
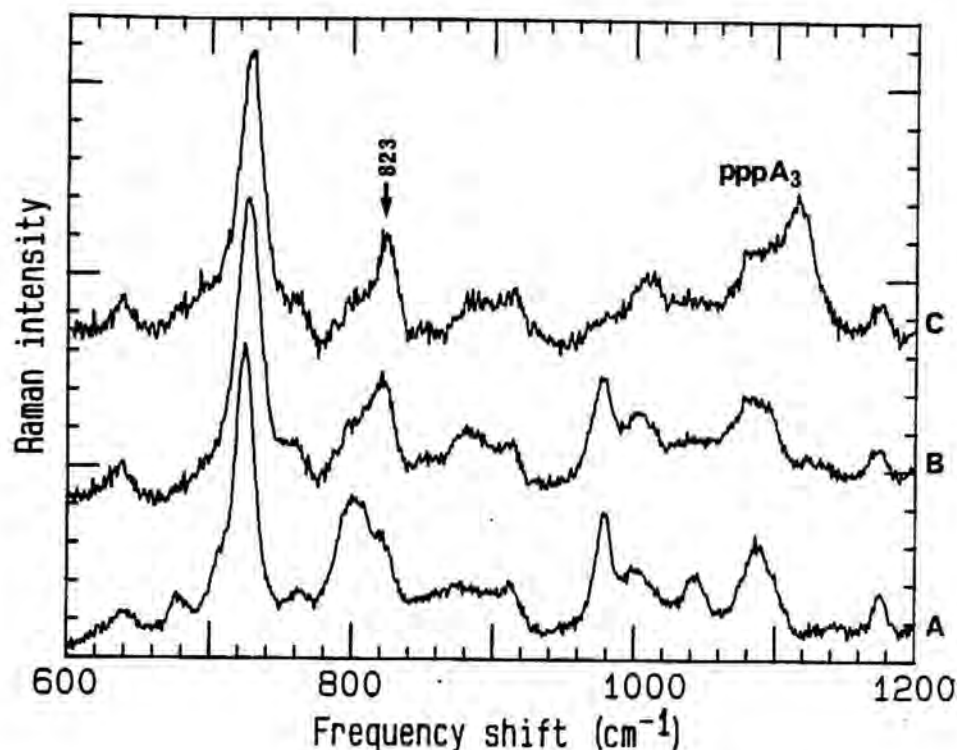
Figure 55. Comparison of the Raman phosphodiester modes in
pA3'pA3'pA, in pA2'pA2'pA, and in pppA2'pA2'pA. Windowed Raman
spectra of (a) pA3'pA3'pA in saline HEPES pH 7.4, sodium salt (b)
pA2'pA2'pA in water pH 7.3, ammonium salt (c) pppA2'pA2'pA in water
pH 7.3, ammonium salt.

Previous studies employing structural analogues of 2-5A have implicated the first 2',5'-linkage as being critical for binding to RNase L. The observation that a brominated monophosphate analogue of 2-5A retained biological activity suggests that the 5'-triphosphate may not be an absolute requirement for RNase L activation. The active analogue, pA2'p(8BrA)2'p(8BrA), was different from the other two bromo-analogues, p(8BrA)2'pA2'pA, and pA2'p(8BrA)2'pA, in regions of the spectrum that suggest a hydrogen bonded structure with possible base stacking.

VII. Appendix

VII.A. "Raman spectroscopy of the Interferon Induced 2',5'-Oligoadenylates," Joseph C. White, Robert W. Williams, and M. I. Johnston, in press.

Raman Spectroscopy of Interferon-Induced 2',5'-Linked Oligoadenylates[†]

Joseph C. White, Robert W. Williams, and Margaret I. Johnston*

* Address correspondence to this author.

1

[1] Abbreviations:

2-5A, trimer triphosphate, 5'-O-triphosphoryladenylyl(2',5')adenylyl
(2',5')adenosine, $pppA2'p(A2'p)_nA$, where n is usually 1-3; trimer monophosphate,
pA2'pA2'pA, 5'-O-monophosphoryladenylyl(2',5')adenylyl(2',5')adenosine;
pA2'pA3'pA, 5'-O-monophosphoryladenylyl(2',5')adenylyl(3',5')adenosine;
pA3'pA2'pA, 5'-O-monophosphoryladenylyl(3',5')adenylyl(2',5')adenosine;
trimer core, A2'pA2'pA, adenylyl(2',5')adenylyl(2',5')adenosine; A3'pA3'pA,
adenylyl(3',5')adenylyl(3',5')adenosine; $pA2'pA^{8Br}2'pA^{8Br}$, 5'-O-monophosphoryl-
adenylyl(2',5')8-bromoadenylyl 8-bromoadenosine; dsRNA, double-stranded
RNA; RNase L, 2-5A dependent endoribonuclease; HEPES, 4-(2hydroxyethyl)-
1-piperazineethanesulfonic acid.

ABSTRACT: Raman spectra of model compounds and of 2',5'-oligoadenylates in D_2O, were utilized to assign the Raman bands of 2',5'-oligoadenylates. The Raman spectra of A2'pA2'pA, pA2'pA2'pA and pppA2'pA2'pA contained features that were similar to those of adenosine, AMP, and ATP respectively. When AMP and pA2'pA2'pA were titrated from a pH of 2 to 9, the normalized Raman intensity of their ionized (980 cm^{-1}) and protonated (1080 cm^{-1}) phosphate bands revealed similar pK_a's for the 5'-monophosphates. The Raman spectrum of pA2'pA2'pA was altered slightly by elevations in temperature, but not in a manner supporting the postulate that 2-5A possesses intermolecular base stacking. Major differences in the Raman spectrum of 2',5'- and 3',5'-oligoadenylates were observed in the 600-1200 cm^{-1} portion of the spectrum that arises predominately from ribose and phosphate vibrational modes. Phosphodiester backbone modes in A3'pA3'pA and pA3'pA3'pA produced a broad band at 802 cm^{-1} with a shoulder at 820 cm^{-1}, whereas all 2',5'-oligoadenylates contained a major phosphodiester band at 823 cm^{-1} with a shoulder at 802 cm^{-1}. The backbone mode of pppA2'pA2'pA contained the sharpest band at 823 cm^{-1}, suggesting that the phosphodiester backbone may be more restrained in the biologically active, 5'-triphosphorylated molecule. The Raman band assignments for 2',5'-oligoadenylates provide a foundation for using Raman spectroscopy to explore the mechanism of binding of 2',5'-oligoadenylates to proteins.

Interferons are recognized as important biological mediators that have numerous effects on the immune system, including inhibition of viral replication. Interferons induce at least two double-stranded RNA-dependent proteins, 2',5'-oligoadenylate synthetase and protein P_1 kinase (reviewed by Johnston & Torrence, 1984). 2',5'-Oligoadenylate synthetase polymerizes ATP into $pppA(2'pA)_n$ where $n > 2$ (2-5A)[1]. 2',5'-Oligoadenylates activate a latent endoribonuclease (RNase L) that degrades RNA and contributes to the translational inhibition caused by double-stranded RNA (dsRNA) (Kerr & Brown, 1978; Kerr et al., 1974; Lebleu et al., 1976; Sen et al., 1976).

The unique nature of these 2',5'-oligoadenylates has prompted investigation into the structural requirements for their binding to and activation of RNase L. The number of 5'-phosphates was shown to be important in determining the biological activity of 2-5A. Trimer 5'-triphosphate, pppA2'pA2'pA, and trimer 5'-diphosphate, ppA2'pA2'pA, bind and activate RNase L. Trimer 5'-monophosphate, pA2'pA2'pA, binds the endonuclease but does not activate the enzyme, and trimer core, A2'pA2'pA, neither binds nor activates RNase L efficiently (Kerr & Brown, 1978; Torrence et al., 1981). However, trimer core at high concentrations has been implicated in the inhibition of DNA and RNA synthesis although the mechanism of core action remains unclear (Kimchi et al., 1981a,b). More detail on the portions of 2-5A critical to binding and activation of RNase L have been obtained through the study of structural analogues of 2-5A. Efficient binding to RNase L requires the N6 amino group of the 5'-terminal adenine (Torrence et al., 1984; Imai & Torrence, 1985; Imai et al., 1985), and two 2',5'-phosphodiester bonds (Lesiak et al., 1983). Activation of RNase L requires the N6 amino group of the 2'-terminal adenine (Torrence et al., 1984; Imai & Torrence, 1985; Imai et al., 1985) and the 3'-OH of the ribose ring (Sawai et al., 1983; Haugh et

al., 1983). An analogue brominated at the C8 position of adenine,
$pA2'pA^{8Br}2'pA^{8Br}$, displayed unexpected biological activity. This 5'-mono-
phosphate shows significant binding and activation of RNase L (Torrence
et al., al., 1985; Torrence & Lesiak, 1986). This unexpected result
demonstrates that biological activity does not always require a 5'-terminal
di- or triphosphate and implies that the biological activity of different
2',5'-oligoadenylates may be dictated by a structural feature other than
the number of 5'-terminal phosphates.

Early Raman spectroscopic studies of mononucleotides (Lord & Thomas,
1967) has led to the emergence of Raman spectroscopy as a useful method
for studying nucleic acid structure. The technique requires small but
concentrated samples that may be in the form of crystal, film, fiber or
aqueous solution. Raman spectroscopy has proven useful in distinguishing
differences in nucleic acid structure. For example, characteristic Raman
"marker" bands have been described for the A, B, C, and Z forms of DNA
(Erfurth et al., 1972; Erfurth et al., 1975; Benevides & Thomas, 1983;
Benevides et al., 1984). Raman spectroscopy may also be employed to
study nucleic acid binding reactions. Ligand-DNA (Manfait et al., 1984)
and protein-cofactor (Yue et al., 1986) binding complexes have been
evaluated using Raman difference spectra. Difference spectra provide
information concerning which part of the ligand or cofactor interacts
with the DNA or protein.

We describe here a qualitative assignment of the Raman bands of the
interferon-induced 2',5'-oligoadenylates based on Raman spectra of model
compounds, and of 2',5'-oligoadenylates under various conditions. Defining
the vibrational modes that are responsible for the bands in the Raman spectrum

spectrum of 2-5A is an obligatory first step in studies designed to explore the molecular binding interactions between 2-5A and proteins. We also observe that the phosphodiester backbone of the biologically active form of 2-5A, pppA2'pA2'pA, differ from those of the inactive forms of 2-5A and of 3'5'-oligoadenylates.

MATERIALS and METHODS

Commercial 2',5'-linked trimer core, A2'pA2'pA, trimer 5'-monophosphate, pA2'pA2'pA, and trimer 5'-triphosphate, pppA2'pA2'pA (ammonium salts) were purchased from Pharmacia Chemical Company (Piscataway, NJ). Synthetic 2',5'-linked trimer core and trimer 5'-monophosphate (sodium salt) were generously supplied by Dr. Paul F. Torrence (NIH). Adenosine (Sigma grade), AMP (Sigma grade), and ATP (Sigma grade), were purchased from Sigma Chemical Company (St. Louis, MO). All samples were dissolved in distilled water or in buffer containing 150 mM NaCl, 10 mM HEPES, pH 7.4. Sample concentration was estimated spectroscopically and ranged from 10-100 mM. Raman experiments were carried out at 15° C except where noted otherwise. The temperature of the brass sample holder was maintained by a thermostatically controlled circulating water bath.

The Raman instrument consisted of a Coherent Innova 90 argon ion laser operating at 514.5 nm with typically 250 mw of light power at the sample, a thermostated brass sample holder, a 300mm focal length f 0.6 aspheric lens for light collection optics, a Spex 1403 double monochrometer with 1800 grove/mm holographic gratings, an RCA 31034 PMT, and a Spex Datamate coupled to a Cromemco Z80 based microcomputer. Spectral bandpass was set to 6 cm^{-1}. Data was collected at 1 cm^{-1} intervals at a scan rate of 1 cm^{-1}/sec. About 15 scans were collected on each spectrum with a 2 sec per cm^{-1} integration time. Samples of approximately 5 microliters were

6

held in melting point capillary tubes. Spectra containing significant noise were 5 point smoothed using the the algorithm of Savitsky & Golay (1967). Water and solvent background peaks, including those from HEPES where appropriate, were subtracted from spectra as described by Williams (1983).

To ensure that samples were pure and were not degraded by the laser beam, or by changes in pH, or by high temperatures employed in certain experiments, samples were analyzed using C-18 reverse phase HPLC. Less than one microliter of sample was removed from each melting point capillary before and after scanning and diluted approximately 20-fold for analysis. The HPLC system consisted of a Waters model 730 data module, a Waters model 720 system controller, a Waters model 710B WISP, 2 Waters model 510 solvent delivery systems, and a Kratos model 769 variable wavelength detector. Buffer A was 50 mM ammonium acetate, pH 5.2, and buffer B was 25% acetonitrile. The flow rate was 1 mL/minute. The column was a Waters µBONDAPACK C-18 3.0 mm x 30 cm stainless steel column. The gradient was programed as follows: 0-5 minutes, 100% A, 5-25 minutes, shallow exponential gradient (curve 07) to 25% B, and 25-35 minutes, steeper exponential gradient (curve 08) to 100% B. Absorbance was monitored at 259 mn. Average retention times in minutes were as follows: pppA2'pA2'pA, 27.2, ppA2'pA2'pA, 24.0, pA2'pA2'pA, 24.2, A2'pA2'pA, 35.6, A2'pA, 34.4, AMP, 9.2, adenosine, 29.9.

Sample pH was measured by insertion of a specially constructed combination pH electrode, measuring 0.9 mm (diameter) by 6.0 cm (length) (Microelectrodes, Inc., Londonderry, NH), into the melting point capillary. Accurate pH measurements were made on volumes as low as two microliters

and were done in duplicate. There was no significant difference in the pH
of a 5μL sample, determined as described above, and the pH of 1 mL of the
same sample measured in a test tube. Sample pH was changed by delivering
less than 1μL of ice cold 0.1 N KOH to the inside of the capillary with
the tip of the pH electrode. The electrode and sample were kept on ice
to minimize possible base-mediated degradation. This procedure changed
the pH by about 0.5 units per addition step without degrading the sample.
The ionized 980 cm^{-1} and protonated 1095 cm^{-1} phosphate peak heights were
measured after each spectrum was normalized to the 729 cm^{-1} band of
adenine using data handling programs described by Williams (1983).

Samples scanned in D_2O were lyophilized and reconstituted on ice
with D_2O from Sigma Chemical Company (St. Louis, MO). The sample was
immediately transferred to the thermostated 15°C brass sample holder for
Raman analysis.

RESULTS

General characteristics of Raman spectra of 2-5A.

The structures of 2',5'-oligoadenylates are depicted in Figure 1.
A clear relationship between the Raman spectrum of each model compound,
adenosine, AMP, and ATP, and the Raman spectrum of 2',5'-oligoadenylates,
A2'pA2'pA, pA2'pA2'pA, and pppA2'pA2'pA, can be seen in Figure 2. These
spectra contain bands that originate from vibrational modes of the
5'-monophosphate at 980 cm^{-1} (Figure 2c, 2d)(Rimai et al., 1969),
the 5'-triphosphate at 1125 cm^{-1} (Figure 2e, 2f)(Rimai et al., 1969),
the phosphodiester backbone at 800-880 cm^{-1} (Brown & Peticolas, 1975; Thomas
& Peticolas, 1983), and the adenine bases, at 729 & 1200-1600 cm^{-1} (Lord &

8

Thomas, 1967; Rimai et al., 1969; Baret et al; 1979; Fodor et al., 1985). Thus, the major differences in the Raman spectra of A2'pA2'pA, pA2'pA2'pA and pppA2'pA2'pA result from differences in the 5'-terminus and the ribose-phosphate backbone.

The major Raman active modes for model compounds and 2',5'-oligo-adenylates at pH 7.3 are summarized in Table I. Ring vibrations were identified by comparison with the frequencies reported for nucleotide monomers (Lord & Thomas, 1967; Fodor et al., 1985; Rimai et al., 1969) and polynucleotides (Baret et al.,1979). Backbone vibrations were identified by comparison with normal coordinate calculations (Brown & Peticolas, 1975; Shimanouchi et al., 1964; Lu et al., 1975). These results show excellent correlation with previously published data on A3'pA3'pA and polyriboadenylic acid (Small & Peticolas, 1971; Prescott et al., 1974).

Adenine Related Modes.

Modes above 1240 cm^{-1} arise from vibrations of adenine bases (Table I). Minor differences between the observed Raman frequency of base bands in the spectra of model compounds and 2-5A may arise from the coupling through the N9-C2' bond. Bands at 1308, 1340, 1378, 1422-1428, 1482-1484, 1510-1515, and 1580-1585 cm^{-1} have been identified previously as adenine ring modes (Lord & Thomas, 1967; Rimai et al., 1969; Baret et al., 1979; Fodor et al., 1985). Peaks at 630-640 and 729 cm^{-1} also arise from the adenine ring, although the width of the 729 cm^{-1} peak may be slightly effected by the state of 5'-phosphorylation (Rimai et al., 1969).

Preliminary studies suggested that a 1455 cm^{-1} band in 2',5'-trimer 5'-monophosphate pA2'pA2'pA, (NIH source), originated from the base moieties (Johnston et al.,1985). However, this 1455 cm^{-1} band originates from a triethyl ammonium ion present from the synthesis or

9

purification of the compound. Subtracting the Raman spectrum of triethyl-
ammonium bicarbonate from the Raman spectrum of pA2'pA2'pA (NIH source)
resulted in a corrected spectrum that was essentially the same as the
Raman spectrum of commercial pA2'pA2'pA (result not shown).

Phosphate modes.

Phosphate mode assignments of 5'-phosphorylated 2',5'-oligoadenylates
were made by comparison with Raman spectra of AMP, ATP, and A2'pA2'pA (Rimai
et al., 1969; Yue et al., 1986). Bands for 5'-monophosphates at 980 cm^{-1}
and triphosphates at 1125 cm^{-1} were observed in AMP and ATP and in 2',5'-
oligoadenylates.

The effect of pH on the ionization state of pA2'pA2'pA as reflected
by the 980 cm^{-1} (ionized) and 1084 cm^{-1} (protonated) phosphate bands was
investigated to determine if the 5'-terminal phosphate of pA2'pA2'pA
interacts with other portions of the 2-5A molecule. Such interactions
might be expected to alter the pK_a of the 5'-terminal phosphate group.
The pH was varied from 2.0 to 9.0. Spectra were normalized to the 729
cm^{-1} adenine base band which is not affected in intensity or frequency by
changes in pH from 5 to 7 (Rimai et al., 1969) or from pH <3 to >5 (Lord &
Thomas, 1967; results not shown). The 729 cm $^{-1}$ band in pA2'pA2'pA was also
not affected by changes in pH from 2 to 9 (results not shown). The band
at 980 cm^{-1} in the control Raman spectrum of AMP showed an apparent pK_a of
6.05 (Figure 3a). The band at 980 cm^{-1} in the Raman spectrum of pA2'pA2'pA
showed a similar pK_a of 6.1.

The 1455 cm^{-1} band due to the triethyl ammonium ion observed in the
synthetic pA2'pA2'pA from NIH showed no change in intensity with pH,
(Figure 3b) relative to the 729 cm^{-1} adenine base band. This further
supports the validity of normalizing spectra to the 729 cm^{-1} band.

10

Deuteration effects.

The spectra of trimer monophosphate, pA2'pA2pA, in H_2O and in D_2O are compared in Figure 4. Only the hydrogens attached to the exocyclic nitrogens of adenine and the ribose hydroxyls would be expected to be exchanged here at the pD of 6.6. Exchange of C8 and C2 protons of adenosine is much slower (Thomas et al., 1975 and references therein) and therefore probably did not occur in this experiment. A minor band at 1650 cm^{-1} in H_2O was shifted down in frequency to 1625 cm^{-1} in D_2O. This band may be related to the high frequency mode found in substituted benzenes since adenine is an aromatic C6-substituted compound (Tsuboi et al., 1973). The band at 1254 cm^{-1}, assigned to the exocyclic N6 amino group of the adenine bases by Tsuboi et al. (1973), is not present in D_2O indicating that this assignment is also correct for the 2',5'-oligoadenylates. This further suggests that the N6 amino groups of adenine moieties of 2-5A do not participate in stable intermolecular interactions in solution.

Deuteration resulted in the appearance of two new bands at 1182 and 1200 cm^{-1}. The 1182 cm^{-1} mode was been assigned to the ND_2 scissor by Tsuboi et al. (1973). The 1200 cm^{-1} band probably arises from adenine, since it also appears when AMP is deuterated (Yue et al., 1986). Most bands above 1300 cm^{-1} also shifted down slightly in frequency as a result of changes in vibrational coupling. Numerous changes in the 700-900 cm^{-1} region of the spectrum, containing ribose and phosphate bands, were also observed.

Assessing Secondary Structure

Raman hyperchromism is observed in the spectra of ordered structures such as poly(rA) when the bases unstack at high temperature. Bands in Raman spectra of poly(rA) and A3'pA3'pA at 729, 1308, and 1510 cm^{-1} increase upon melting at 90°C (Prescott et al., 1974).

Our studies at 16° C and at higher temperatures enable us to make four observations (spectra discussed below were normalized to either the 1095 O-P-O symmetric stretch or the 1338 adenine bond). 1. We observed a linear increase in intensities of lines in the spectrum of pA2'pA2'pA at 1308, 1378, and 1510 cm^{-1} (21, 16, and 33% respectively) with increasing temperature (Figure 5A). 2. The intensities of bands in the spectra of AMP and pA2'pA2'pA at 1308, 1378 and 1510 cm^{-1} at 16°C were essentially the same (Figure 2). 3. The intensities of bands in the spectra of pA3'pA3'pA at 1308, 1378 and 1510 cm^{-1} were slightly decreased with respect to the same bands in AMP which is consistant with observations by Prescott et al. (1974), (data not shown). 4. The 814 cm^{-1} line in the Raman spectrum of A3'pA3'pA at 20°C shifts to 798 cm^{-1} at 90°C and has been used as a measure of "disorder" (lack of secondary structure) in this and other 3',5'-linked RNA's (Prescott et al., 1974). No shift of the 823 cm^{-1} line in the spectrum of pA2'pA2'pA was observed at 90° C (Figure 5A).

Linkage Isomers.

Spectra of A2'pA2'pA, A3'pA3'pA, and pA3'pA3'pA were examined to investigate the effect of the 2',5'-phosphodiester bond on Raman active modes. The $PO_3^=$ mode at 980 cm^{-1} (Rimai et al., 1969) was observed for both pA2'pA2'pA and pA3'pA3'pA (Figure 6c,d). pA3'pA3'pA had well-resolved bands at 680 and 760 cm^{-1} (Figure 6d); these modes appeared as shoulders on the 729 cm^{-1} band of pA2'pA2'pA (Figure 6c). The ratio of the intensities at 1510 cm^{-1}

12

and 1482 cm^{-1} was smaller in 3-5A than in 2-5A (Figure 6). The major difference between A2'pA2'pA and A3'pA3'pA was in the frequency of the phosphodiester backbone bands found in the 800-825 cm^{-1} region of the spectrum (Figure 6). The Raman spectrum of 3',5'-linked trimer core, A3'pA3'pA, revealed the presence of a strong backbone mode at 802 cm^{-1} and a relatively weaker mode at 820 cm^{-1}. 2',5'-Oligoadenylates contained both of these bands but the band at 823 cm^{-1} was stronger and sharper relative to the 820 cm^{-1} band of 3-5A. The form of 2'5'-oligoadenylate which is capable of activating the cellular endonuclease, pppA2'pA2'pA, had the sharpest band at 823 cm^{-1} (Figure 6e). The possible significance of these results is discussed below.

DISCUSSION

Previously published physiochemical studies on the conformation of 2',5'-linked oligoadenylates in solution have yielded mixed results. Studies using CD to estimate base stacking revealed that hypochromicity of 2',5'oligoadenylates was higher than that of the corresponding 3',5'-oligoadenylates (Sawai, 1983; Doornbos et al., 1981, 1983). This result suggests that 2',5'-oligoadenylates possess more base stacking than 3',5'-oligoadenylates. In contrast, a CD comparison of 2-5A and 3-5A tetramer, pentamer, and hexamer at 20° C showed that $\Delta\varepsilon$ for 3',5'-oligoadenylates increases with increasing chain length, but $\Delta\varepsilon$ for 2',5'-oligoadenylates remains constant with increasing chain length. The conclusion was that stacking in 2',5'-oligoadenylates is weaker than in 3',5'-oligo(A)'s (Hirao et al., 1983; Dhingra & Sarma, 1978). X-ray analysis of the structure of crystals of A2'pC implied that a very compact right handed helix can exist; intramolecular O4' ribose-adenine stacking (rather than intermolecular base stacking) was proposed (Parthasarathy et al., 1982).

13

Our spectra were normalized to both the 1095 cm^{-1} PO_2^- band and the 1338 cm^{-1} adenine band. We observed no change in the relative intensities of these bands with temperature indicating that the 1338 band may be a good band to normalize under these circumstances.

Spectra of pA2'pA2'pA and AMP have the same relative intensities at (16°C) in bands that are sensitive to base stacking (Figure 2) in contrast to observations made by Prescott et al. (1974) in a comparison of AMP and 3-5A core. This suggests that there is little or no base stacking in 2-5A. The relative intensities of bands at 1308, 1378 and 1510 cm^{-1} increased and the relative intensity of the 823 cm^{-1} band decreased as temperature was increased from 16 - 90°C (Figure 5A). The linearity of these changes (Figure 5B) suggests that the 2-5A molecule was undergoing a change in structural equilibrium that is not related to base stacking. If base stacking was disrupted, changes in these bands would be expected to follow a typical melting curve, as observed for poly(A)·poly(U) (Small & Peticolas, 1971) and for GpC (Prescott et al., 1974).

pA3'pA3'pA but not A3'pA3'pA has weak but well-resolved bands at 680 and 760 cm^{-1} that were signficantly less discernable in both A2'pA2'pA and pA2'pA2'pA (Figure 6). These bands are also not present in poly(rA) (Prescott et al., 1974). Rimai et al. (1969) assigned bands at these positions to the polyphosphate chain at the 5'-terminus of ADP and ATP because they were absent in AMP (see Figure 2). This assignment does not explain our results since pA3'pA3'pA does not contain polyphosphate. Preliminary studies of pA3'pA2'pA and pA2'pA3'pA have provided further clues to the nature of the 680 and 760 cm^{-1} bands in oligonucleotides. When the first ribose was 3',5'-linked, as in pA3'pA2'pA, both the 680 and 760 cm^{-1} bands were present (not shown), as observed with pA3'pA3'pA (Figure 6d). However, when the first linkage was 2',5'-linked, as in pA2'pA3'pA, the Raman spectrum appears similar to pA2'pA2'pA, which lacks

14

well-resolved bands at 680 and 760 cm^{-1} (Figure 6c and results not shown). These results imply that the 680 and 760 cm^{-1} bands may arise from the presence of a phosphate at the 5'-terminus of certain oligonucleotides. Changes in backbone parameters such as the glycosyl torsion angle, which may accompany differences in the phosphodiester linkage, may account for the observed difference between 2'5'- and 3'5'-linked oligoadenylates.

Raman spectroscopy has been used to identify the ribose pucker of nucleic acids. A-genus DNA possesses a C3'-endo ribose conformation and has a strong sharp band in the 807-815 cm^{-1} region. (Erfurth et al., 1972; Thomas & Hartman, 1973; Erfurth et al., 1975; Goodwin & Brahms, 1978). Raman spectra of B and C-genus DNA has weak, broad bands at 835 and 875 cm^{-1} respectively (Brown & Peticolas., 1975; Lu et al., 1975). For ribonucleotides, the Raman A-genus "marker" bands are shifted up about 7 cm^{-1} to 814-822 cm^{-1} (Erfurth et al., 1972; Erfurth et al., 1975; Goodwin et al., 1978; Hartman et al., 1973; Peticolas & Tsuboi, 1979). Marker modes have been shown to exist in low temperature Raman scans of mononucleotides (Small & Peticolas, 1971), and in U3'pA, G3'pC an dT3'pdT (Thomas & Peticolas, 1983). Based on these results Peticolas et al. (1983) proposed that the position of the phosphodiester backbone marker mode for ribonucleotides in the 814-822 range depends on the coupling through the 5'-ribose ester linkage. Assignment of the 823 cm^{-1} line in the spectrum of 2-5A as resulting from phospohdiester group vibrations seems reasonable (Figure 6). Wartell and Harrell (1986) recently reported that an "extra" 823 cm^{-1} backbone band was required to reproduce the 800-850 cm^{-1} region of poly[d(A-T)]·poly[d(A-T)] by curve-fitting procedures. The relationship of this band to the clearly visible 823 cm^{-1} band in the Raman spectra of 2-5A's has not been ascertained.

15

NMR studies have indicated that the ribose pucker of A2'pA2'pA is mixed at 20° C while the deoxy analogue, d(A2'pA2'pA), is almost exclusively C3'-endo at 20° C (Doornbos, et al., 1981,1983). If a mixed population of ribose puckers is observed by NMR, on a time scale of 10^{-6} sec, then Raman spectroscopy, on a time scale of $< 10^{-13}$ sec, should identify these populations of ribose pucker.

We assign the band at 823 cm^{-1} to phospohdiester group vibrations in 2-5A's (Figure 6). NMR evidence indicates that a mixture of ribose puckers exists in 2-5A. We observed a major band at 823 cm^{-1} and a minor band at 802 cm^{-1}. These bands may represent the relative predominance of one ribose pucker type over the other since the position of the backbone marker has been shown to be sensitive to furanose pucker (Thomas & Peticolas, 1983). The broadness or sharpness of the band may also be influenced by furanose pucker. We propose that the biologically active molecule, pppA2'pA2'pA has a more uniform ribose pucker than pA2'pA2'pA, since the band at 823 cm^{-1} in pppA2'pA2'pA is subtantially sharper than the 823 cm^{-1} band in pA2'pA2'pA (Figure 7). Alternatively, changes in other backbone torsion angles may affect the appearance of this band. In either case, the Raman spectra demonstrates that the backbone structure in the biologically active pppA2'pA2'pA differs from that found in non-biologically active forms of 2-5A and 3',5'-oligoadenylates.

2',5'-Oligoadenylates probably present unique conformational properties that are important in binding and activating RNase L. Previous studies employing structural analogues of 2-5A have implicated the first 2',5'-linkage as being critical for binding to RNase L. The observation that a brominated monophosphate analogue of 2-5A retained biological activity suggests that the 5'-triphosphate may not be an absolute requirement for RNase L activation. We are presently exploring the possibility that

16

bromination forces the ribose of pA2'pA2'pA into a more rigid conformation as reflected by a sharp 823 cm^{-1} band. Rigidity of the phosphodiester backbone and possibly of the furanose pucker may be related to the ability of the 2',5'-oligoadenylates to activate RNase L. These assignments reported here will also be useful in studying the interaction of 2',5'-oligoadenylates with proteins.

REFERENCES

Baret, J. F., Carbone, G. P., & Sturm, J. (1979) J. Raman Spec. 8, 291-304.

Benevides, J. M., & Thomas, G. J., Jr. (1983) Nucleic Acids Res. 11, 5747-5761.

Benevides, J. M., LeMeur, D., & Thomas, G. J., Jr. (1984) Biopolymers 23, 1011-1024.

Brown, E. B., & Peticolas, W. L. (1975) Biopolymers 14, 1259-1271.

Dhingra, M. M., & Sarma, R. H. (1978) Nature 272, 798-801.

Doornbos, J., DenHartog, J. A., VanBoom, J. H. & Altona, C. (1981) Eur. J. Biochem. 116, 403-412.

Doornbos, J., Charubala, R., Pfleiderer, W., & Altona, C. (1983) Nucleic Acids Res. 11, 4569-4582.

Erfurth, S. C., Kiser, E. J., & Peticolas, W. L. (1972) Proc. Natl. Acad. Sci. 69, 938-941.

Erfurth, S. C., Bond, J., & Peticolas, W. L. (1975) Biopolymers 14, 1245-1257.

Fodor, P. A., Rava, R. P., Hays, T. R., & Spiro, T. G. (1985) J. Am. Chem. Soc. 107, 1520-1529.

Goodwin, D. C. & Brahms, J. (1978) Nucleic Acids Res. 5, 835-850.

Hartman, K. A., Lord, R. C., & Thomas, G. J., Jr. (1973) in Physicochemical Properties of Nucleic Acids, Vol 2, pp. 92-143. (Duchesne, J., ed.) Academic Press, New York.

Haugh, M. C., Cayley, P. J., Serfinoska, H. Norman, D. C. Reese, C. B., & Kerr, I. M. (1983) Eur. J. Biochem. 132, 77-84.

Hirao, I., Ishido, Y., & Miura, K. (1983) Nucleic Acids Res. Symposium Series 12, 193-196.

Imai, J., & Torrence, P. F. (1985) J. Org. Chem. 50, 1418-1426.

Imai, J., Lesiak, K., & Torrence, P. F. (1985) J. Biol. Chem. 260, 1390-1393.

Johnston, M. I. & Torrence, P. F. (1984) in Interferon, Vol. 3, pp. 189-298. (Freidman, R. M., ed.) Elsevier Science, New York.

Johnston, M. I., Hearl, W. G., White, J. C., Imai, J., Torrence, P. F., & Williams, R. W. (1985) in Progress in Clinical and Biological Research Vol. 202 pp. 37-45 (Williams, B. R. C. & Silverman, R. G. eds.) Alan R. Liss Inc., New York.

Kerr, I. M., & Brown. R. E. (1978) Proc. Natl. Acad. Sci. U. S. A. 75, 256-260.

Kerr, I. M., Brown, R. E., & Ball, L. A. (1974) Nature London 250, 57-59.

Kimchi, A., Shure, H., Lapidot, Y., Rapoport, S., Panet, A. and Revel, M. (1981a) FEBS Lett. 134, 212-216.

Kimchi, A., Shure, A., & Revel, M. (1981b) Eur. J. Biochem. 114, 5-10.

Lebleu, B., Sen, G. C., Shaila, S., Carber, B., & Lengyel, P. (1976) Proc. Natl. Acad. Sci. U. S. A. 73, 3107-3111.

Lesiak, K. Imai, J., Floyd-Smith, G., & Torrence, P. F. (1983) J. Biol. Chem. 258, 13082-13088.

Lord, R. C., & Thomas, G. J., Jr. (1967) Spectrochim Acta. Part A, 23A, 969.

Lu, K. C., Prohofsky, E. W., Van Zant, L. L. (9175) Biopolymers 16, 2491-2506.

Manfait, M., Theophanides, T., Alix, A.J.P. & Jeannesson, P. (1984) in Spectroscopy of Biological Molecules, pp 113-136 (Sandorfy, C. & Theophanides, T., eds.) Reidel, Dordredlt, Holland.

Parthasarathy, R., Malik, M. & Fridey, S. M. (1982) Proc. Natl. Acad. Sci. U. S. A. 79, 7292-7296.

Peticolas, W. L., & Tsuboi, N. (1979) in Infrared and Raman Spectroscopy of Biological Molecules, pp. 153-165 (Theophanidies, T. M., ed.) Reidel, Dordredlt, Holland.

Prescott, B., Gamache, R., Liveramento, J., & Thomas, G. J., Jr. (1974) Biopolymers 13, 1821-1845.

Rimai, L., Cole, T., Parsons, J. L., Hickmott, J. T., Jr., & Carew, E. B. (1969) Biophys. J. 9, 320-329.

Savitsky, A., & Golay, M., (1967) Anal. Chem. 36, 1627-1639.
Sawai, H., Imai, J., Lesiak, K., Johnston, M. I. & Torrence, P. F. (1983) J. Biol. Chem. 258, 1671-1677.

Sawai, H. (1983) Nucliec Acids Res. Symposium Series 12, 189-192.

Sawai, H., Imai, J., Lesiak, K., Johnston, M.I., & Torrence, P.F. (1983) J. Biol. Chem. 258, 1671-1677.

Sen, G. C., LeBleu, B., Brown, G. E., Kawakita, M., Slattery, E., & Lengyel, P. (1976) Nature London 264, 370-373.

Shimanouchi, E. B., Tsuboi, M., & Kyogoku, Y. (1964) in Chemical Physics Vol. VII, pp. 435- 498 (Duchesene, J., Ed.) Interscience, London.

Small, E. W., & Peticolas, W. L. (1971) Biopolymers 10, 1377-1425.

Thomas, G. J., Jr., & Hartman, K. A. (1973) Biochim. Biophys. Acta. 312, 311-322.

Thomas, G. J., Jr., & Livramento, J. (1975) Biochemistry 23, 5210-5218.

Thomas, G. A., & Peticolas, W. L. (1983) J. Am. Chem. Soc. 105, 986-992.

Torrence, P. F. & Lesiak, K. (1986) J. Med. Chem. 29, 1015-1022.

Torrence, P. F., Imai, J., & Johnston, M. I. (1981) Proc. Natl. Acad. Sci. U. S. A. 78, 5993-5997.

Torrence, P. F., Imai, J., Lesiak, K., Jamoulle, J. C. & Sawai, H. (1984) J. Med. Chem. 27, 726-733.

Torrence, P. F., Imai, J., Wong, A., & Lesiak, K. (1985) in Progress in Clinical and Biological Research Vol. 202 pp 75-80 (Williams, B. R. C., & Silverman R. G. eds.) Alan R. Liss Inc., New York.

Tsuboi, M., Takahushi, S., & Harada, I. (1973) in Physio-chemical Properties of Nucleic Acids Vol. 2, p 91 (Duchesne J., ed.) Academic Press, New York.

Wartell, R.M., & Harell, J.T. (1986) Biochemistry 25, 2664-2671.

Williams, R. W. (1983) J. Mol. Bio. 166, 581-603.

Yue, T. K., Martin, C. L., Chen, D., Nelson, P., Sloan, D. L., & Chandler, R. (1986) Biochemistry 25, 4981-4987.

Table I. Raman active modes for model and 2',5'-linked compounds.

Observed Raman frequency shift (cm^{-1})[a]						Calculated frequency shift (cm^{-1})[b]	Potential Energy Distribution[c]
adenosine	A2'pA2'pA	AMP	pA2'pA2'pA	ATP	pppA2'pA2'pA		
1650		1650		1650			C=N(19) C-C(25) C-N(23)N-C=(19)
1582	1580	1580	1578	1585	1580	1581	C5C4(48) - C4N3(31)
1512	1510	1510	1510	1515	1510	1531	C5C4(25) - C2N3(23)
1486	1480	1482	1480	1487	1480	1468	δC2H(29)-N9C8(19) + δC8H
1458	1460	1460	1458	1462	1460	1464	ribosyl CH_2 bending[d]
1428	1422	1422	1422	1422	1425	1689	C4N(44) - δC8H(15)
1378	1378	1378	1378	1380	1380	1351	C-N(50)C=C(16)
1340	1340	1340	1340	1340	1340	1329	N7C5(39) + C8N7(12)
1308	1310	1308	1305	1305	1310	1309	N9C8(30) + N3C2(14) + δC8H(14) - δC2H
1254	1254	1254	1254	1254	1254	1424	N1C6(31) + C6N6'(26)
1214	1220	1220	1218	1220	1222	1218	adenine ring bending
1178	1180	1180	1180	1180	1178	1171	N1-C2-N3(25) N1-C2(23) C2=N3(14) N6-C6=N1(14)
				1113	1115	1125	$PO_3^=$ 5'-triphosphate[e]

Table I. (Con't)

Observed Raman frequency shift (cm^{-1})[a]						Calculated frequency shift (cm^{-1})[b]	Potential Energy Distribution[1]
¡nosine	A2'pA2'pA	AMP	pA2'pA2'pA	ATP	pppA2'pA2'pA		
	1085		1075		1080		O-P-O symetric diester stretch[d]
)05	1010	1000	1010	1015	1010		adenine torsion
		980	980				$PO_3^=$ 5' monophosphate[e]
			918	918	918		not assigned
	880	882	895	892	890		not assigned
865							not assigned
		854		855	850		asymetric O-P-O[d], backbone[e]
	825	822	825	830	825		not assigned
		802	802	805	802		symetric O-P-O[d]
	780		795		780		C4-N9-C1'(16) C1'O5'(11)
29	729	729	729	729	729	681	δN7C8N9(19) – N9ribose(14) + δC5N7C8(12) + δC4N9C8(11)
30	638	640	638	640	640		backbone-A bending

[a] Frequency shifts experimentally observed in this report.
[b] Frequency shifts assigned by normal mode analysis by Fodor et al. (1985) and/or Baret et al. (1979)
[c] Potential enegery distributions based on normal mode analysis by Fodor et al. (1985) and/or Baret et al. (1979), except where noted otherwise.
[d] Assignment from Thomas et al., (1983).
[e] Assignment from Rimai et al. (1969).

FIGURE LEGENDS

Figure 1: Schematic of 2',5'-oligoadenylates. R=H for A2'pA2'pA, R=PO$_3^=$ for pA2'pA2'pA, and R=P$_3$O$_{10}^{4-}$ for pppA2'pA2'pA2.

Figure 2: Raman spectra of 2',5'-oligoadenylates and model compounds. (a) adenosine in saline HEPES, pH 7.4, (b) A2'pA2'pA in water, pH 7.3, (c) AMP in water, pH 7.3, (d) pA2'pA2'pA in water, pH 7.3, (e) ATP in water, pH 7.3 (f) pppA2'pA2'pA in water, pH7.3. Samples were prepared and scanned as described under Materials and Methods.

Figure 3: Effect of pH on the phosphate modes of AMP and pA2'pA2'pA. (A) Raman intensity of the Phosphate modes of AMP, 980 cm^{-1} ($\square$); 1080 cm^{-1}($\triangle$).   (B) Raman intensity of pA2'pA2'pA 980 cm^{-1} ($\square$); 1080 cm^{-1}($\triangle$); 1455 cm $^{-1}$($\diamondsuit$).   Ten units were added to the 1455 cm^{-1} intensities. Spectra were normalized to the 729 cm^{-1} band of adenine a described under Materials and Methods.

Figure 4: Effect of D$_2$O on the Raman spectrum of pA2'pA2'pA. (a) in water, pH 6.6, (b) in D$_2$O, pD 5.8. pH was estimated by spotting a small sample on pH paper.

Figure 5: Effect of temperature on the Raman spectrum of pA2'pA2'pA. (A) The Raman spectrum of pA2'pA2'pA, pH 7.3, was taken at, (a) 16°C, (b) 23°C, (c) 37°C, (d) 56°C, (e) 70°C, (f) 90°C. (B) Raman intensities of the bands at ($\triangle$), 823 cm^{-1}; ($\blacktriangle$), 1308 cm^{-1}; ($\blacksquare$), 1378 cm^{-1}; and ($\blacklozenge$), 1510 cm^{-1}.
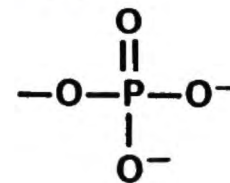
Figure 6: Comparison of the Raman spectra 2',5'- and 3',5'-oligoadenylates. Raman spectra were obtained in water, pH 7.3 as described under Materials and Methods. (a) A2'pA2'pA, (b) A3'pA3'pA, (c) pA2'pA2'pA, commercial source, (d) pA3'pA3'pA. (e) pppA2'pA2'pA.

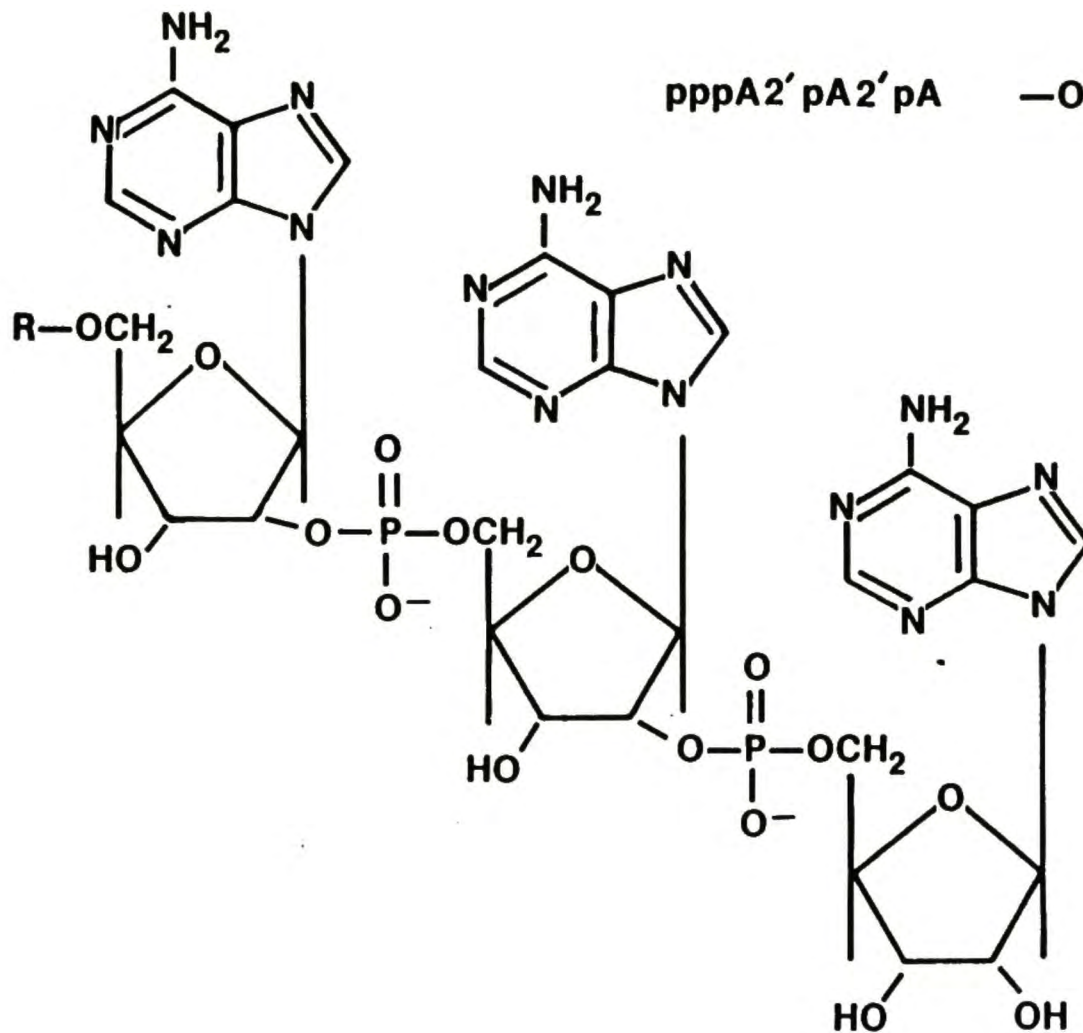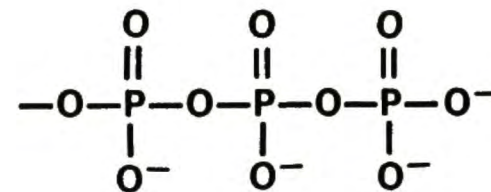Figure 7: Comparison of the Raman phosphodiester backbone modes (a) pA3'pA3'pA, (b) pA2'pA2'pA, (c) pppA2'pA2'pA.
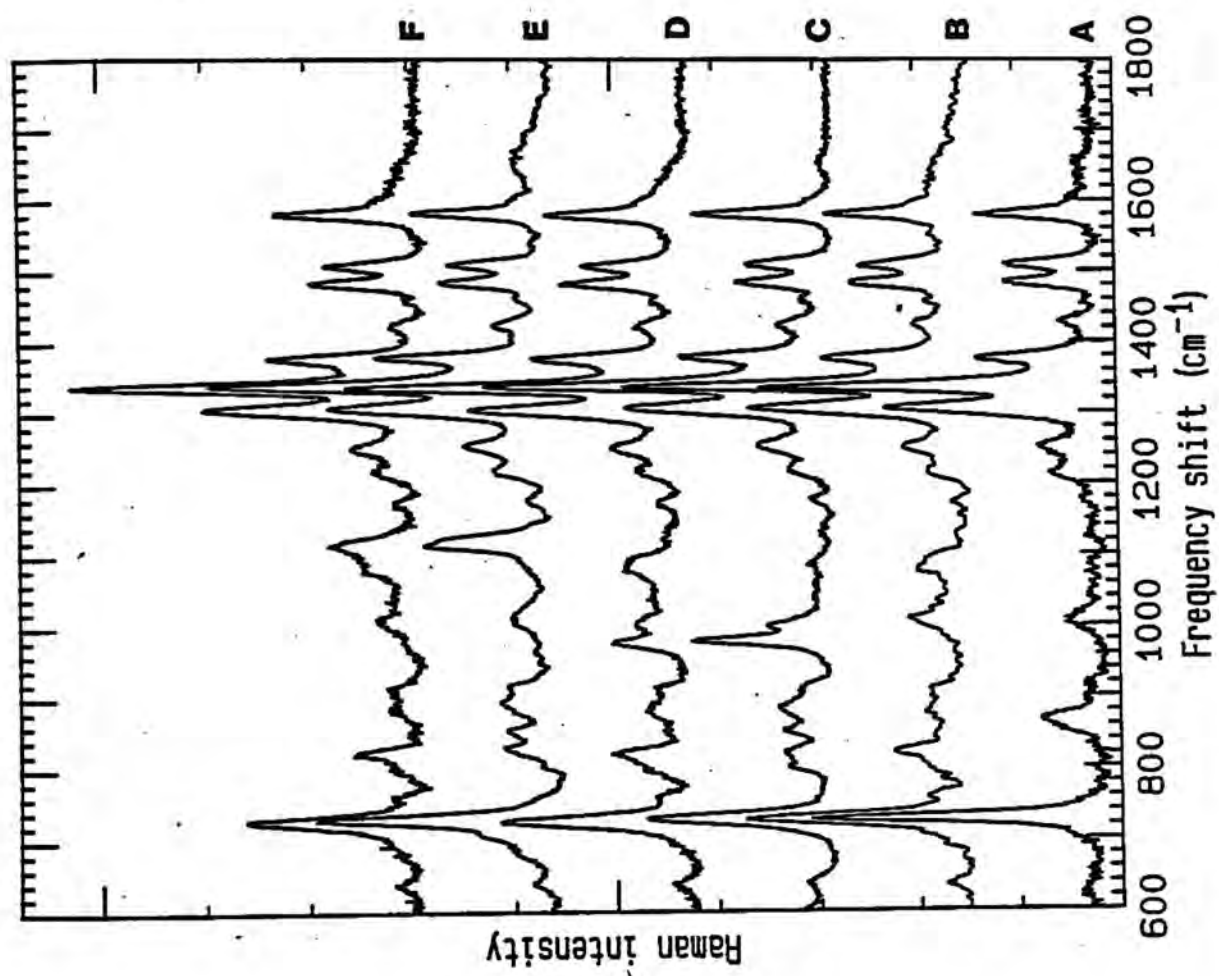
Frequency shift (cm⁻¹)
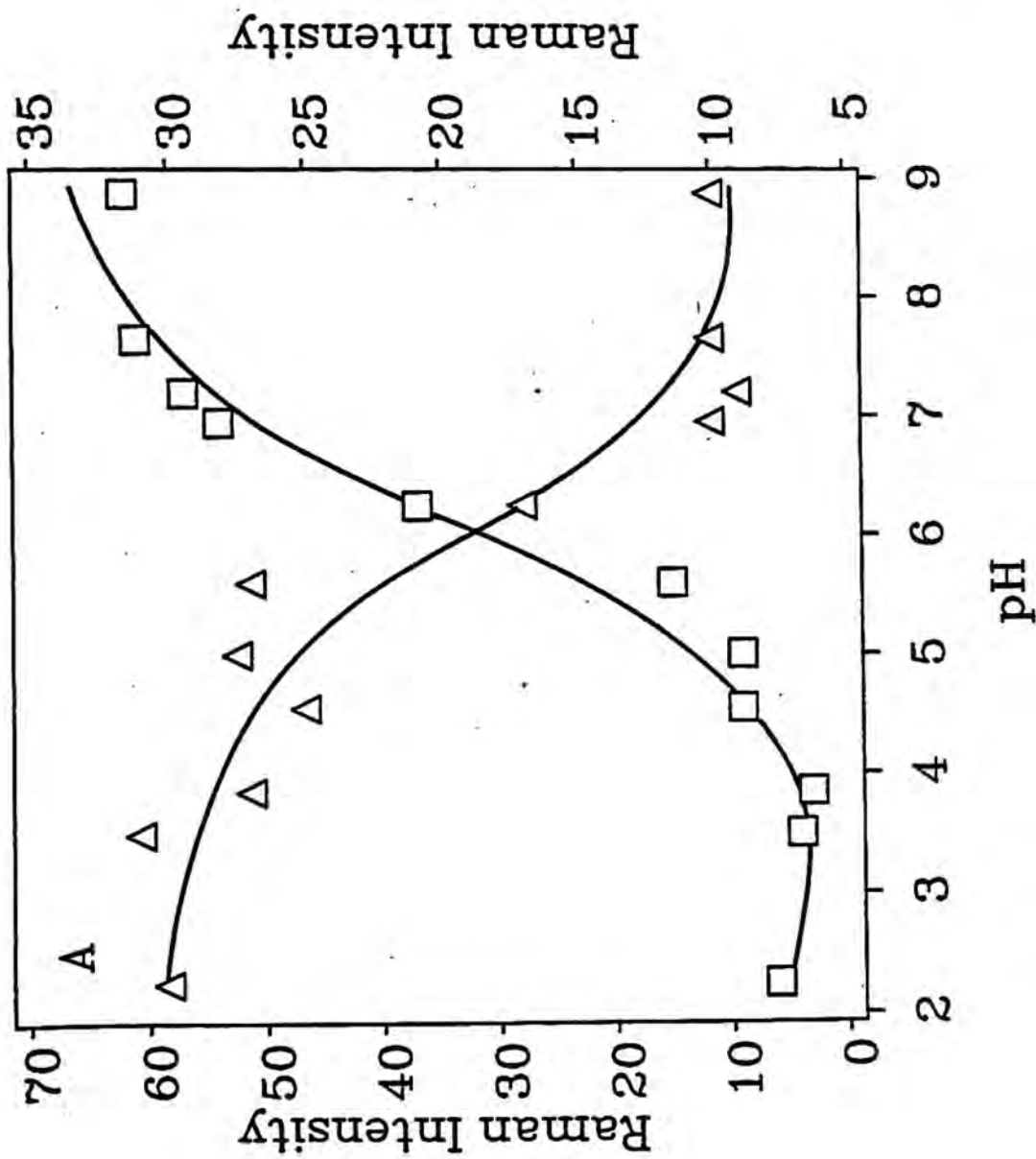
Raman intensity

F
E
D
C
B
A

600 800 1000 1200 1400 1600 1800

WHITE ET AL. FIG. 2

WHITE ET AL. FIG. 3 A.

WHITE ET. AL. FIG. 3B

WHITE ET AL FIG.4

WHITE ET AL. FIG. 5A

WHITE ET AL. FIG. 6

WHITE ET AL. FIG. 7
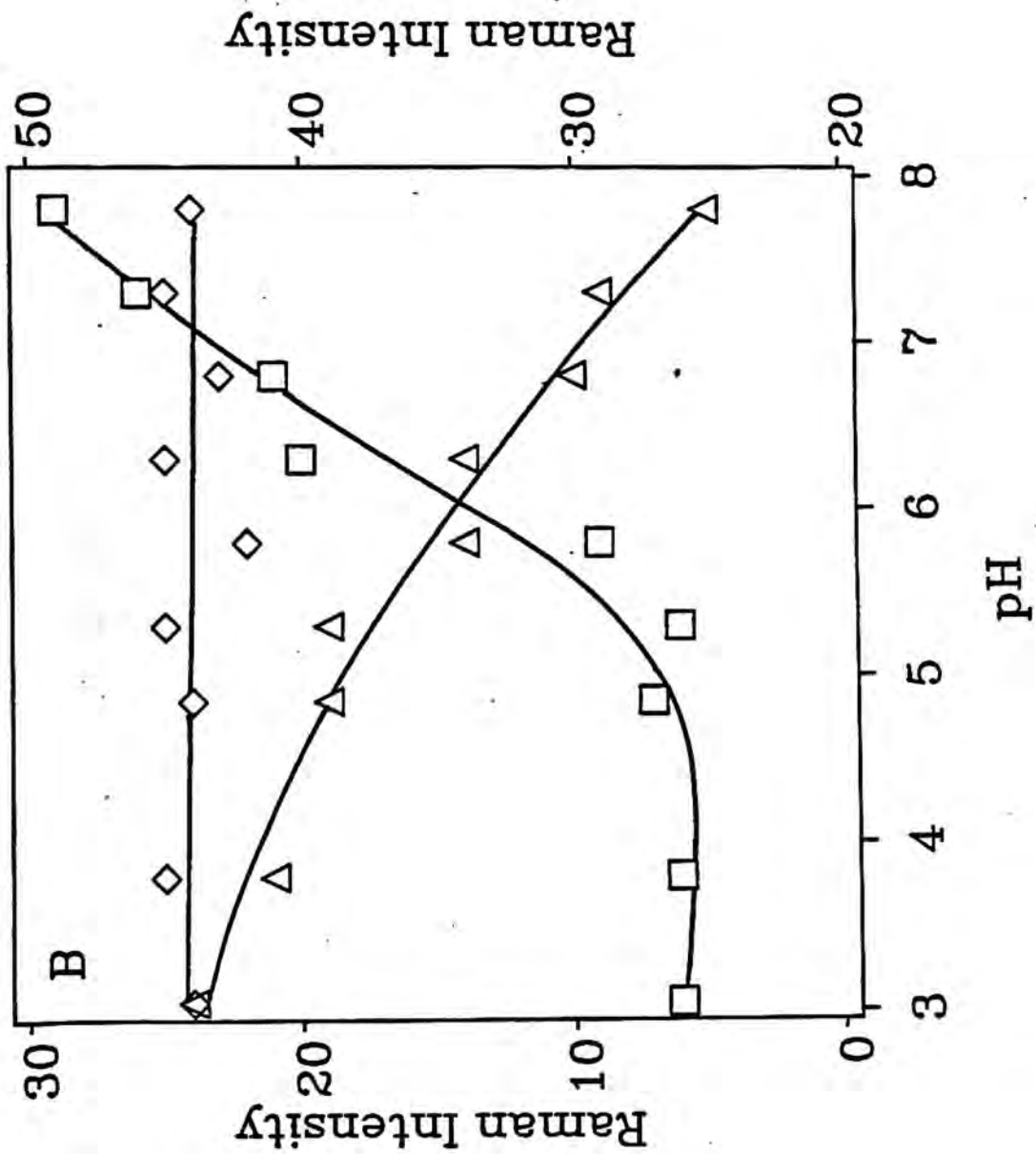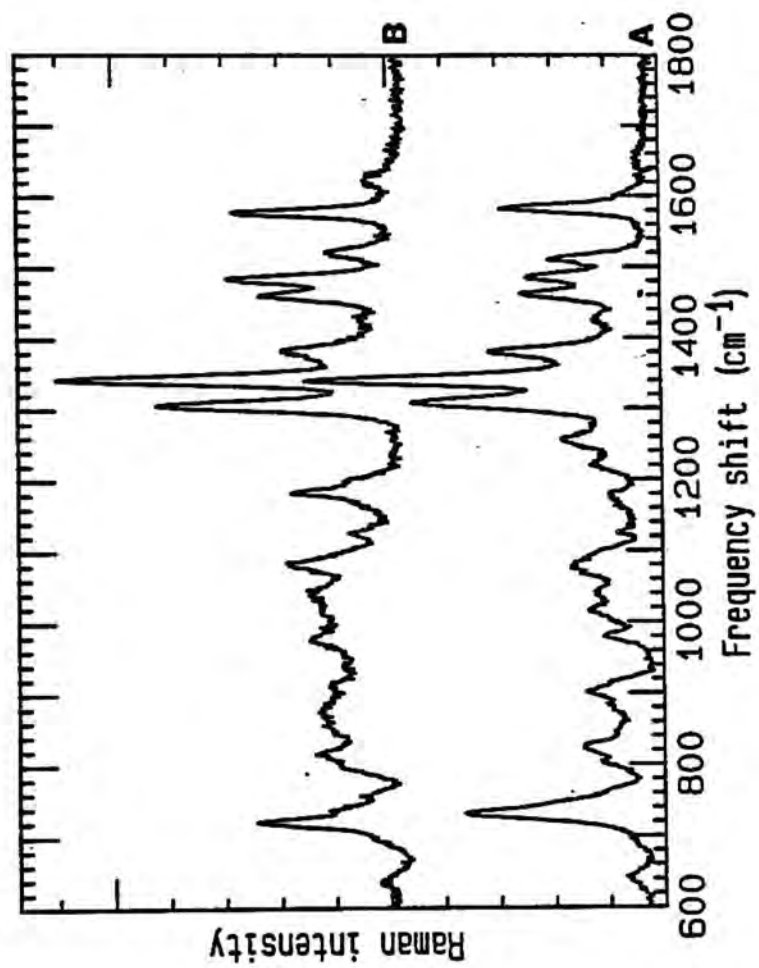
VIII. REFERENCES

Aguet, M. (1980) Nature (London) 284, 459-461.

Aguet, M. & Mogensen, K. E. (1983) in Interferon 5 (Gresser, I. ed.), pp. 1-22, Academic Press, New York.

Aguet, M., & Blanchard, B. (1981) Virology 115, 249-261.

Baglioni, C. & Nilson, T. W. (1983) in Interferon 5 (Gresser, I. ed.), pp. 23-42, Academic Press, New York.
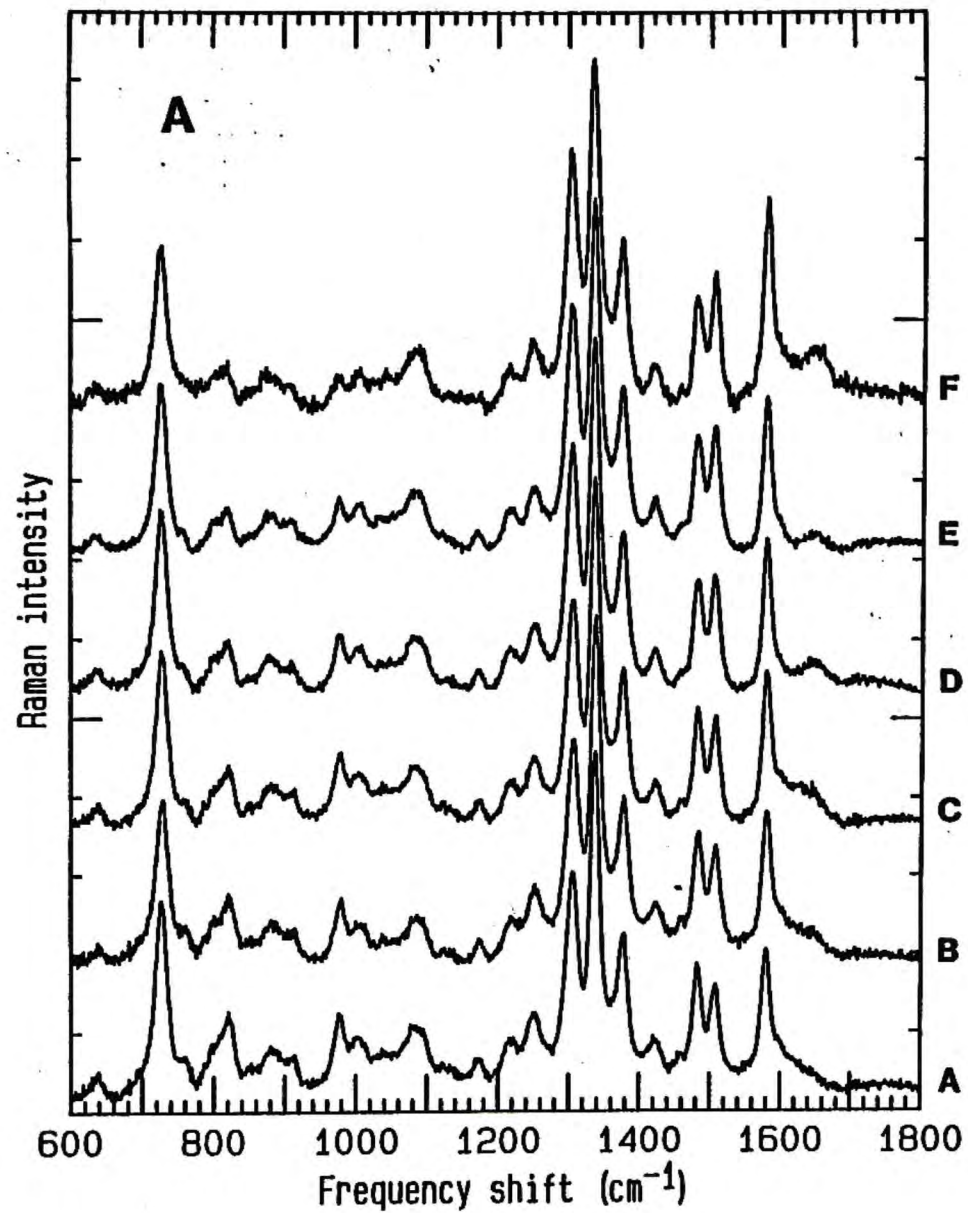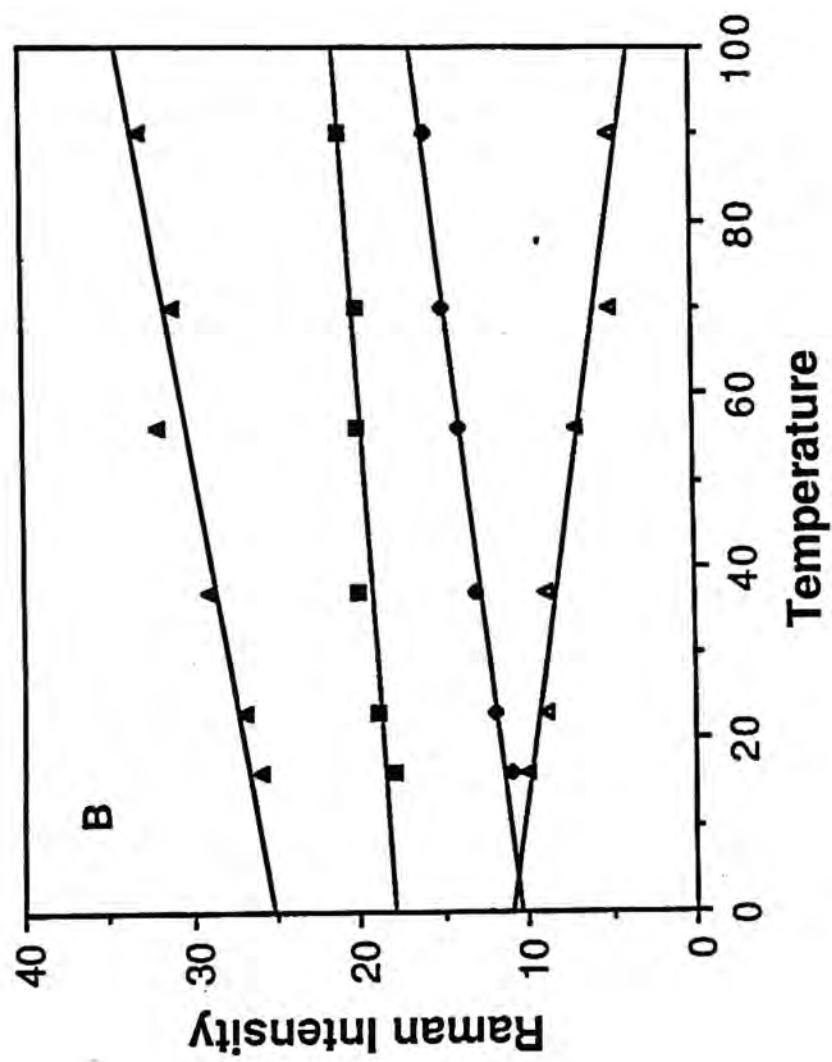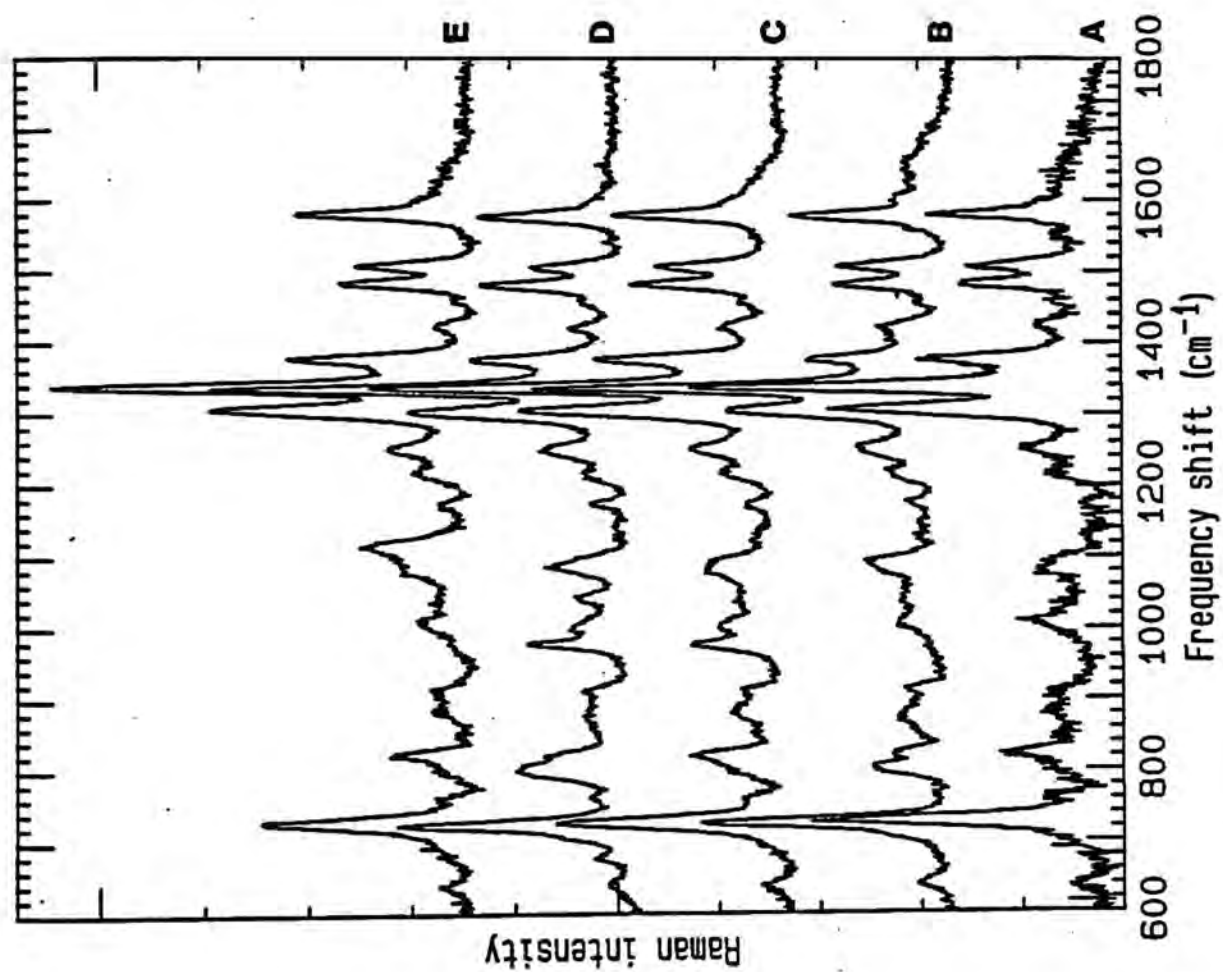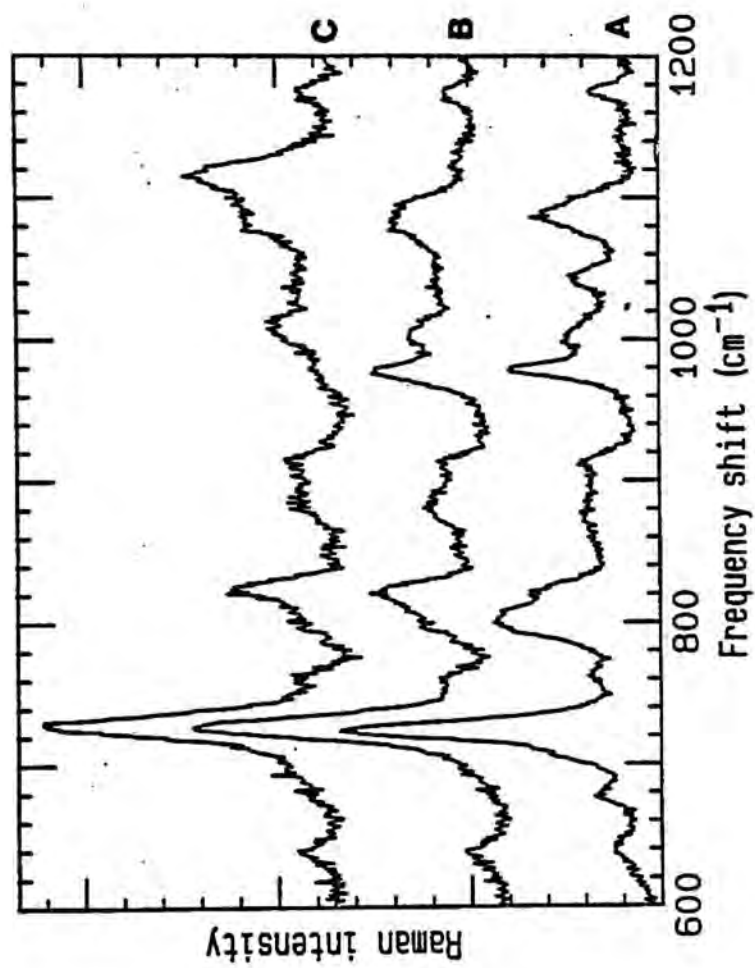
Ball, L. A., (1980) Virology, 94, 282-296.

Ball, L. A., & White, C. N. (1978) Virology 84, 496-508.
Ankel, H., Chany, C., Galliot, B., Chevalier, M. J. & Robert, M. (1973) Proc. Natl. Acad. Sci. USA 70, 223-231.

Baret, J. F., Carbone, G. P., & Sturm, J. (1979) J. Raman Spec. 8, 291-304.

Benevides, J. M., LeMeur, D., & Thomas, G. J., Jr. (1984) Biopolymers 23, 1011-1024.

Benevides, J. M., & Thomas, G. J., Jr. (1983) Nucleic Acids Res. 11, 5747-5761.

Berry, M. J., Knutson, G. S., Lasky, S. R., Munemitsu, S. M., & Samuel, C. E. (1985) J. Biol. Chem. 260, 11240-11247.

Bischoff, J. R., & Samuel, C. E. (1985) J. Biol. Chem. 260, 8237-8239.

Brown, E. B., & Peticolas, W. L. (1975) Biopolymers 14, 1259-1271.

Brown, G. E., Lebleu, B., Kawakita, M., Shaila, S., Sen, G. C., & Lengyel, P. (1976) Biochem. Biophys. Res. Commun. 69, 114-122.

Bugany, H., Bosch, J. V., Ferdinand, F. J., & Friis, R. R. (1983) Virology 127, 290-298.

Cayley, P. J., Silverman, R. H., Balkwill, F. R., McMahon, M., Knight, M., & Kerr, I. M. (1982) in The 2-5A System and Interferon Action, (Merigan, T. C., & Freidman, R. M., eds.), pp. 143-157 Academic Press, New York.

Chany, C. (1984) in Interferon 3 (Friedman R. M. ed.), pp 11-22, Elsever Science Publishers, New York.

Chany, C., Ankel, H., Galliot,B., Chevalier, M. J., & Gregoire, A. (1974) Proc. Soc. Exp. Biol. Med. 147, 293-299.

Chebath, J., Benech, P., Havanessian, A., Galbru, J., & Revel, M. (1987) J. Biol. Chem. 262, 3852-3857.

Collins, T., Korman, A. J., Wake, C. T., Boss, J. M., Kappes, D. J., Feirs, W., Ault, K. A., Gimbrone, M. A., Strominger, J. L., & Pober, J. S. (1984) Proc. Natl. Acad. Sci. USA 81, 4917-4921.

Cotton, F. A. (1971) in Chemical Applications of Group Theory, Wiley-Interscience, New York.

DeFilippi, P., Heuz, G., Verhaegen-Lewalle, M., DeClercq, E., Imai, J., Torrence, P. F., & Content, J. (1985)

De Maeyer-Guignard, J., & De Maeyer, E. (1985) in Interferon 6 (Gresser, I., ed.), pp. 69-91, Academic Press, New York.

Dhingra, M. M., & Sarma, R. H. (1978) Nature 272, 798-801.

Doornbos, J., DenHartog, J. A., VanBoom, J. H. & Altona, C. (1981) Eur. J. Biochem. 116, 403-412.

Doornbos, J., Charubala, R., Pfleiderer, W., & Altona, C. (1983) Nucleic Acids Res. 11, 4569-4582.

Elvidge, J. A., Jones, J. R., O'Brian, C., & Evans, E. A. (1971) Chem Commun. 394-395.

Erfurth, S. C., Kiser, E. J., & Peticolas, W. L. (1972) Proc. Natl. Acad. Sci. 69, 938-941.

Erfurth, S. C., Bond, J., & Peticolas, W. L. (1975) Biopolymers 14, 1245-1257.

Eyester, J. M., & Prohofsky, E. W. (1974) Spectrochim. Acta Part A 30, 2041-2049.

Floyd-Smith, G., Slattery, E. & Lengyel, P. (1981) Science 212, 1030-1032.

Floyd-Smith, G., Yoshie, O., & Lengyel, P. (1982) J. Biol. Chem. 257, 8584-8587.

Floyd-Smith, & Lengyel, P. (1986) Methods Enzymol.

Fodor, P. A., Rava, R. P., Hays, T. R., & Spiro, T. G. (1985) J. Am. Chem. Soc. 107, 1520-1529.

Friedman, R. M. (1977) Bacteriolo. Rev. 41, 543-567.

Friedman, R. M., Esteban, R. M., Metz, D. H., Tovell, D. R., & Kerr I. M. (1972a) FEBS Lett. 24, 273-277.

Friedman, R. M., Metz, D. H., Esteban, R. M., Tovell, D. R., Ball, L. A. & Kerr, I. M. (1972b) J. Virol. 10, 1184-1198.

Geer, C. L., Javor, B., & Abelson, J. (1983) Cell 33, 899-906.

Goodwin, D. C. & Brahms, J. (1978) Nucleic Acids Res, 5, 835-850.

Gresser, I., Banduu, M. T., & Brouty-Boyle, D. (1974) J. Natl. Cancer Inst. 52, 553-559.

Hartman, K. A., Lord, R. C., & Thomas, G. J., Jr. (1973) in Physicochemical Propreties of Nucleic Acids, Vol 2, pp. 92-143. (Duchesne, J.,ed.) Academic Press, New York.

Haugh, M. C., Cayley, P. J., Serfinoska, H. Norman, D. C. Reese, C. B., & Kerr, I. M. (1983) Eur. J. Biochem. 132, 77-84.

Hearl, W. H., & Johnston, M. I. (1984) in Progress in Clinical and Biological Research 202, pp. 37-45 (Williams, B. R. C. & Silverman, R. G. eds.) Alan R. Liss Inc., New York.

Hearl, W. H., & Johnston, M. I. (1987) J. of Virol. 61, 1586-1592.

Hirao, I., Ishido, Y., & Miura, K. (1983) Nucleic Acids Res. Symposium Series 12, 193-196.

Hovanessian, A. G., Brown, R. E. & Kerr I. M. (1977) Nature 268, 537-540.

Ilson, D. H., Torrence, P. F., & Vilcek, J. (1986) J. Interferon Res. 6, 5-12.

Imai, J., Johnston, M. I., & Torrence, P. F. (1982) J. Biol. Chem. 257, 12739-12745.

Imai, J., & Torrence, P. F. (1985) J. Org. Chem. 50, 1418-1426.

Imai, J., Lesiak, K., & Torrence, P. F. (1985) J. Biol. Chem. 260, 1390-1393.

Jacobsen, H., Czarniecki, C. W., Krause, D., Freidman, R. M., & Silverman, R. H. (1983a) Virology 125, 496-501.

Jacobsen, H., Krause, D., Freidman, R. M., & Silverman, R. H. (1983b) Proc. Natl. Acad. Sci. 80, 4954-4958.

Jamoulle, J.-C., Imai, J., Lesiak, K., & Torrence P. F. (1984) Biochemistry 23, 3063-3069.

Johnston, M. I. & Torrence, P. F. (1984) in Interferon 3, pp. 189-298. (Freidman, R. M., ed.) Elsevier Science, New York.

Johnston, M. I., Hearl, W. G., White, J. C., Imai, J., Torrence, P. F., & Williams, R. W. (1985) in Progress in Clinical and Biological Research 202, pp. 37-45 (Williams, B. R. C. & Silverman, R. G. eds.) Alan R. Liss Inc., New York.

Kerr, I. M., Brown, R. E. & Hovansessian, A. G. (1977) Nature 268 540-542.

Kerr, I. M., & Browm. R. E. (1978) Proc. Natl. Acad. Sci. USA 75, 256-260.

Kerr, I. M., Brown, R. E., & Ball, L. A. (1974) Nature (London) 250, 57-59.

Knight, E., Jr., Fahey, D. & Blomstrom, D. C. (1985) J. Interferon Res. 5, 305-313.

Knight, M., Cayley, P. J., Silverman, R. H., Wreschner, D., Gilbert, C. S., Brown, R. E., & Kerr I. M. (1980) Nature 288, 189-197.

Kimchi, A., Zilberstein, A., Schmidt, A., Shulman, L. & Revel, M. (1979) J. Biol. Chem. 254, 9846-9853.

Kimchi, A., Shure, H., Lapidot, Y., Rapoport, S., Panet, A. and Revel, M. (1981a) FEBS Lett. 134, 212-216.

Kimchi, A., Shure, A., & Revel, M. (1981b) Eur. J. Biochem. 114, 5-10.

Krause, D., Silverman, R. H., Jacobsen, H., Leisy, S. A., Dieffenbach, C. W. & Freidman, R. M. (1985) Eur J. Biochem. 146, 611-618.

Krishnan, I., & Baglioni, .C. (1981) Virology 111, 666-670.

Kushnaryov, V. M., MacDonald, H. S., Sedmark, J. J., & Grossber, S. E. (1985) Proc. Natl. Acad. Sci. USA 82, 3281-3285.

Lebleu, B., Sen, G. C., Shaila, S., Carber, B., & Lengyel, P. (1976) Proc. Natl. Acad. Sci. USA 73, 3107-3111.

Lee, S., & Suhadolnik, RT. J. (1985) Biochemistry 24, 551-555.

Lengyel, P., (1982) Ann. Rev. Biochem. 151, 251-282.

Lesiak, K. & Torrence, P. F. (1983) FEBS Lett. 151, 291-296.

Lesiak, K., & Torrence, P. F. (1986) J. Med. Chem. 29, 1015-1022.

Lesiak, K. Imai, J., Floyd-Smith, G., & Torrence, P. F. (1983) J. Biol. Chem. 258, 13082-13088.

Levitt, M., & Warshel, A. (1978) J. Amer. Chem. Soc. 100, 2607-2613.

Lord, R. C., & Thomas, G. J., Jr. (1967) Spectrochim Acta. Part A, 23A, 969.

Lu, K. C., Prohofsky, E. W., & Van Zant, L. L. (1975) Biopolymers 16, 2491-2506.

Manfait, M., Theophanides, T., Alix, A. J. P., & Jeannesson, P. (1984) in Spectroscopy of Biological Molecules, pp. 113-136 (Sandorfy, C. & Theophanides, T., eds) Reidel, Dordredlt, Holland.

Martin, J. C., & Wartell, R.. M. (1982) Biopolymars 21, 499-507.

Merlin, G. Chebath, J., Benech, P., Metz, R., & Revel, M. (1983) Proc. Natl. Acad. Sci. USA 80, 4904-4908.

Metz, D. H., (1975) Cell 6, 429-439.

Minks, M. A., Benvin, S., Maroney, P.A. & Baglioni, C. (1979) J. Biol. Chem. 254, 5058-5064.

Nishimura, Y., Tsuboi, M., Nakano. T., Higuchi, S., Sato, T., Shida, T.,Uesugi, S., Ohtsuka. E., & Ikehara, M. (1983) Nucleic Acids Res. 11, 1579-1588.

Nishimura, Y., Tsuboi, M., & Sato, T. (1984) Nucleic Acids Res. 12, 6901-6908.

Nishimura, Y., Hirakawa, Y., & Tsuboi, M. (1978) in Advances in Infrared and Raman Spectroscopy (Clark, R. J. H., & Hester, R. E., eds.), pp. 217-275 Heydon, London.

Padgett, R. A., Konarska, M. M., Grabowski, P. J., Hardy, S. F. & Sharp, P. A. (1984) Science 225, 898-903.

Parthasarathy, R., Malik, M. & Fridey, S. M. (1982) Proc. Natl. Acad. Sci. USA 79, 7292-7296.

Peticolas, W. L., & Tsuboi, N. (1979) in Infrared and Raman Spectroscopy of Biological Molecules, pp. 153-165 (Theophanidies, T. M., ed.) Reidel, Dordredlt, Holland.

Prescott, B., Gamache, R., Liveramento, J., & Thomas, G. J., Jr. (1974) Biopolymers 13, 1821-1845.

Raman, C. V., & Krishnan, K. S. (1928) Nature 121, 501.

Raziuddin, A., Sarker, F. H., Dutkowsky, R., Shulman, L., Ruddle, F. H. & Gupta, S. L. (1984) Proc. Natl. Acad. Sci. USA 81, 5504-5508.

Revel, M., Kimchi, A., Freidman, M., Wolf, D. Merlin, G., Panet, A., Rapoport, S., & Lapidiot, Y. (1982) Tex. Biol. Med. 41, 452-462.

Revel, M. (1984) in Antiviral Drugs and Interferon (Becker, Y., ed), pp. 357-433, Martinus Nijhoff, Paris.

Revel, M., & Chebath, J. (1986) TIBS 11, 166-170.

Revel, M., Wallach, D., Merlin, G., Schattner, A., Schmidt, A. & Freidman, M. (1981) Method Enzymol. 79, 149-161

Revel, M., Mory, Y., Rubinstein, M., Segev, D., Fellows, M., Hahn, T., & Wallach, D. (1985) in Immunopharmacology, Serono Symposia 23 (Miescher, P. A., & Ghhione, M., eds), pp. 67-68, Raven Press.

Rimai, L., Cole, T., Parsons, J. L., Hickmott, J. T., Jr., & Carew, E. B. (1969) Biophys. J. 9, 320-329.
Roberts, W. K., Clemens, M. J., & Kerr I. M. (1976) Proc. Natl. Acad. Sci. USA 73, 3136-3140.

Rosa, F., & Fellous, M. (1984) Immunol. Today 5, 261-262.

Ruskin, B., Krainer, A. R., Maniatis, T., & Green, M. R. (1984) Cell 38, 317-331.

Safer, B., (1983) Cell 33, 7-8.

Savitsky, A., & Golay, M., (1967) Anal. Chem. 36, 1627-1639.

Sawai, H., & Ohno, M. (1981a) Bull. Chem. Soc. Jpn. 54, 2759-2752.

Sawai, H., & Ohno, M. (1981b) Chem. Pharm. Bull. 29, 2237-2245.

Sawai, H., Imai, J., Lesiak, K., Johnston, M. I. & Torrence, P.F. (1983) J. Biol. Chem. 258, 1671-1677.

Sawai, H. (1983) Nucliec Acids Res. Symposium Series 12, 189-192.

Schmidt, A., Zilberstein, A., Shulman, L., Federman, P., Berissi, H. & Revel, M. (1978) FEBS Lett. 95, 257-264.

Schmidt, A., Chernajovsky, Y., Shulman, L., Federman, P., Berissi, H., & Revel, M., (1979) Proc. Natl. Acad. Sci. USA 76, 4788-4792.

Sen, G. C., LeBleu, B., Brown, G. E., Kawakita, M., Slattery, E., & Lengyel, P. (1976) Nature (London) 264, 370-373.

Shimanouchi, E. B., Tsuboi, M., & Kyogoku, Y. (1964) in Chemical Physics Vol. VII, pp. 435-498 (Duchesene, J., Ed.) Interscience, London.

Silverman, R. H., Krause, D., Jacobsen, H., Leisy, S. A., Barlow, D. P. (1983) in The Biology of the Interferon System (De Maeyer E., & Schellekens, eds.) pp. 189-200. Elsevier Science

Silverman, R. H. (1985) Anal. Biochem. 144, 450-460.

Silverman, R. H., Cayley, P. J., Knight, M., Gilbert, C. S., & Kerr I. M. (1982a) Eur. J. Boichem. 124, 131-138.

Silverman, R. H., Watling, D., Balkwill, F.R., Trowsdale, J. & Kerr, I. M. (1982b). Eur. J. Biochem. 126, 333-341.

Slattery, E., Ghoh, N., Samanta, H. & Lengyel, P. (1979) Proc. Natl. Acad. Sci. USA 76, 4778-4782.

Small, E. W., & Peticolas, W. L. (1971a) Biopolymers 10, 69-88.

Small, E. W., & Peticolas, W. L. (1971b) Biopolymers 10, 1377-1425.

Sonnabend, J. A. & Freidman, R. M. (1973) in Interferons and Interferon Inducers, (Finter, N. B., ed.) pp 201- 239, North-Holland, Amsterdam.

Stewart, W. E. II (1979) in Interferon 1 (Gresser, I., ed.), pp.29-51, Academic Press, New York.

Stewart, W. E. II (1981) The Interferon System, 2nd ed., pp.200-207, Springer-Verlag, New York.

St. Laurent, G., Yoshie, O., Floyd-Smith, G., Samanta, H., Sehgal, P. B. & Lengyel, P. (1983) Cell 33, 95-102.

Taylor-Papadimitriou, J., (1980) in Interferon 2 (Gresser, I., ed.) pp. 13-46, Academic Press, New York.

Thomas, G. A., & Peticolas, W. L. (1983a) J. Am. Chem. Soc. 105, 986-992.

Thomas, G. A., & Peticolas, W. L. (1983b) J. Am. Chem. Soc. 105, 993-996.

Thomas, G. J., Jr., & Kyogoku, Y. (1977) Pract. Sprctrosc. 1C, 717-723.

Thomas, G. J., Jr., & Livramento, J. (1975) Biochemistry 23, 5210-5218.

Thomas, G. J., Jr., & Hartman, K. A. (1973) Biochim. Biophys. Acta. 312, 311-322.

Torrence, P. F. (1985) in Biological Response Modifiers (Torrence, P. F., ed.) pp. 77-105, Academic Press, New York.

Torrence, P. F. & Lesiak, K. (1986) J. Med. Chem. 29, 1015-1022.

Torrence, P. F., & Lesiak, K. (1987) J. Biol. Chem. 262, 1961-1966.

Torrence, P. F., Lesiak, K., Imai, J., Johnston, M. I., Sawai, H. (1983) in Nucleosides, Nucleotides, and Their Biological Applications (Ridout, J. L., Henry B. W., Beachham L. M., eds.) pp. 67-115. (Academic Press, New York.

Torrence, P. F., Imai, J., & Johnston, M. I. (1981) Proc. Natl. Acad. Sci. USA 288, 5993-5997.

Torrence, P. F., Imai, J., Lesiak, K., Johnston, M. I., Jacobsen, H., Freidman, R . M. Sawai, H., & Safter, B. (1982) in Interferons UCLA symposia on Molecular and Cellular Biology, pp.123-142 (Merigan, T., Freidman, R., & Fox, C. F., eds), Vol. XXV, Academic Press, New York.

Torrence, P. F., Imai, J., Lesiak, K., Jamoulle, J. C. & Sawai,H. (1984) J. Med. Chem. 27, 726-733.

Torrence, P. F., Imai, J., Wong, A., & Lesiak, K. (1985) in Progress in Clinical and Biological Research 202, pp. 75-80 (Williams, B.R. C., & Silverman R. G. eds.) Alan R. Liss Inc., New York.

Tsuboi, M., Takahushi, S., & Harada, I. (1973) in Physio-chemical Properties of Nucleic Acids Vol. 2, p. 91 (Duchesne J., ed.) Academic Press, New York.

Van Zandt, L. L., Lu, K.C., & Prohofsky, E. W. (1977a) Biopolymers 16, 2481-2490.

Van Zandt, L. L., Lu, K.C., & Prohofsky, E. W. (1977b) Biopolymers 16, 2490-2506.

Verhaegen-Lewalle, M., & Content, J. (1982) Eur. J. Biochem. 126, 638-643.

Wartell, R.M., & Harell, J.T. (1986) Biochemistry 25, 2664-2671.

Wallace, J. C., & Edmonds, M. (1982) Proc. Natl. Acad. Sci. 80, 950-954.

Wallach, D., Fellous, M., & Revel, M. (1982) Nature 299, 834-836.

Whitaker-Dowling, P.A., Wilcox, D. K., Widnell, C. C. & Younger, J. S. (1983) Proc. Natl Acad. Sci. USA 80, 1083-1086.

Williams, B. R. G. & Kerr, I. M. (1978) Nature 176, 88-90.

Williams, R. W. (1983) J. Mol. Bio. 166, 581-603.

Wilson, E. B., Decius, J. C., & Cross, P. C. (1980) in Molecular Vibrations; The Theory of Infrared and Raman Vibrational Spectra. Dover Publications, New York.

Wreschner, D. H., James, T. C., Silverman, R. H. & Kerr I. M. (1981a) Nucleic Acids Res. 9, 1571-1581.

Wreschner, D. H., McCauley, J. W., Skehel, J. J., & Kerr I. M. (1981b) Nature 289, 414-417.

Wreschner, D. H , Silverman, R. H., James, T. C., Gilbert, C. S. & Kerr, I. M. (1982) Eur. J. Biochem. 124, 261-268.

Yang, K., Samanta, H., Dougherty, J., Jayaram, B., Broeze, R. & Lengyel, P. (1981) J. Biol. Chem. 256, 9324-9328.

Yarden, A., Shure-Gottlied, H., Chebath, J., Revel, M., & Kimchi, A (1984) EMBO J. 3, 969-973.

Yue, T. K., Yang, J.-P., Martin C. L., Lee, S. K., Sloan, D., & Callender, R. H. (1984) Biochemistry 23, 6480-6483.

Yue, T. K., Martin, C. L., Chen, D., Nelson, P., Sloan, D. L., & Chandler, R. H. (1986) Biochemistry 25, 4981-4947.